NASA TECHNICAL NOTE

NASA TN D-2983

A GENERAL DESCRIPTION OF THE ST124-M INERTIAL PLATFORM SYSTEM

by Herman E. Thomason

George C. Marshall Space Flight Center
Huntsville, Ala.

NATIONAL AERONAUTICS AND SPACE ADMINISTRATION • WASHINGTON, D. C. • SEPTEMBER 1965

NASA TN D-2983

A GENERAL DESCRIPTION OF THE ST124-M INERTIAL PLATFORM SYSTEM

By Herman E. Thomason

George C. Marshall Space Flight Center
Huntsville, Ala.

NATIONAL AERONAUTICS AND SPACE ADMINISTRATION

For sale by the Clearinghouse for Federal Scientific and Technical Information
Springfield, Virginia 22151 – Price $3.00

TABLE OF CONTENTS

LIST OF ILLUSTRATIONS

LIST OF ILLUSTRATIONS (Cont'd)

LIST OF ILLUSTRATIONS (Cont'd)

LIST OF ILLUSTRATIONS (Concluded)

NOMENCLATURE

θ_X	Middle gimbal angle with respect to inner gimbal
β	Single axis gyro pickoff output angle
α	Single axis gyro input axis angle
G(s)	Gyro transfer function
K	Servoloop dc gain
H	Gyro angular momentum in cm g/s^2
T_α	Disturbance torques about gyro input axes
T_m	Applied torque resulting from closed loop servosystem
T_β	Disturbance torques about gyro output axis
ω	Frequency in radians per second
J_α	Platform input axis (stabilized axes) moment of inertia
J_β	Gyro output axis moment of inertia
ζ	Servoloop damping coefficient
F	Electronics feedback function
σ	Total gyro pickoff output with three-axis system
Δ	Determinant of three-axis matrix

A GENERAL DESCRIPTION OF THE ST124-M INERTIAL PLATFORM SYSTEM

SUMMARY

~~33~~ 34434

A general description of the ST124-M inertial platform system is presented. The major subsystems of the platform system are discussed and a brief explanation of the launch electrical support equipment is provided. Servoloop design theory for use with gas bearing components and an extension of this theory into the three-axis platform servosystem is presented. The effects of gyro cross-coupling and three-axis stabilization problems are discussed.

Each of the platform's subsystems is discussed to the extent that a general understanding of its function is possible. References are provided to facilitate further investigation.

Author

SECTION I. INTRODUCTION

The inertial platform and its associated black box assemblies (Fig. 1) is a major part of the guidance and control (G&C) system of the Saturn launch vehicles. The block diagram in Figure 2 illustrates the manner in which the ST124-M platform system fits into the total G&C system of the Saturn V vehicles. The platform system originates the guidance parameters used to compute the necessary steering commands for vehicle attitude control and navigation; the system also provides the mechanics for thrust vector attitude programing.

The total platform system consists of six assemblies: the inertial platform, the platform electronics assembly, the accelerometer signal conditioner, the ac power supply, the 56-volt dc power supply, and the nitrogen gas supply (Fig. 3). The ST124-M system is self-contained and requires only inputs from the environmental conditioning system and the 28-volt dc power source. Guidance parameters flow from the platform system via the data adapter to the guidance computer. The inputs to the platform system are vehicle acceleration along the navigation coordinates, vehicle movement about the vehicle control coordinate, and computer commands. Its outputs are vehicle velocity along the inertial navigation coordinates and vehicle attitude, as referenced to the inertial coordinates. The guidance computer takes these inertial platform guidance parameters and generates steering commands that reduce vehicle attitude error to zero and navigate the vehicle onto predetermined trajectories and into predetermined orbits.

INERTIAL STABILIZED PLATFORM SYSTEM SATURN V&IB

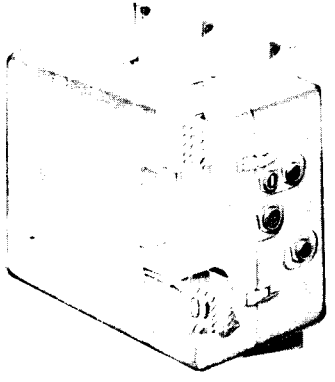

AC POWER SUPPLY

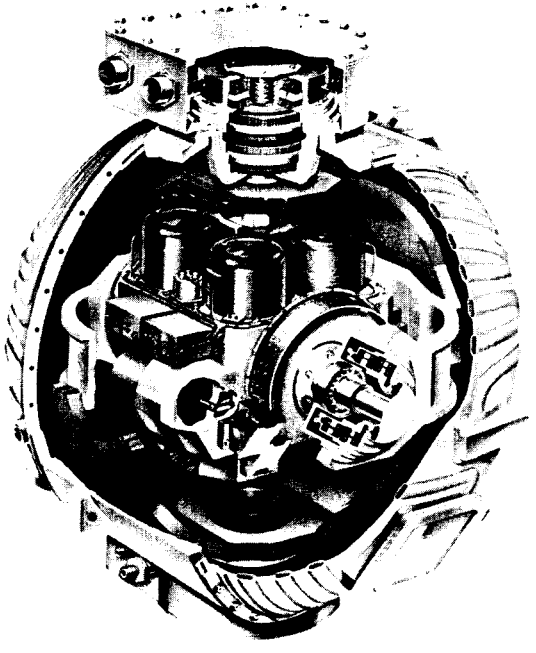

ST 124-M
STABLE PLATFORM

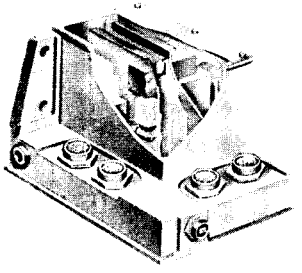

ACCELEROMETER
SIGNAL
CONDITIONER

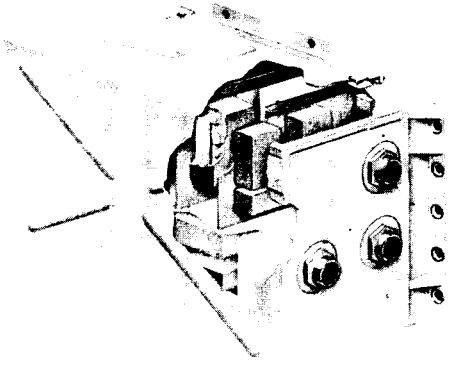

PLATFORM
SERVOAMPLIFIER

SYSTEM FUNCTIONS

A. ACCELEROMETER SENSING & REFERENCE.
B. VEHICLE ATTITUDE & PROGRAMING.
C. GUIDANCE REFERENCE COORDINATES.

FIGURE 1. ST124-M STABLE PLATFORM.

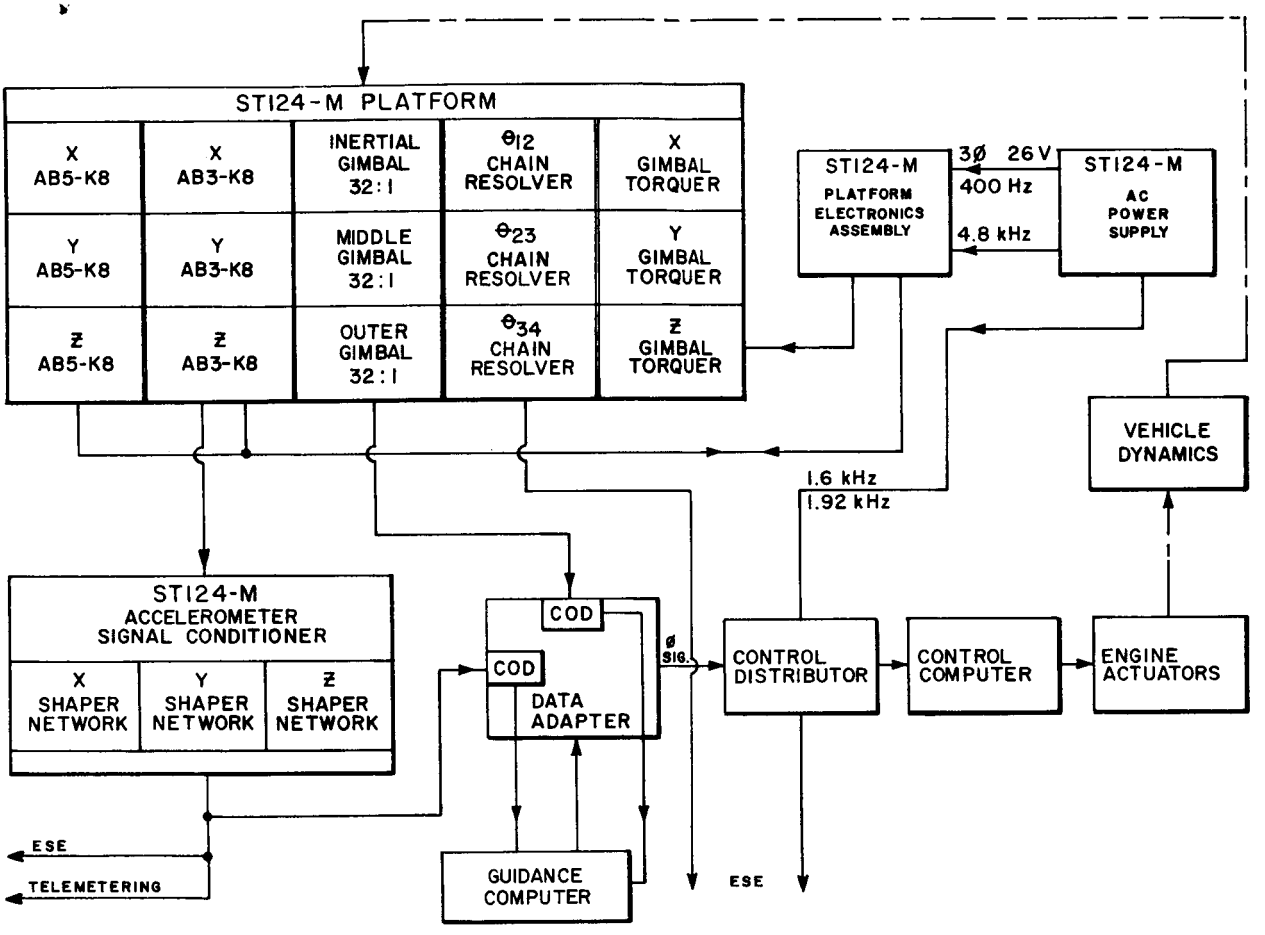

FIGURE 2. BLOCK DIAGRAM OF SYSTEM INTERCONNECTION.

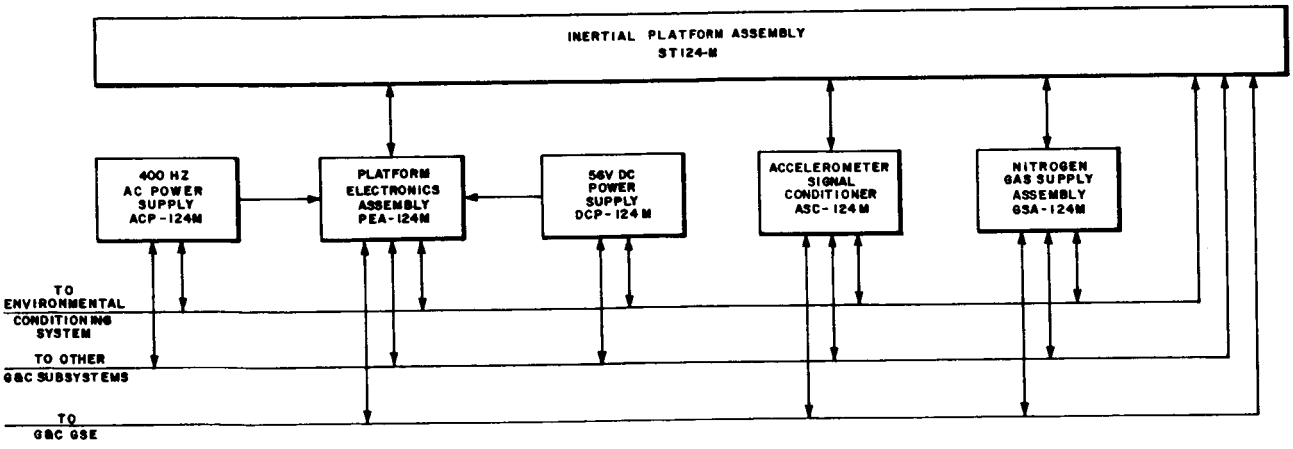

FIGURE 3. BLOCK DIAGRAM OF ST124-M SYSTEM.

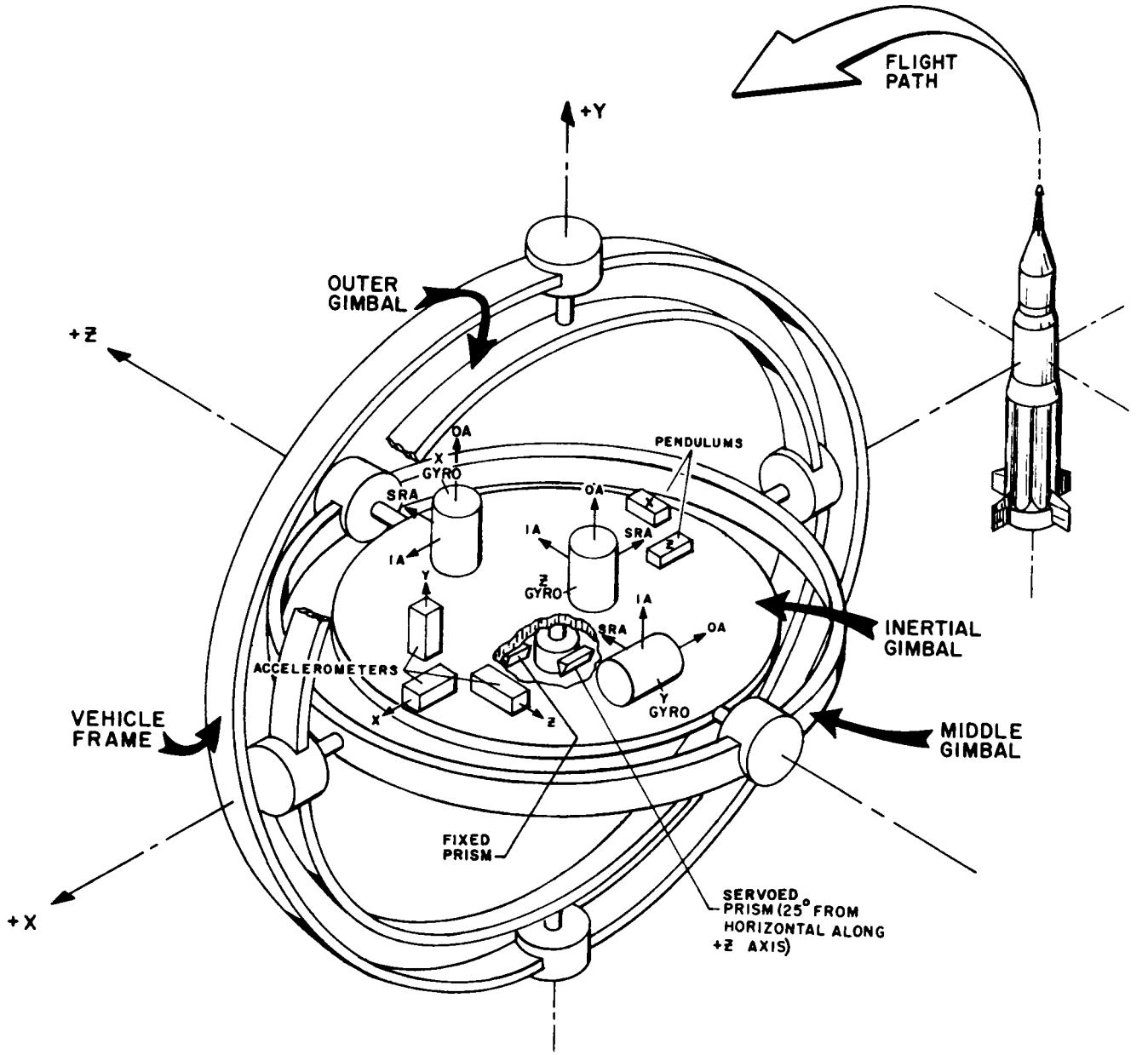

FIGURE 4. ST124-M GIMBAL CONFIGURATION.

There is much in common between the ST124-2 platform, developed for Saturn I-class vehicles, and the ST124-M platform, developed for Saturn IB/V-class vehicles; but there are some major differences. Two significant differences are a change in gimbal order and the method of generating attitude parameters. The attitude parameters are generated by multispeed resolvers in the gimbal pivots. The gimbal order is base, roll, yaw, and pitch (Fig. 4).

An area of growth in complexity and hardware associated with the platform system is the ground support equipment. This growth can be attributed to the requirement for complete automation and the consequent interfacing with the launch control computers and the extremely long data link to the launch control center. System tests and updating requirements on the launch pad also have contributed to further complicate the ground support equipment (GSE). Electrical support equipment (ESE) associated with the platform system is located at the launch site and the launch control center (LCC). At the launch site, the azimuth laying theodolite is located approximately 700 feet from the base of the vehicle. The theodolite installation transmits signals via underground cables to the platform ESE located in the mobile launcher. Platform ESE in the mobile launcher consists of the inertial data box, the alignment amplifier panel, the azimuth control panel, the theodolite amplifier panel, and the accelerometer monitor panels. The equipment contained in the mobile launcher interfaces with the onboard ST124-M system, the RCA-110A mobile launcher computer, and the data link. In the LCC, additional ST124-M ESE interfaces with the LCC RCA-110A computer and data link. This equipment consists of the platform checkout and monitor panel, the platform control panel, the azimuth laying panel, and the azimuth laying video monitor panel. Total remote control and automation of the platform system is accomplished from the LCC by use of the platform ESE, the launch control computer, and the data link.

SECTION II. ST124-M INERTIAL PLATFORM

ST124-M is the nomenclature of a mission-oriented stabilized platform that can take either of two configurations. These two configurations are designated ST124-M3 and ST124-M4 and are three- and four-gimbal systems, respectively. In the basic design of the ST124-M platform, the outer, middle, and inertial gimbals are identical in both models. The ST124-M4 has a fourth, or redundant, gimbal and a larger base structure; it requires a different Instrument Unit (IU) mounting frame. The IU intercabling and wiring for these two systems are identical.

The gimbal configuration of the ST124-M4 offers unlimited freedom about all three inertial reference axes, while the ST124-M3 is limited to ±45 degrees about its X axis (vehicle yaw at launch). The vehicle mission dictates the configuration required. The Apollo mission uses the ST124-M3 configuration.

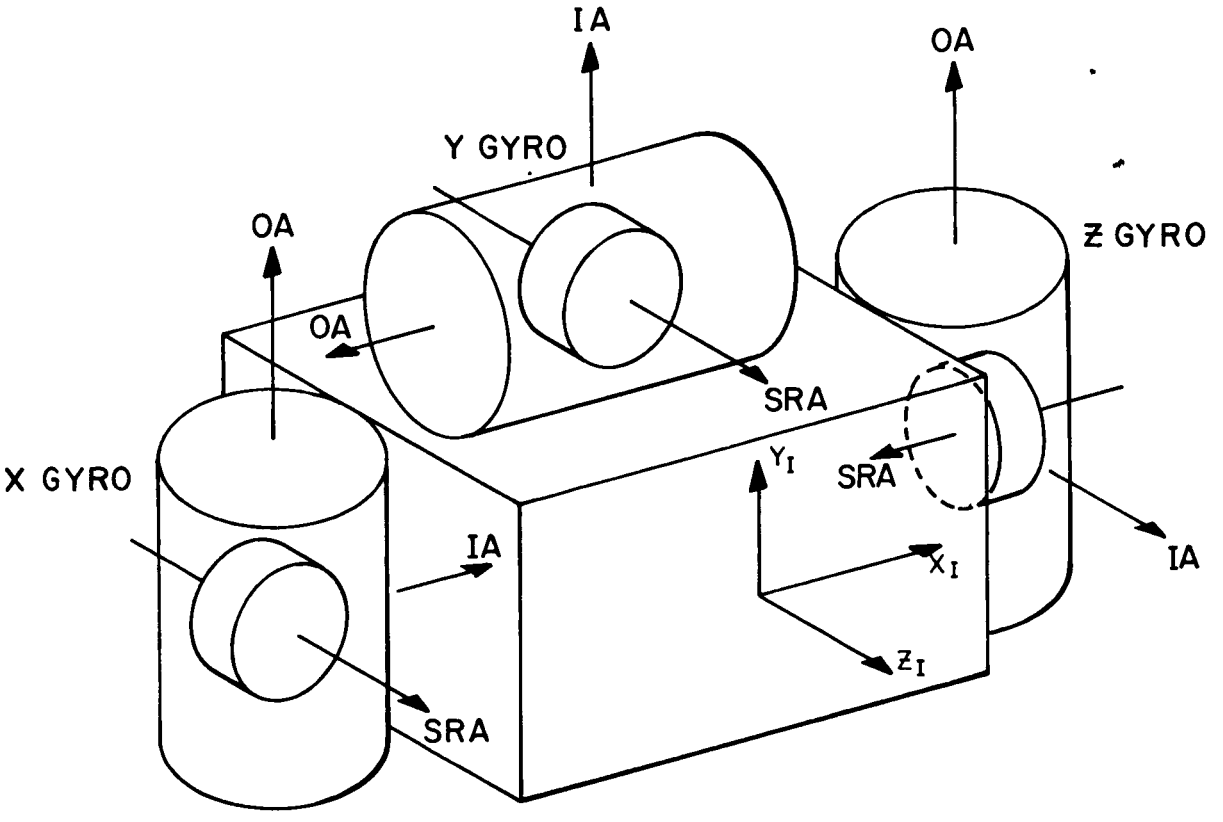

FIGURE 5. GYROSCOPE ORIENTATION ON INERTIAL GIMBAL.

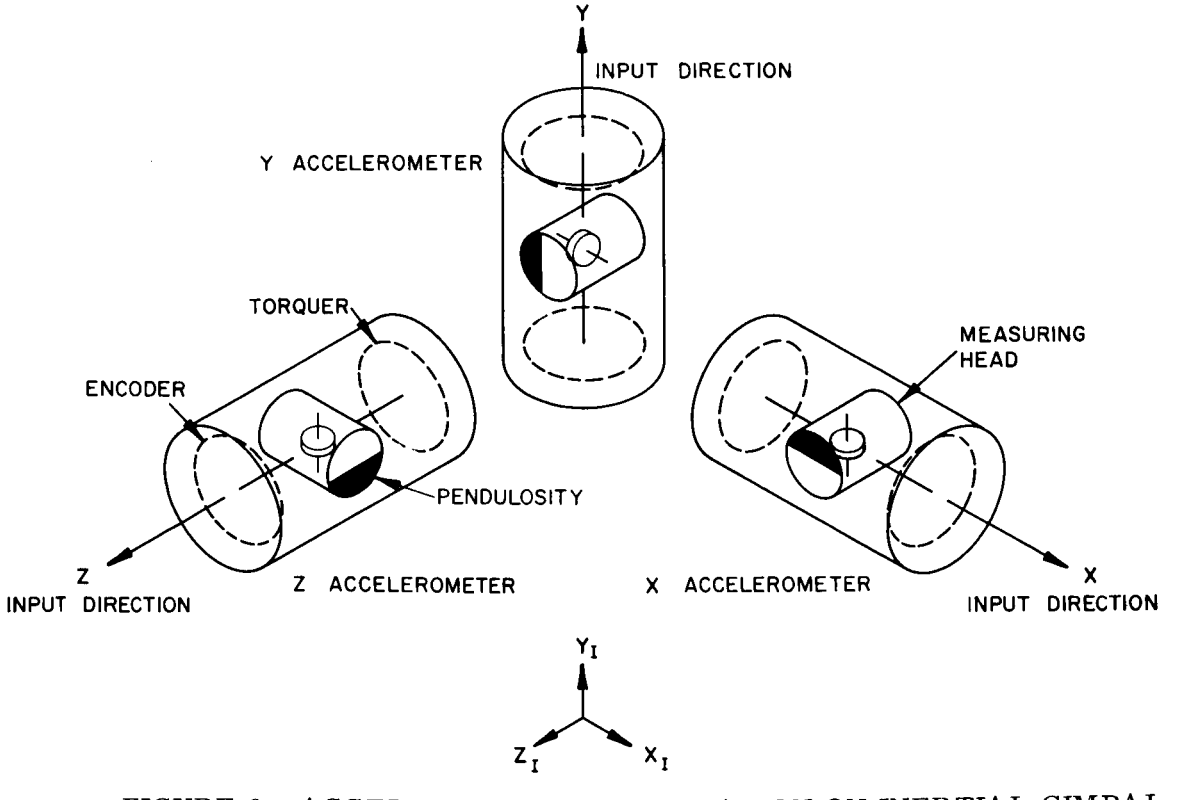

FIGURE 6. ACCELEROMETER ORIENTATION ON INERTIAL GIMBAL.

The inertial, or inner, gimbal provides a rotationally-stabilized table upon which are mounted three inertial accelerometers. The gimbaling system allows the inertial gimbal rotational freedom. Three single-degree-of-freedom gyroscopes provide the reference for the stabilized table. The gyros have their input axes aligned along an orthogonal coordinate system X_I, Y_I, and Z_I of the inertial gimbal as shown in Figure 5. The signal generator, which is fixed to the output axis of the gyro, generates electrical signals proportional to torque disturbances. These signals are transmitted to the servoelectronics which terminate in the gimbal pivot servotorque motors. The servoloops maintain the inertial gimbal rotationally fixed in inertial space.

The inertial gimbal has three pendulous integrating gyro accelerometers oriented along the inertial coordinates X_I, Y_I, and Z_I (Fig. 6). Each accelerometer measuring head contains a pendulous single-degree-of-freedom gyro; the angular position of the measuring head is a measure of integrated acceleration along the input axis of the accelerometer. The Z accelerometer measures acceleration perpendicular to the thrust vector and provides the cross range guidance to the guidance computer. The velocity outputs of the X and Y accelerometers are used by the guidance computer to establish the pitch attitude of the vehicle acceleration vector and the required cutoff velocity.

The inertial coordinate erection and orientation system of the ST124-M platform aligns the Y_I coordinate along the launch local vertical parallel to the gravity vector and aligns the Z_I coordinate perpendicular to the vehicle mission azimuth. The coordinate orientation is accomplished by use of an automatic alignment system which is a part of the electrical support equipment. The leveling alignment servoloops (X and Z) generate torquing voltages which are a function of the earth's angular velocity, the latitude of the launch site, and the azimuth of the X_I inertial coordinate. These voltages are applied to the X and Z gyro torquers and cause the gyros to torque their respective gimbals until the servos are nulled. The inertial coordinates are established in azimuth with the roll alignment servoloop. The output of the roll alignment servoloop is a function of the earth's angular velocity and the latitude of the launch site. Azimuth alignment, being a commanded function, is accomplished by injecting azimuth alignment signals directly into the roll alignment loop and positioning the inertial coordinates by torquing the roll gimbal with the Y gyro. The azimuth alignment position can be updated at any time by the launch control computer.

The inertial coordinates of the ST124-M platform maintain a fixed relationship to the inertial gimbal. These coordinates are accurately positioned prior to vehicle liftoff and remain inertially fixed after vehicle liftoff. The gimbals of the platform have the basic function of allowing the inertial coordinate rotational freedom with respect to the vehicle. The gimbal pivots are the axes about which the gimbals turn with respect to each other. The ±Z pivots couple the inertial gimbal to the middle gimbal; the Z pivot axis is normally along the vehicle pitch axis. The ±X pivots couple the middle gimbal to the outer gimbal; the X pivot axis is normally along the vehicle yaw axis. The ±Y pivots couple the outer gimbal to the platform mounting base; the Y pivot axis is along the vehicle roll axis. The platform pivot scheme is shown in Figure 7. The X, Y, and Z pivots are controlled by dc torque motors; the Y pivot torquer has approximately twice the torque

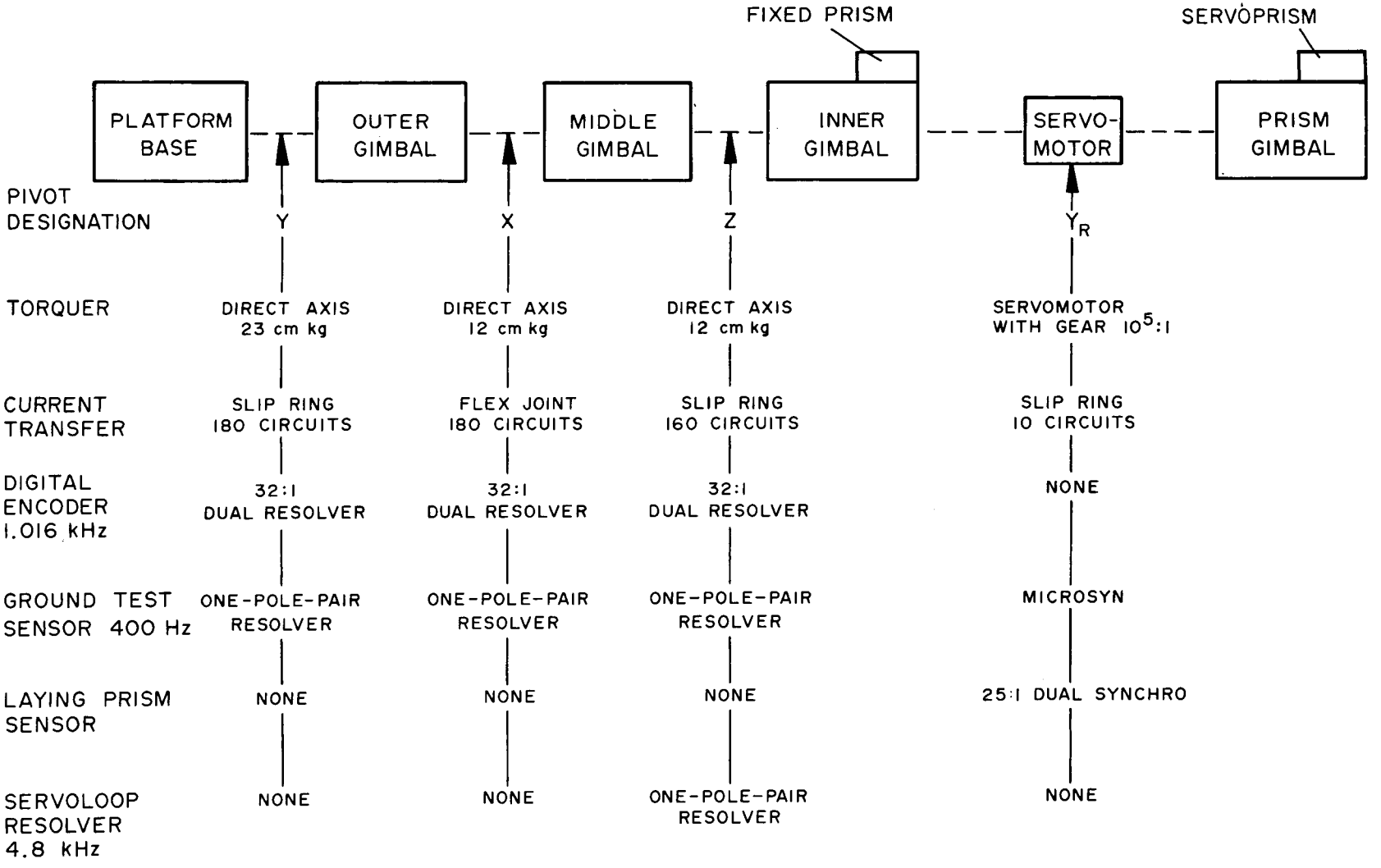

FIGURE 7. PLATFORM PIVOT SCHEME.

capacity of the other pivot torquers. This accommodates the reflected torque when the middle gimbal is not orthogonal with the outer gimbal. For transfer of electrical potentials across the ±Y and ±Z pivots, slip ring capsules are used. A flex cable is used on the ±X pivot because of its limited freedom.

Dual-speed resolvers (32:1) are used as digital shaft encoders on the +X, +Y, and +Z pivots. The system also has an analog resolver chain that utilizes single-speed resolvers on each pivot and three program resolvers in the inertial data box. This is used with the ground electrical support equipment to facilitate checkout and test. If required, the resolver chain system can be used as flight equipment to measure the gimbal angles and to provide the vehicle attitude signals.

The Y_R prism gimbal pivot is controlled through a gear reduction of 10^5:1 by a servomotor mounted to the inertial gimbal. The angle between the prism gimbal and the inertial gimbal is accurately sensed by a dual synchro (25:1) and controlled with a followup servo. A microsyn is also mounted on the Y_R pivot to initially align the prism gimbal to the inertial gimbal and to facilitate laboratory checkout and test.

The three-gimbal ST124-M3 platform, as defined, is the normal launch pad configuration and is illustrated in Figure 8. The configuration of the four-gimbal platform is shown in Figure 9. It is similar to the three-gimbal structure with the addition of the redundant gimbal and the $\pm X_R$ pivots. The redundant gimbal is controlled either by a time program or an angular sensor on the +X pivot.

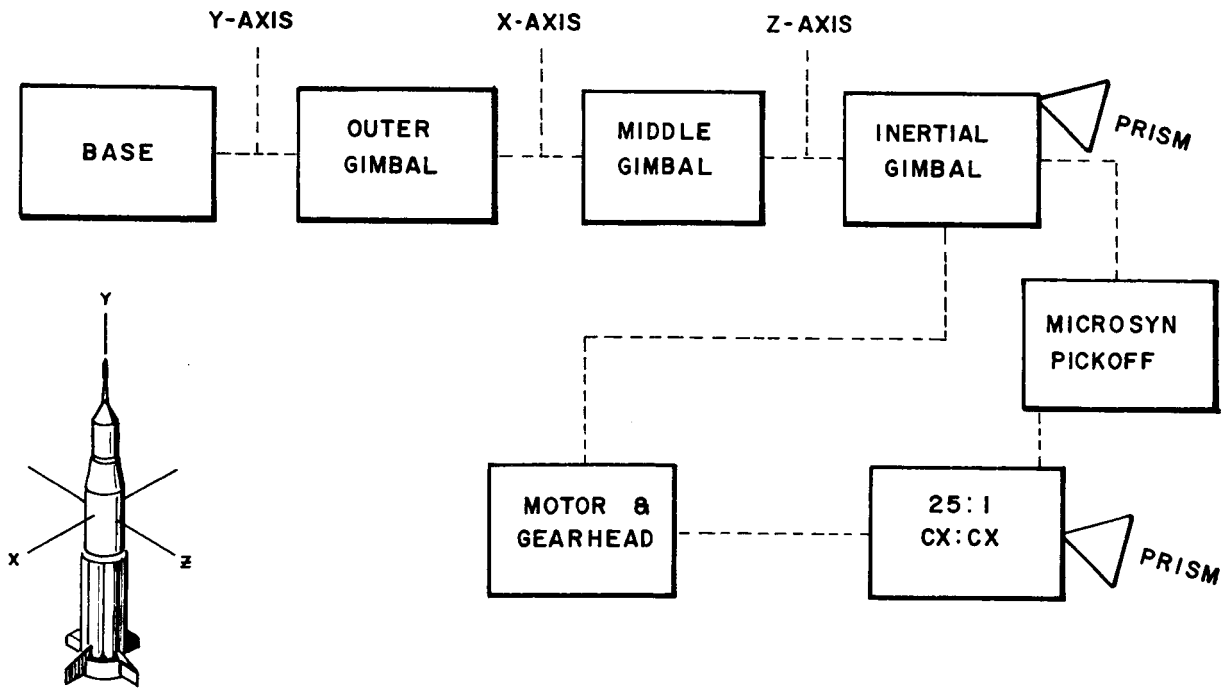

FIGURE 8. BLOCK DIAGRAM OF ST124-M3 GIMBAL.

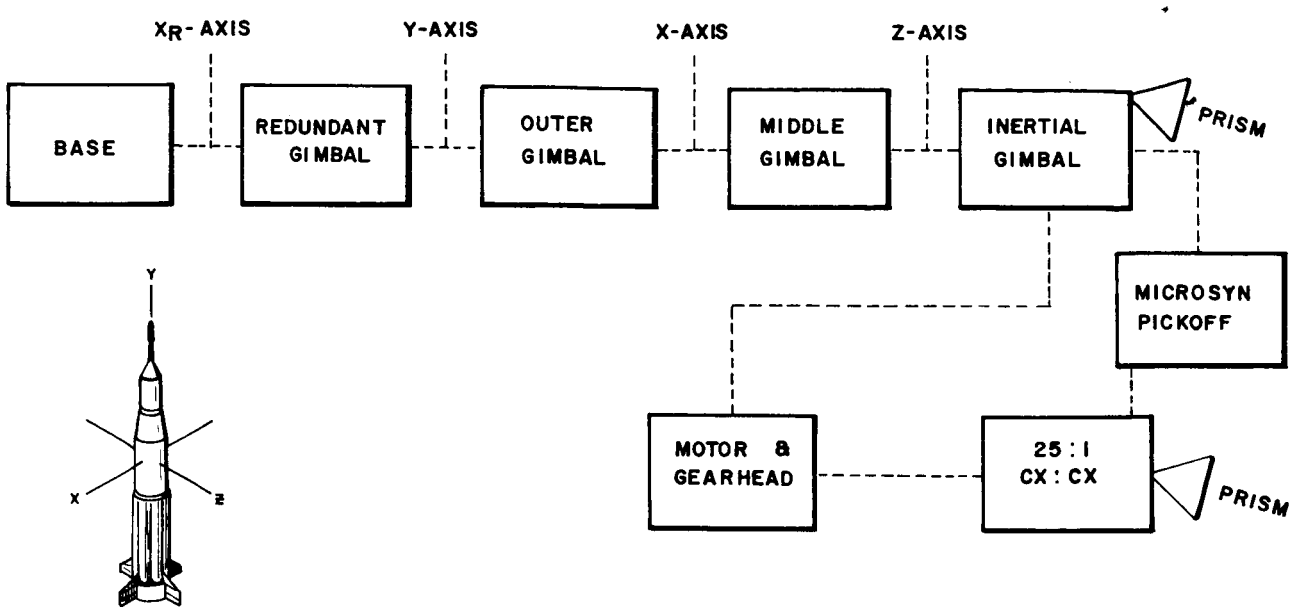

FIGURE 9. BLOCK DIAGRAM OF ST124-M4 GIMBAL

The weights of the ST124-M3 and ST124-M4 are 48 kg (107 lb) and 65.5 kg (145 lb), respectively. The platform mounts to the Saturn IB and V IU at control position IV on accurately machined surfaces which are qualified to the IU coordinates to ±3 arc minutes. A window in the IU at control position IV provides a line of sight to the platform azimuth laying prisms for penetration of the azimuth laying theodolite light source (Fig. 10).

The electrical connectors and hemispherical covers of the platform are sealed so that exhaust gas from the gas bearing components must pass through a special orifice in the platform base. This orifice is a pressure-regulating device that stabilizes the internal ambient pressure at 8.3 N/cm^{2}a (12 psia). Because of the characteristics of this orifice, the internal pressure will rise to approximately 12 N/cm^{2}a (17 psia) in a one atmosphere ambient and will drop to the controlled pressure of 8.3 N/cm^{2}a (12 psia) as the vehicle ascends in approximately one minute after liftoff.

The covers also serve as heat exchangers for removing excess heat from the platform. The water-methanol coolant from the environmental conditioning system flows through passages in the covers, removing the excess heat. The water-methanol solution is maintained at 15 ±1° C by the IU environmental conditioning system. The mass temperature of the platform stabilizes at approximately 42° C. The hemispherical covers are aluminum and are secured to the platform base with cap screws and sealed with full volume 0 rings.

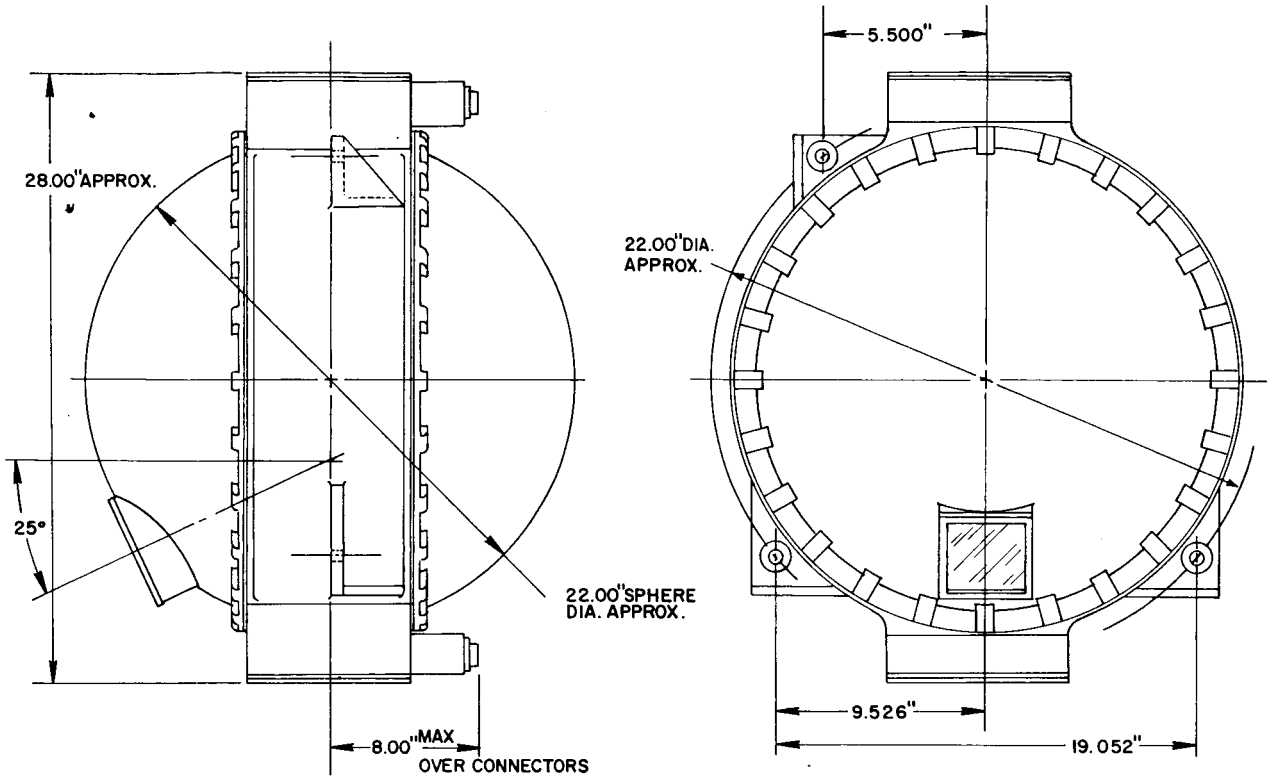

FIGURE 10. ST124-M3 OUTLINE.

The platform gimbals, pivot housings, and base are machined from beryllium, which provides the greatest stiffness-to-weight ratio, stability after machining, and excellent heat transfer characteristics.

The inertial gimbal is geometrically the most complicated gimbal and thus is the most difficult to fabricate (Fig. 11). This gimbal supports the three stabilizing gyros, three accelerometers, two pendulums, the inertial prism, the synchro prism assembly, and electronic modules. The mounting surfaces for the gyros, accelerometers, pendulums, and prisms are precision machined. Orthogonality of the mounting surfaces for the accelerometers and gyros is ±3 arc seconds and ±2 arc minutes, respectively. The pendulums are matched to the accelerometers to ±3 arc seconds, and the prisms are matched to the inertial coordinates to ±3 arc seconds. Gas supply passages are machined inside the inertial gimbal, and special fittings on the gas bearing components allow them to be plugged directly into the gas supply passages.

The gimbal rings are designed as spherical sections. This geometry was chosen to give maximum mechanical rigidity and stability and also to provide symmetrical moments of inertia for servoloop design.

Gimbal load bearings are designed so that minimum shear is placed on the gimbal. This is accomplished by using on one pivot of each gimbal a pair of bearings preloaded against each other with 36.3 kg (80 lb) load. The other pivot of each gimbal has a single gothic-arch-type bearing preloaded to 2.27 kg (5 lb).

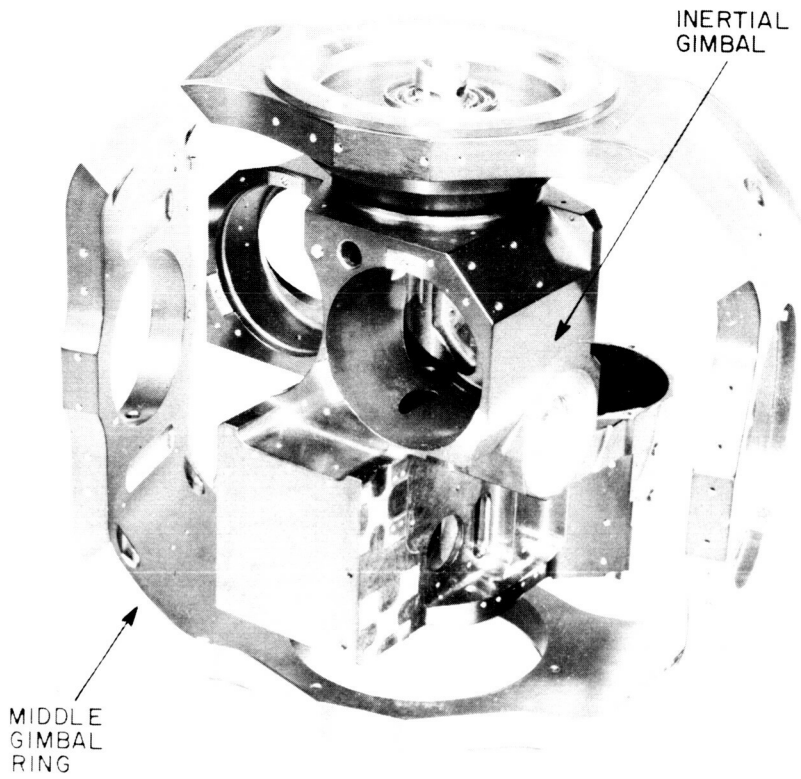

FIGURE 11. INERTIAL AND MIDDLE GIMBALS.

Gimbal pivot resolvers are assembled in separate beryllium housings and attached to the pivots with stiff diaphragms. This allows a minimum eccentricity between resolver rotor and stator, bench testing of the assembled resolver, and easy replacement without disassembly of the gimbal structure at the load bearings.

Nitrogen gas is transported across the pivots through an annulus with 0 ring seals. The total leak rate of the pivot annulus will be less than 1400 cm^3/min STP (0.05 CFM).

Structural resonances of the outer and middle gimbals are 265 Hz and 330 Hz, respectively. The structural resonant frequency of 120 Hz is obtained on the inertial gimbal because of the stiffness of the beryllium gimbal rings. There is a secondary resonant frequency of the inertial gimbal at 280 Hz which is obtained from the bearings and pivot trunnions. Above 280 Hz, the gimbals attenuate base vibration inputs, providing a smooth support for the components.

SECTION III. GYRO AND ACCELEROMETER SERVOSYSTEM

Functional block diagrams of the gyro and accelerometer servoloops are shown in Figures 12 and 13, respectively. The servoloops use a 4.8 kHz suppressed carrier modulation system with the signal generator outputs being amplified and demodulated on

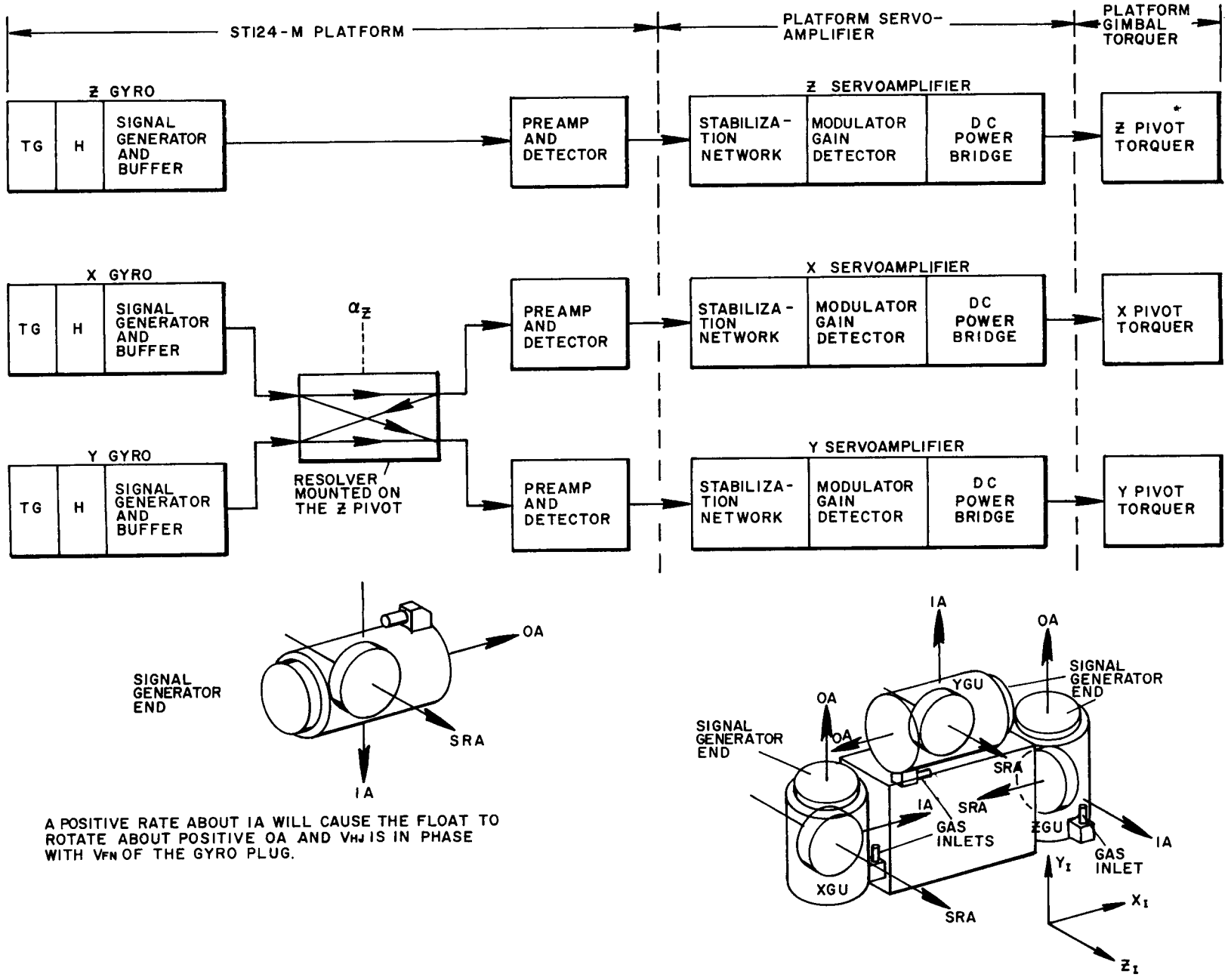

FIGURE 12. GYRO SERVOLOOP BLOCK DIAGRAM.

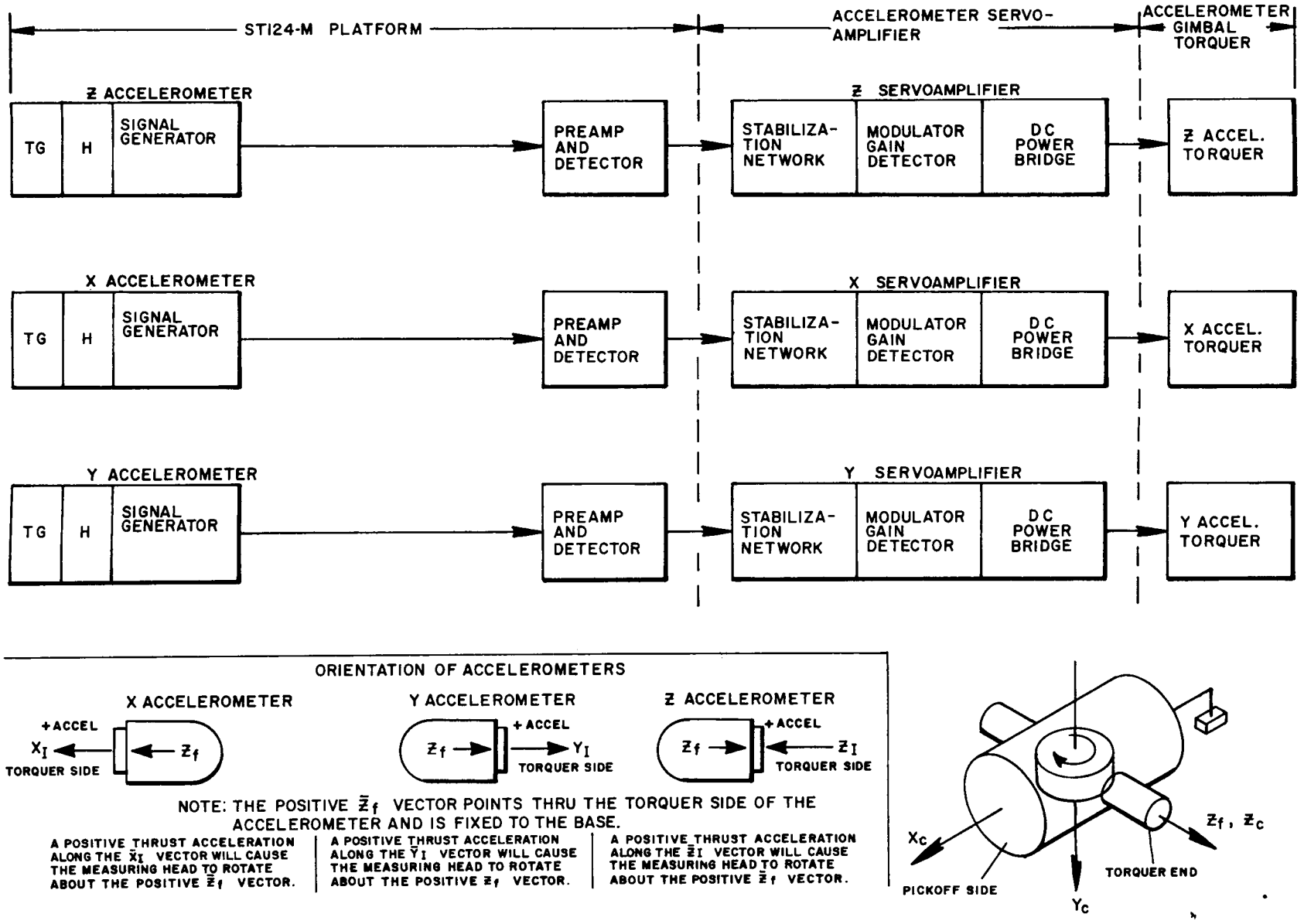

FIGURE 13. ACCELEROMETER SERVOLOOP BLOCK DIAGRAM.

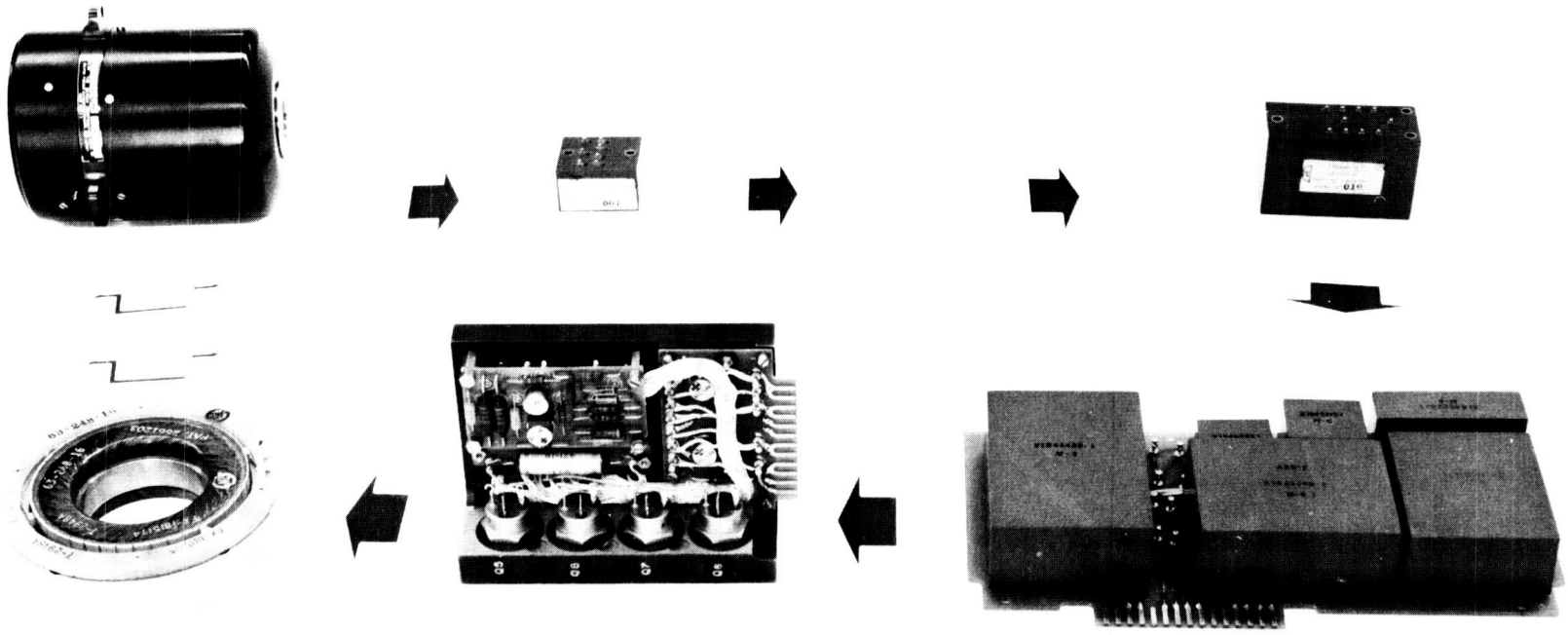

FIGURE 14. SERVOLOOP COMPONENTS.

the gimbals of the platform. The dc signal from the detector output is transferred from the platform to the platform electronics box. The dc signal is shaped by a lag-lead stabilization network, remodulated at 4.8 kHz, amplified, and then demodulated prior to entering the dc power bridge. This dc power bridge provides a current source drive for the direct axis dc gimbal torquer. The 4.8 kHz carrier provides sufficient bandwidth for the servoloop while the current driver for the torquer maintains the gain in the servoloop independent of torquer heating and commutator brush resistance.

The Z servoloop has the Z gyro output signal phase-shaped and amplified and sent to the Z pivot torquer. The X and Y gyro output signals are resolved along the X and Y coordinates of the middle gimbal by a resolver mounted along the minus Z pivot. The outputs of the resolver are amplified and demodulated. The resolved signals are shaped and amplified and fed to their corresponding gimbal pivot dc torquer. No gain compensation such as secant θ_X is used in the outer gimbal servoloop for middle gimbal angle deviation. Figure 14 shows the hardware that comprises a gimbal servoloop.

The three accelerometer servoloops are identical and are similar to the Z gyro servoloop.

The design of each servoloop is based on the single axis block diagram shown in Figure 15. Equation 1 is the closed loop transfer function for the system:

$$\frac{\beta(s)}{T_\alpha(s)} = \frac{\omega_N^2/H}{s^3 + \omega_N^2 s + \omega_N^2/HKG(s)} \quad . \tag{1}$$

The absence of a second order term in the denominator indicates that the system is unstable without compensation; therefore, KG(s) must be synthesized to include the compensation necessary for system stability. Proper compensation has been obtained by the use of frequency response and root locus techniques. Figure 16 is a root locus plot of the open loop poles for G(s) equal to unity. As the gain is increased, the poles move to the right half plane and an unstable condition exists. A pair of complex zeros at a frequency ω_{N_1} (very close to ω_N) would satisfy the second order term requirement. An associated pair of complex poles (necessary with a passive system) is generated with the pair of complex zeros. The optimal location of these poles is one decade to the left of the zeros and along the same constant damping ratio line. The poles cannot be located too far into the left half plane because the further separated the poles and zeros, the more insertion loss associated with the function; hence, more gain is required in the electronics. To increase the zero frequency gain, a lag function $\left(\frac{s + A}{s + B}\right)$ is also added. This dipole is inserted at a low frequency so its effect on the rest of the network is negligible. A schematic diagram of the passive network is shown in Figure 17. The lag function dipole is shown enclosed with dotted lines. The transfer function KG(s) for the compensation network of Figure 17 is

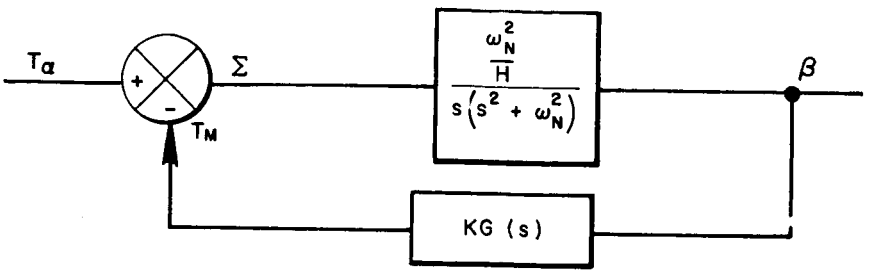

FIGURE 15. GAS BEARING GYROSCOPE STABILIZING SYSTEM.

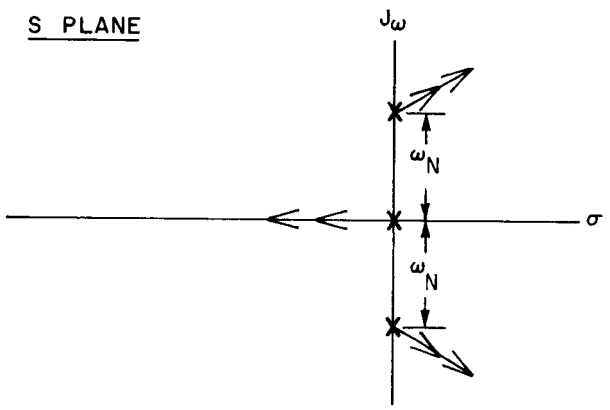

FIGURE 16. ROOT LOCUS OF GAS BEARING GYROSCOPE.

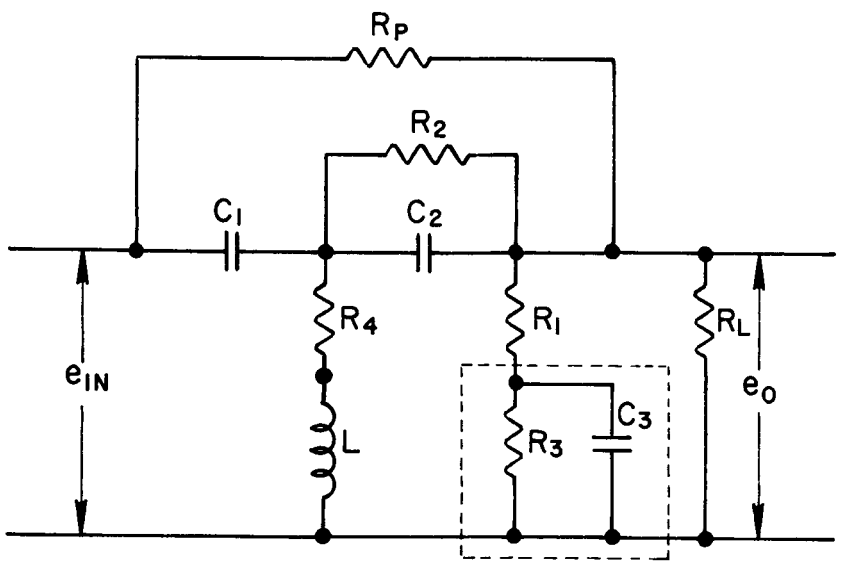

FIGURE 17. COMPENSATION NETWORK SCHEMATIC.

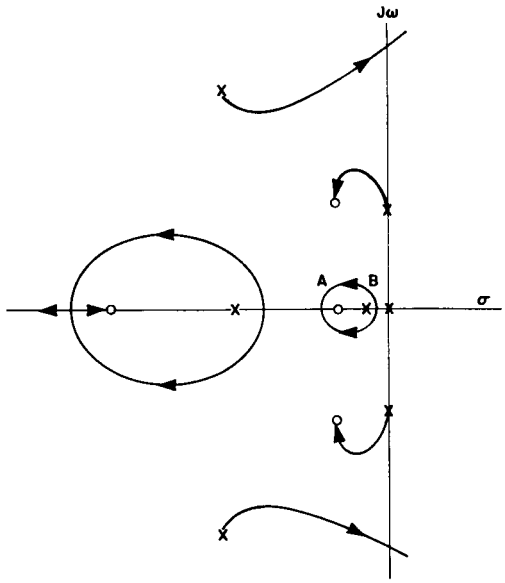

FIGURE 18. ROOT LOCUS OF GAS BEARING GYROSCOPE SERVOLOOP.

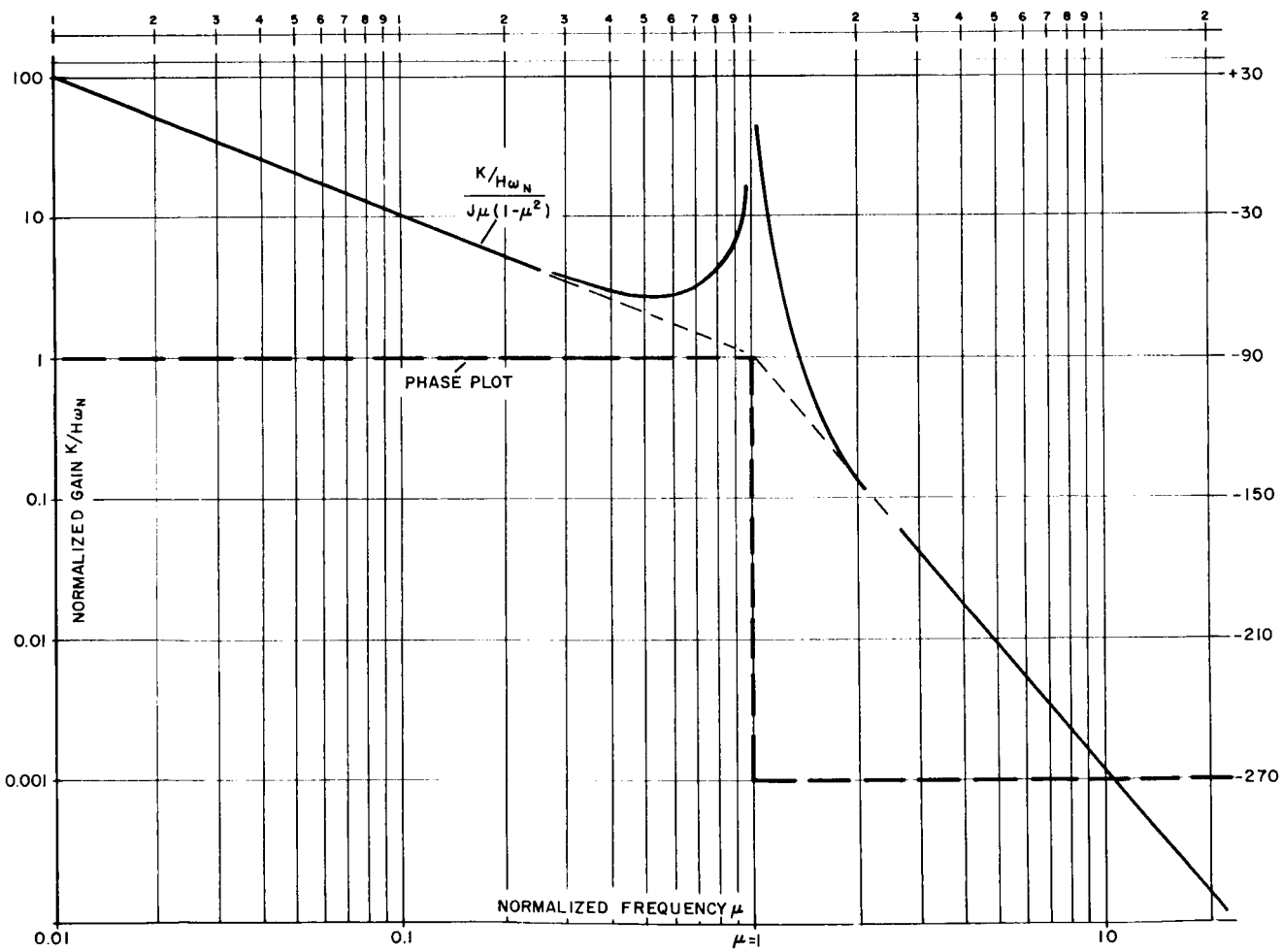

FIGURE 19. FREQUENCY RESPONSE OF GAS BEARING GYROSCOPE.

$$\frac{e_o}{e_{in}} = \frac{(s + A)\ (s + \omega_1)\ (s^2 + 2\zeta_1\omega_{N_1}\, s + \omega_{N_1}^2)}{(s + B)\ (s + \omega_2)\ (s^2 + 2\zeta_2\omega_{N_2}\, s + \omega_{N_2})} \quad . \tag{2}$$

A typical root locus of the servosystem is shown in Figure 18.

The design steps to determine the exact location of the poles and zero are outlined below. A Bode plot of the mechanical portion of the loop gain versus normalized frequency is shown in Figure 19. It can be seen that if gain crossover is located at a frequency higher than $\omega = 1$, the system is unstable since the slope here is 3:1 (60 db/decade), and the phase angle is everywhere equal to -270 degrees. To stabilize this, a minimum phase lead of 90 degrees must be introduced at crossover. To realize a satisfactory transient response, an acceptable phase margin must be attained. A phase lead of 120 degrees is desirable. This is accomplished by inserting the pair of complex zeros such that peak lead will occur at gain crossover. The frequency at which the leading phase is inserted will determine whether the system is conditionally stable. Figure 20, a Nyquist sketch of the system, best shows this characteristic. Curve 1 shows that if a phase lead of 90 degrees is reached at or lower than the mechanical resonance the locus crosses the negative real axis only once. Whereas, if the 90 degree point is reached at a higher frequency (curve 2), the locus crosses the negative real axis twice and the system will be unstable for low gain as well as high gain. It is desirable to raise the loop gain as high as possible; the higher the frequency at which the crossover is made, the greater the gain that can be realized. However, because of a nonlinear effect, the placing of the complex zeros must be held near the natural frequency of the mechanical system.

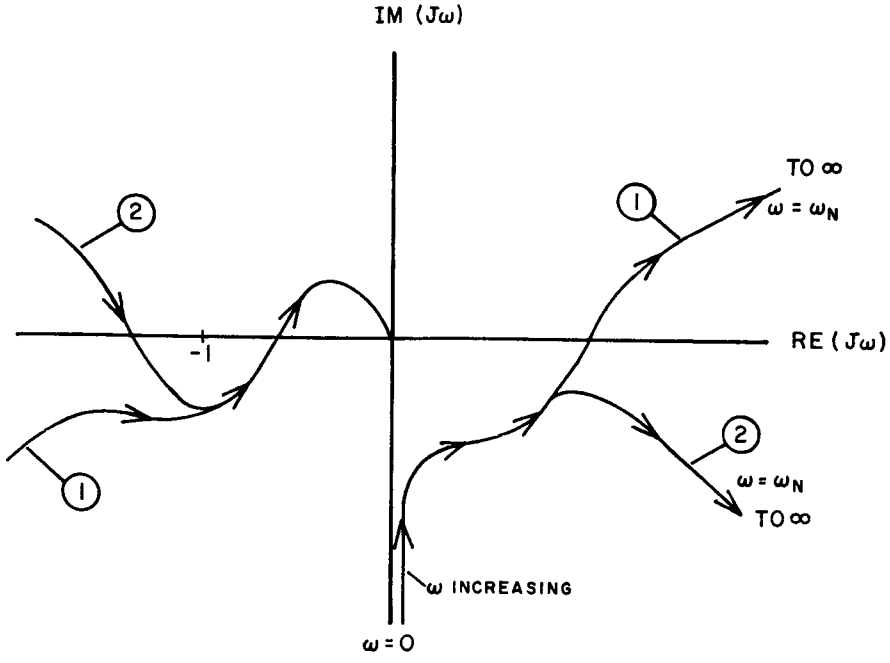

FIGURE 20. SYSTEM NYQUIST SKETCHES.

The network transfer function (equation 2) shows a third pole-zero combination (ω_1 and ω_2) located on the real axis. This combination is set approximately one octave apart with the pole at the lowest frequency. The algebraic mean between the pole and zero is approximately the mean between ω_{N_1} and ω_{N_2} (complete pole-zero pair) at the cross-over frequency. Thus the peak lag, which is introduced, is located at the frequency where the leading phase angle is the greatest. This also flattens the phase curve out and reduces the phase margin; however, it allows more gain in the system by limiting the bandwidth. The effect of this pole pair is shown in the Bode plot in Figure 21.

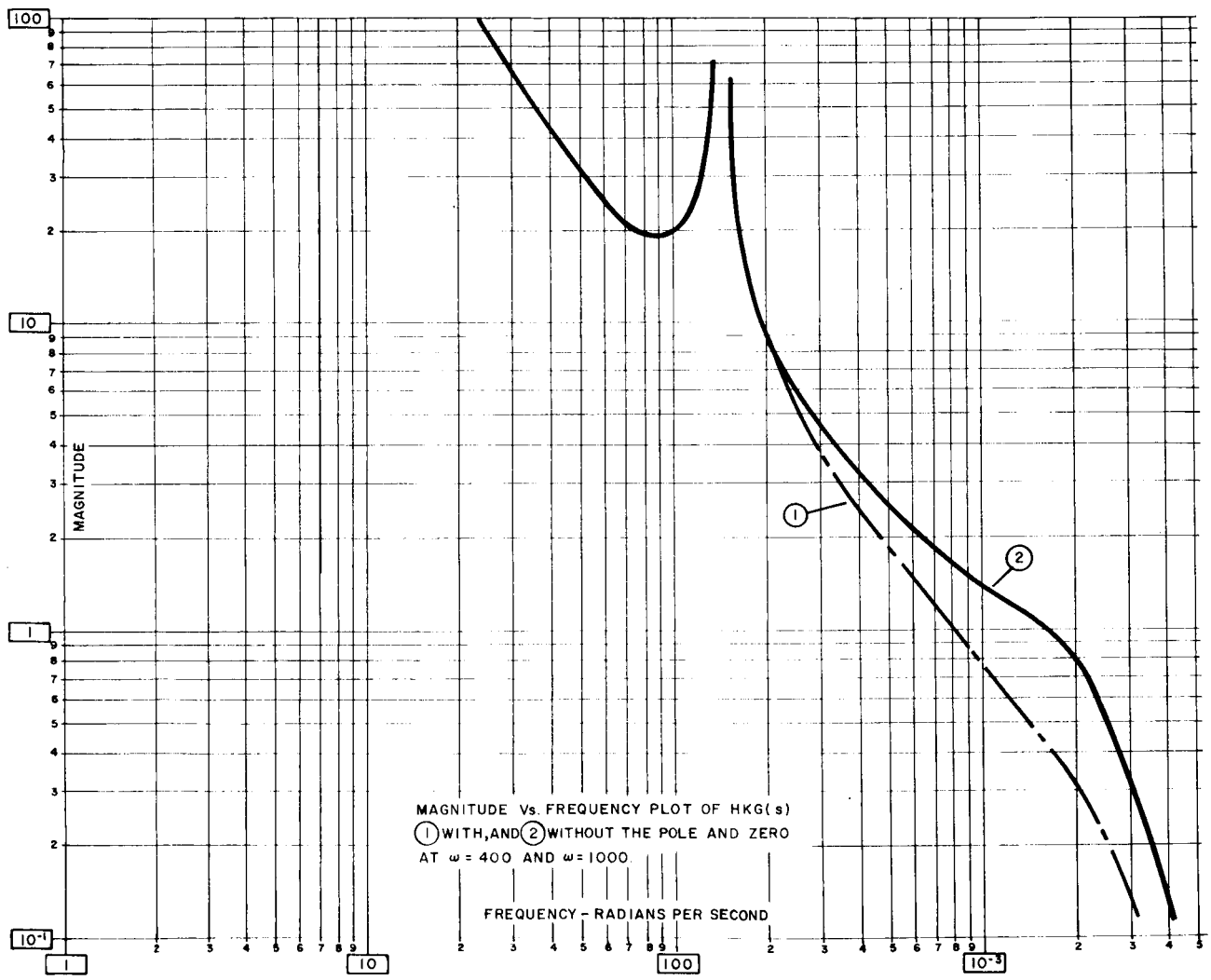

FIGURE 21. FREQUENCY RESPONSE OF GYROSCOPE WITH AND WITHOUT POLE ZERO.

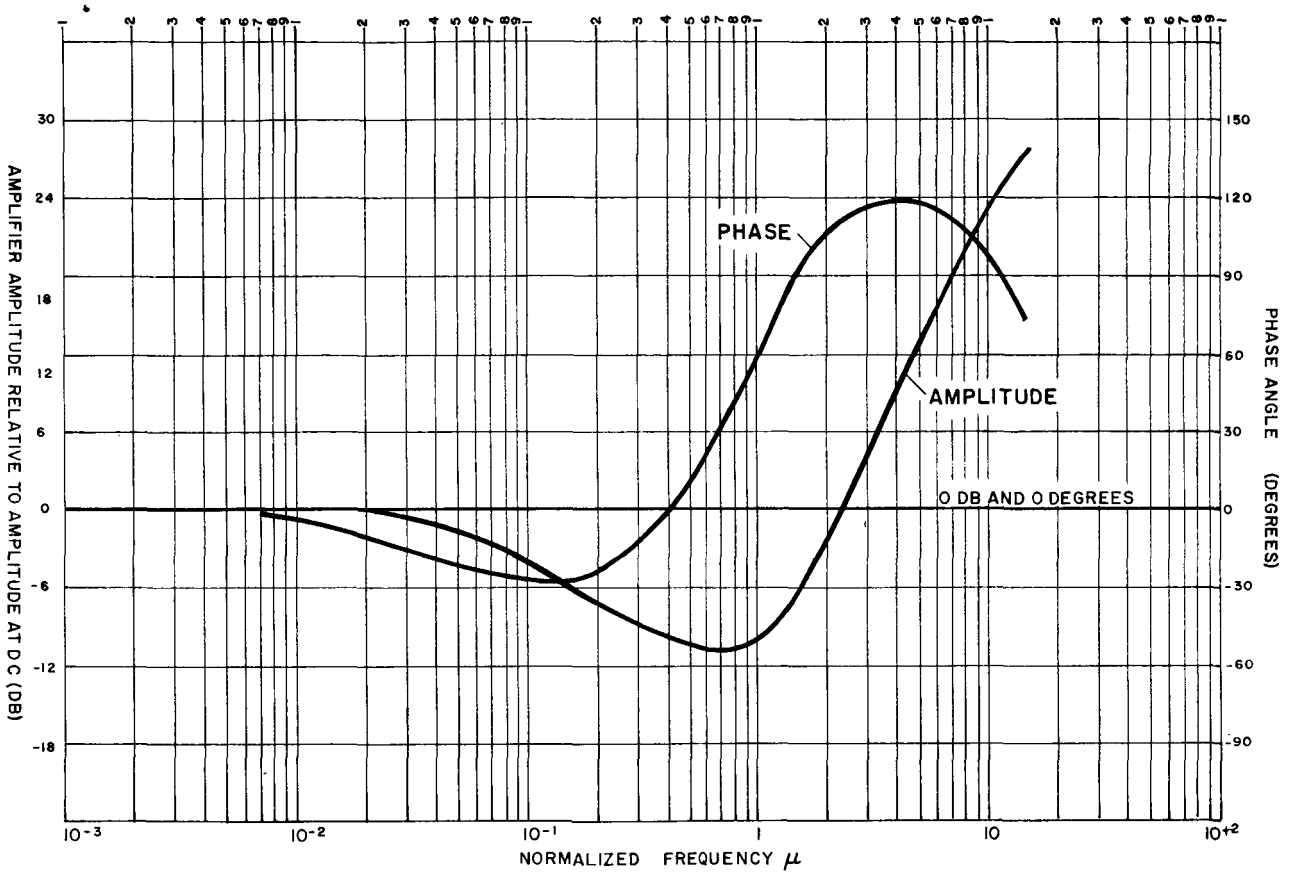

FIGURE 22. ST124-M GYROSCOPE SERVOAMPLIFIER FREQUENCY RESPONSE.

The final phase of the design is the insertion of the lag function dipole to boost the low frequency gain. The location of the dipole is inserted to produce negligible phase lag in the area of crossover; hence, the highest frequency associated with the dipole is at least an order of magnitude below crossover and two octaves below the mechanical resonance frequency. Figure 22 is a frequency response plot of the servoamplifier with the frequency axis normalized. It can be seen that 90 degree lead occurs at $\mu = 1.5$ and the lead network has a bandwidth of 9.5, with a maximum lead angle of 120 degrees at $\mu = 4$. The effect of the lag dipole network is from $\mu = 0.07$ to $\mu = 0.3$. The amplifier gain is minimum in the vicinity of the mechanical resonant frequency $\mu = 0.7$; however, the amplifier is capable of delivering maximum torque at the notch point within the limit stops of the gyro. A complete loop block diagram for the gyro and accelerometer is shown in Figures 23 and 24, respectively.

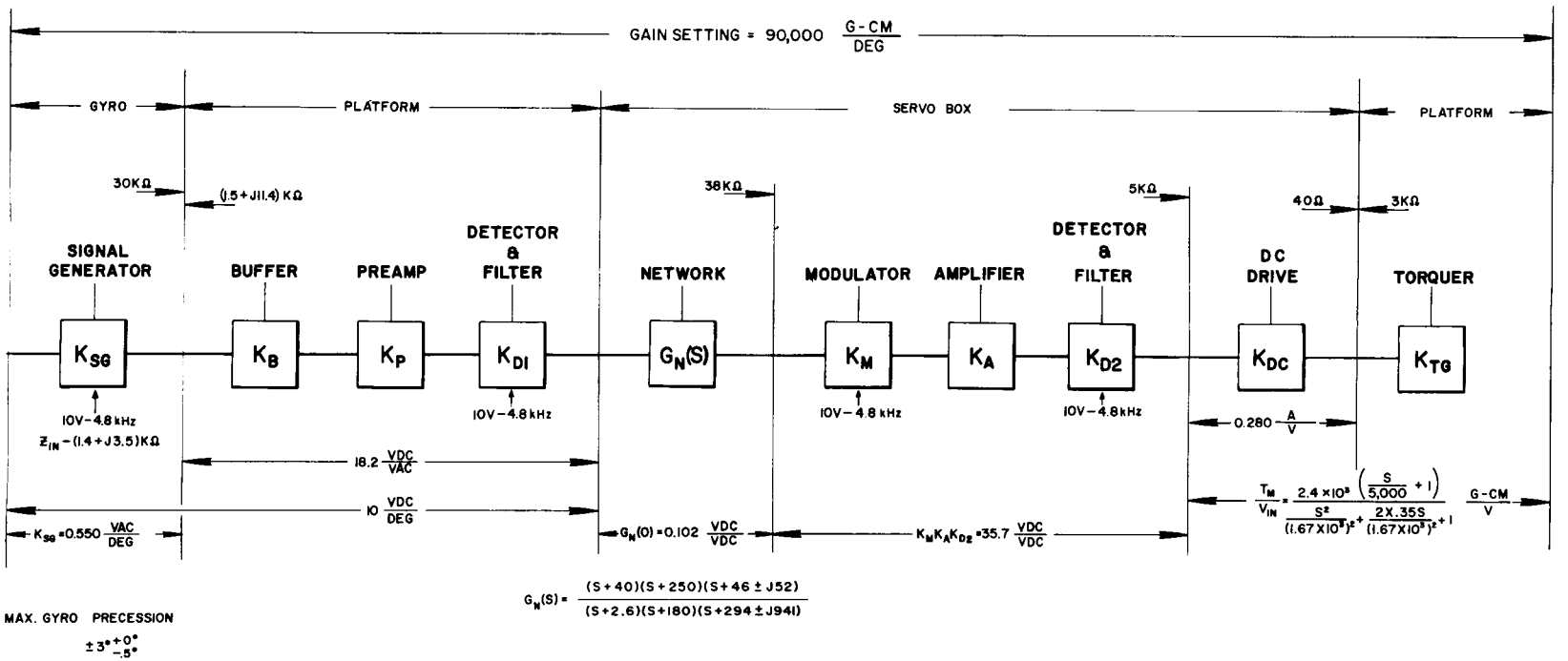

FIGURE 23. BLOCK DIAGRAM OF GIMBAL ELECTRONICS.

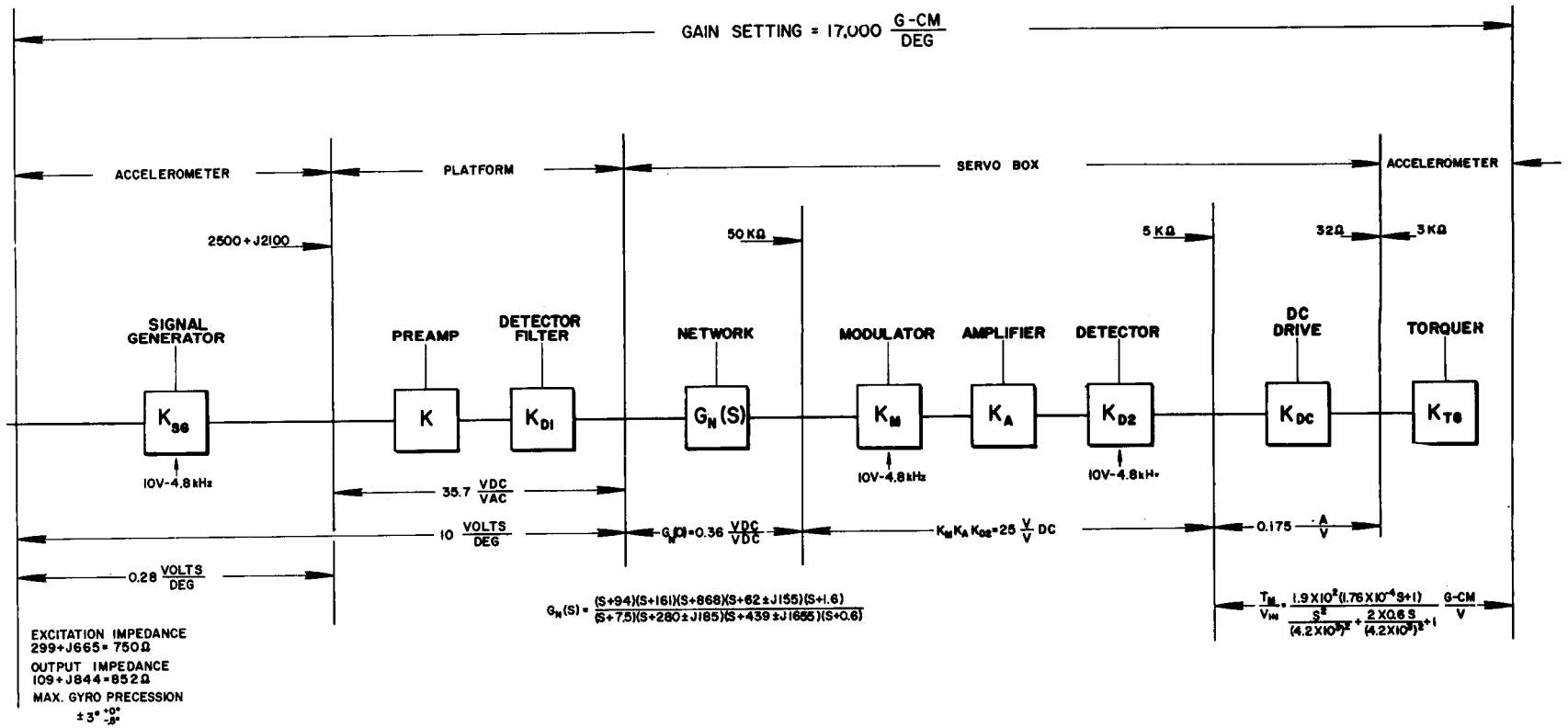

FIGURE 24. BLOCK DIAGRAM OF ACCELEROMETER ELECTRONICS.

SECTION IV. THREE-AXIS SYSTEM EQUATIONS

The previous section analyzed the design of the servosystem based on a single-axis system. The analysis ignored the effects of mechanical and electromechanical interaxis coupling. Applying Euler's equation in a single-axis gyro, the following equations can be formulated. Refer to Figure 25 for a definition of the gyro coordinate system.

$$T_\alpha - T_m = J_\alpha \frac{d^2\alpha}{dt^2} + H \frac{d\beta}{dt}$$

$$T_\beta = J_\beta \frac{d^2\beta}{dt^2} - H \frac{d\alpha}{dt} + D \frac{d\beta}{dt} + K\beta. \tag{3}$$

Laplace transformation of equation 3 gives

$$T_\alpha(s) - T_m(s) = J_\alpha s^2 \alpha(s) + Hs\beta(s)$$

$$T_\beta(s) = J_\beta s^2 \beta(s) + Ds\beta(s) + K\beta(s) - Hs\alpha(s). \tag{4}$$

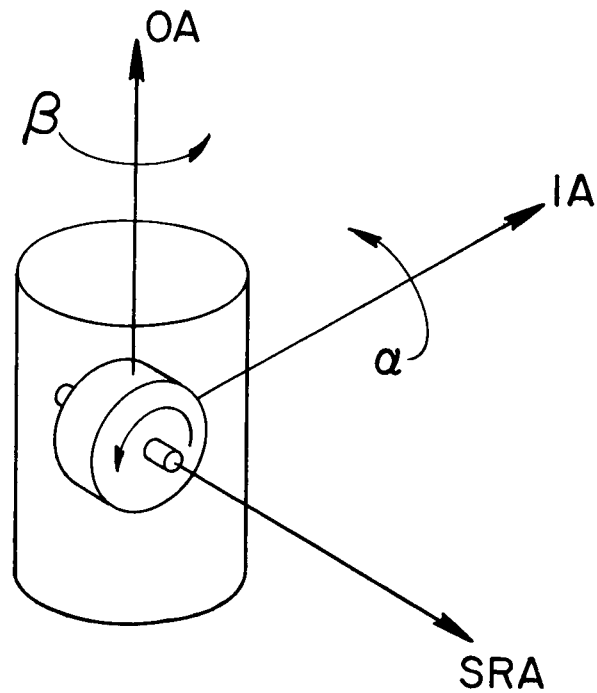

FIGURE 25. GYRO COORDINATE SYSTEM.

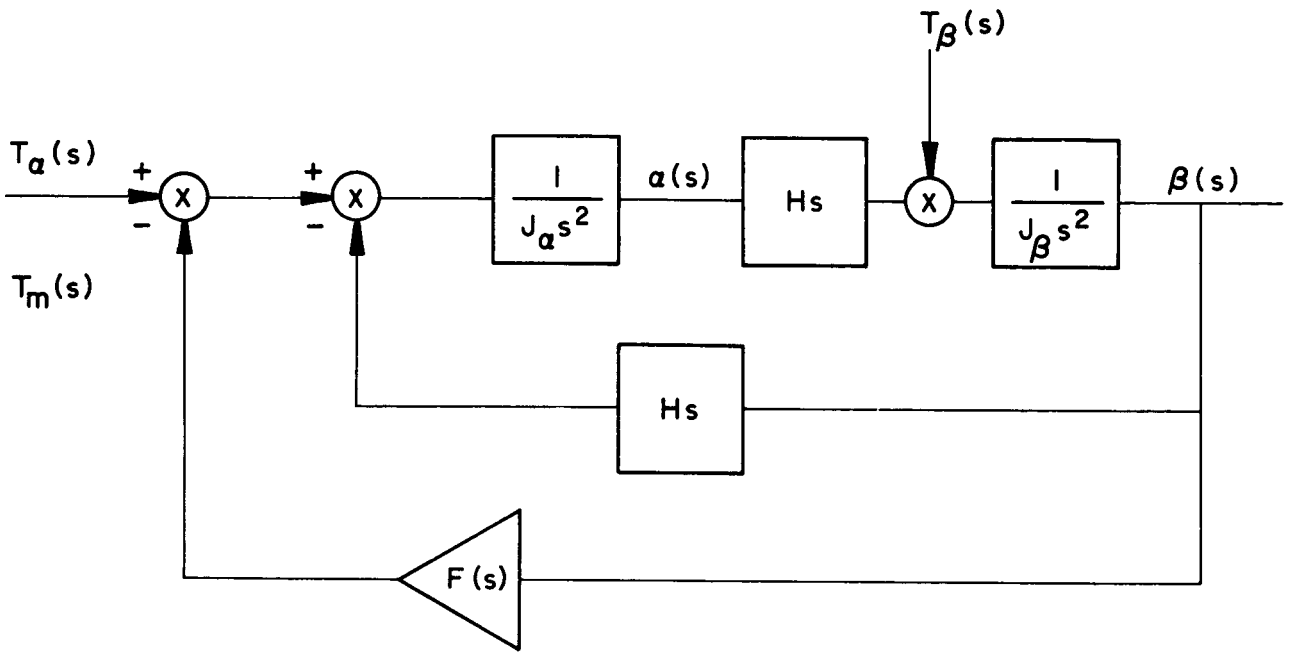

FIGURE 26. SINGLE-AXIS GYRO BLOCK DIAGRAM.

Since the damping constant D and spring constant K are very small in a gas bearing, their influence has little effect on the dynamics of the system and will be dropped. Thus the single-axis element described will be an integrating gyro. The block diagram for the single-axis gyroscope using equation 4 is shown in Figure 26. Assuming $T_\beta(s) = 0$, the transfer functions relating input torque to precession motion and to gyro input motion are

$$\frac{T_\alpha(s)}{\beta(s)} = \left(F(s) + Hs + \frac{J_\alpha J_\beta s^3}{H} \right)$$

and (5)

$$\frac{T_\alpha(s)}{\alpha(s)} = \frac{H}{J_\beta s} \left(F(s) + Hs + \frac{J_\alpha J_\beta s^3}{H} \right).$$

Note that $\frac{T_\alpha(s)}{\beta(s)}$ is $\frac{T_\alpha(s)}{\alpha(s)}$ multiplied by the gyroscope transfer function.

$$\frac{\beta(s)}{\alpha(s)} = \frac{H}{J_\beta s}. \tag{6}$$

The principal function of the servosystem is to maintain α near 0 in the presence of various disturbances. A logical measure of system performance is the ratio $\frac{T_\alpha}{\alpha}$ which describes the maximum angular deviation for specified inputs. For instrumentation reasons, $\frac{T_\alpha}{\beta}$ is used because α is very small for frequencies below ten times the resonant frequency. The angular motion β resulting from α is normally a much larger signal by the multiplication factor $\frac{H}{J_\beta s}$ (the gyro transfer function) and is easily measured at the input to the servoamplifier, $F(s)$. In system design, the ratio $\frac{T_\alpha}{\beta}$ is made as large as possible to be consistent with good transient response.

The single-axis approach to the design of the servosystem is expedient, but it ignores the effect of mechanical and electromechanical interaxis coupling. Mechanical interaxis coupling will occur if the principal axes of the inertial gimbal do not coincide with the input axes of the gyroscopes. Also, products of angular motion will occur if the moments of inertia are unequal. Fortunately, in the design and fabrication of the inertial gimbal, close tolerance controls make these effects negligible relative to other interaxis coupling.

The output signal β of the single-axis gyro is a measure of the angle between the gyro float and the gyro case. This is the signal used in the platform servoloop. Because the gyro case is mounted to the inertial gimbal, disturbances about its output axis are reflected into other servoloops. Therefore, motions of the gyro case about its output axis are coupled into the servoloop for that gyro.

The effect of servostability of this pickoff coupling depends on the orientation of the gyros on the platform. A multiplicity of possible gyro orientations exists for a platform, but it is not possible to orient three single-axis gyros with mutually orthogonal input axes in such a way that there is not at least one closed loop of gyro pickoff interaxis coupling. Additional considerations for orientation of the gyros on the inertial gimbal must be made. These include the coning or rectification drift and the unequal elasticity (anisoelasticity) in the gyro spin axis and input axis which give rise to a steady state drift rate. The effect of gyro orientation is a function of the direction of applied linear acceleration or vibration and varies sinusoidally as the acceleration vector is rotated about the gyro's output axis.

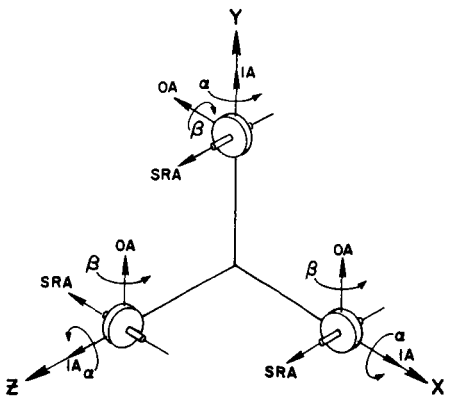

FIGURE 27. ST124-M PLATFORM GYRO COORDINATE DEFINITION.

Figure 27 is a sketch of the ST124-M gyro orientation. The inertial gimbal is gimbal-mounted for three degrees of freedom relative to the vehicle about the three mutually-perpendicular axes identified as α_x, α_y, and α_z. The gyroscopes are represented by mutually-perpendicular vectors which define the angular momentum H, the input angular motion α, and the output motion β. The gyroscopes are identified with their particular platform axes. Platform angular motion about the input axis of the Y gyro is coupled into the pickoff of the X and Z gyros, and angular motion about the input axis of the X gyro is coupled into the pickoff of the Y gyro.

The actual pickoff signals that are fed to the amplifier can be expressed as:

$$\sigma_x = \beta_x + \alpha_y \qquad \sigma_y = \beta_y - \alpha_x \qquad \sigma_z = \beta_z + \alpha_y \,. \tag{7}$$

The three axis servosystem block diagram shown in Figure 28 illustrates this coupling through the gyro output axes. The platform motion about the Y axis is coupled into the Z axis servo but does not feed back into either of the other two gyro servoloops. Therefore, the Z axis servo will be disturbed by motion of the Y axis but no stability problem results. There is coupling of the input angles α_x and α_y to the output motions β_y and β_x, respectively. Therefore, a closed loop is formed which, in addition to causing cross axis disturbances, must also be considered as to its effect on servo performance. A resolver (α_z) provides continuous coupling between the inertial components and the gimbal about which compensating servotorques are applied. This effect is shown by the sinusoidal coupling between the X and Y axes.

Essentially, the basic single-axis characteristic, as defined with equation 3 and Figure 26, is retained in the three-axis system. The important difference is that

$$T_m(s) = \sigma F(s). \tag{8}$$

Therefore, substituting equations 7 and 8 into the single axis expression of equation 3 and assuming all three gyros have the same inertia and momentum characteristics will yield a series of expressions defining the three-axis system.

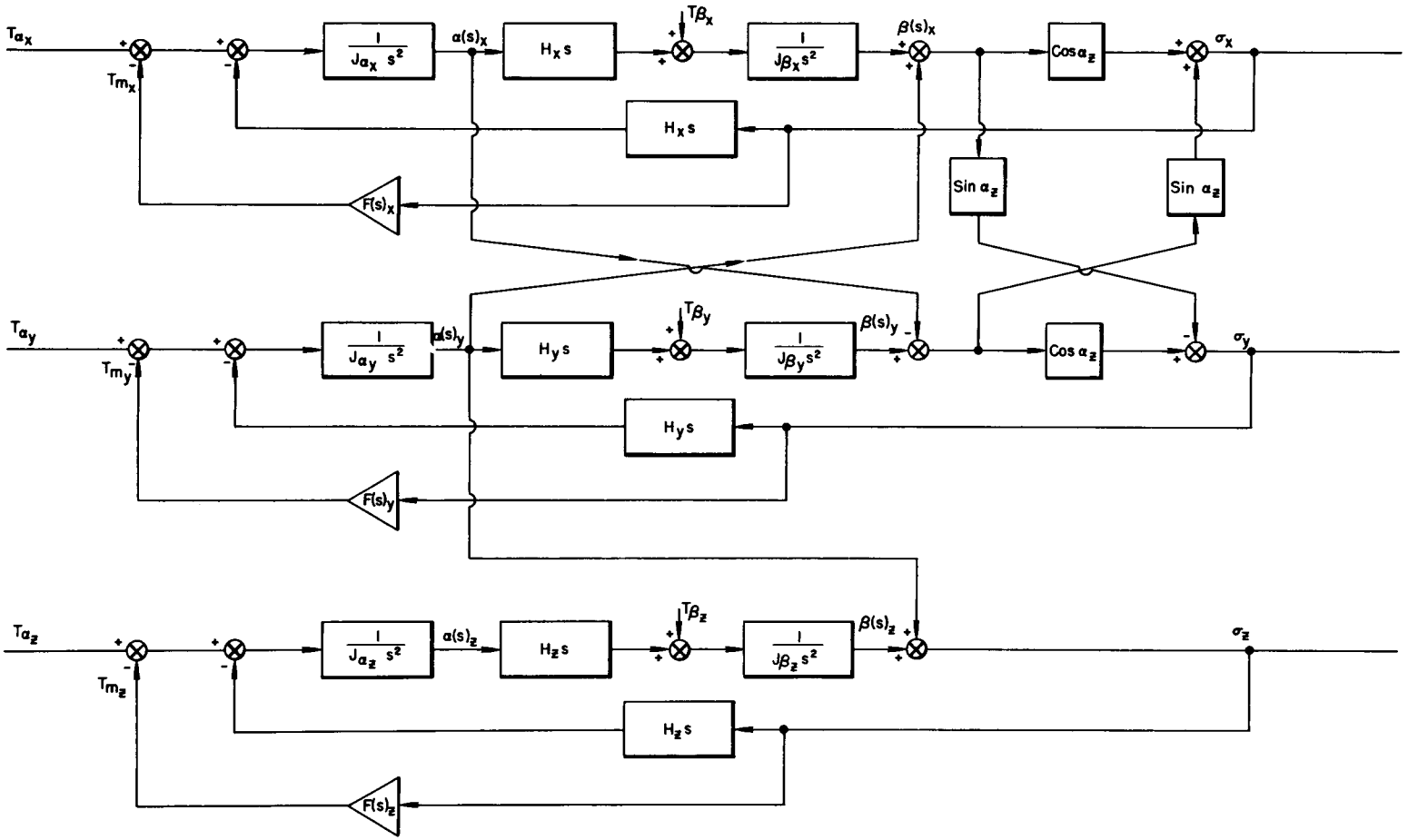

FIGURE 28. BLOCK DIAGRAM OF THREE-AXIS STABILIZED PLATFORM.

$$\begin{bmatrix} T_{\alpha_x} \\ T_{\alpha_y} \\ T_{\alpha_z} \end{bmatrix} = \begin{bmatrix} \frac{J_\alpha J_\beta s^3}{H_x} + H_x s + F(s)_x & (H_x s + F(s)_x)\frac{J_\beta s}{H} & 0 \\ -(H_y s + F(s)_y)\frac{J_\beta s}{H_y} & \frac{J_\alpha J_\beta s^3}{H_y} + H_y s + F(s)_y & 0 \\ 0 & (H_z s + F(s)_z)\frac{J_\beta s}{H_z} & \frac{J_\alpha J_\beta s^3}{H_z} + H_z s + F(s)_z \end{bmatrix} \begin{bmatrix} \beta_x \\ \beta_y \\ \beta_z \end{bmatrix} \quad (9)$$

The main diagonal contains the single axis terms. Other nonzero terms in the determinant are caused by cross coupling. Multiplying all the expressions in the determinant by the gyro transfer function expresses equation 9 in terms of the input angle α and yields the following set of equations:

$$\begin{bmatrix} T_{\alpha_x} \\ T_{\alpha_y} \\ T_{\alpha_z} \end{bmatrix} = \begin{bmatrix} J_{\alpha_x} s^2 + \frac{H_x^2}{J_{\beta_x}} + \frac{H_x}{J_{\beta_x} s} F_x & H_x s + F_x & 0 \\ -(H_y s + F_y) & J_{\alpha_y} s^2 + \frac{H_y^2}{J_{\beta_y}} + \frac{H_y}{J_{\beta_y} s} & 0 \\ 0 & H_z s + F_z & J_{\alpha_z} s^2 + \frac{H_y^2}{J_{\beta_z}} + \frac{H_z}{J_{\beta_z} s} F_z \end{bmatrix} \begin{bmatrix} \alpha_x \\ \alpha_y \\ \alpha_z \end{bmatrix} \quad (10)$$

The main diagonal of equation 10 now contains the single axis terms with the loops defined in terms of input disturbing torque to input angle. This equation can be modified for ease in handling by letting:

$$\gamma_x = \left[J_{\alpha_x} s^2 + \frac{H_x^2}{J_{\beta_x}} + \frac{H_x}{J_{\beta_x} s} F_x \right] \frac{1}{F_x} = \frac{H_x}{J_\beta s} \frac{T_{\alpha_x}}{T_{m_x}}$$

$$m_x = \pm \left[H_x s + F_x \right] \frac{1}{F_x} . \quad (11)$$

Equation 10 can be made applicable for all spin directions by the appropriate sign for the cross coupling terms. Note the simple relation of γ to the inverse torque function and the gyro transfer function. This relation simplifies the three-axis analysis. Substitution of equation 11 into equation 10 yields the following series of equations:

$$\begin{bmatrix} \frac{T_{\alpha_x}}{F_x} \\ \frac{T_{\alpha_y}}{F_y} \\ \frac{T_{\alpha_z}}{F_z} \end{bmatrix} = \begin{bmatrix} \gamma_x & m_x & 0 \\ -m_y & \gamma_y & 0 \\ 0 & m_z & \gamma_z \end{bmatrix} \begin{bmatrix} \alpha_x \\ \alpha_y \\ \alpha_z \end{bmatrix}. \tag{12}$$

The determinant or characteristic function is

$$\Delta = \gamma_x \gamma_y \gamma_z + \gamma_z m_x m_y. \tag{13}$$

The zeros of the determinant Δ determine the stability of the three-axis system. The difficulty of analysis is apparent from the fact that γ varies for each axis independent of the others since the inertias J_α cannot feasibly all be equal.

Solving equation 12 in terms of the input function yields a series of equations:

$$\begin{bmatrix} \alpha_x \\ \alpha_y \\ \alpha_z \end{bmatrix} = \begin{bmatrix} \frac{\gamma_y \gamma_z}{F_x} \frac{1}{\Delta} & \frac{-m_x \gamma_x}{F_y} \frac{1}{\Delta} & 0 \\ \frac{m_y \gamma_z}{F_x} \frac{1}{\Delta} & \frac{\gamma_x \gamma_z}{F_y} \frac{1}{\Delta} & 0 \\ \frac{-m_y m_z}{F_x} \frac{1}{\Delta} & \frac{-m_z \gamma_x}{F_y} \frac{1}{\Delta} & \frac{1}{F_z \gamma_z \Delta} \end{bmatrix} \begin{bmatrix} T_{\alpha_x} \\ T_{\alpha_y} \\ T_{\alpha_z} \end{bmatrix}. \tag{14}$$

These equations illustrate that platform motion about one axis can be caused by torque about another axis. To solve this equation in terms of the gyro output axis, simply multiply by the gyro transfer function.

SECTION V. GIMBAL ANGLE MULTISPEED RESOLVERS

As shown in Figure 29, the plus X, Y, and Z gimbal pivots have multispeed analog resolvers for angular readouts. The phase shift of their output voltage is measured by digital techniques. A schematic block diagram is shown in Figure 30. The dual resolver provides the demanded high readout accuracy. The digital computer system processes the measured gimbal attitude signals and computes the pitch, roll, and yaw vehicle body rates for the attitude control system.

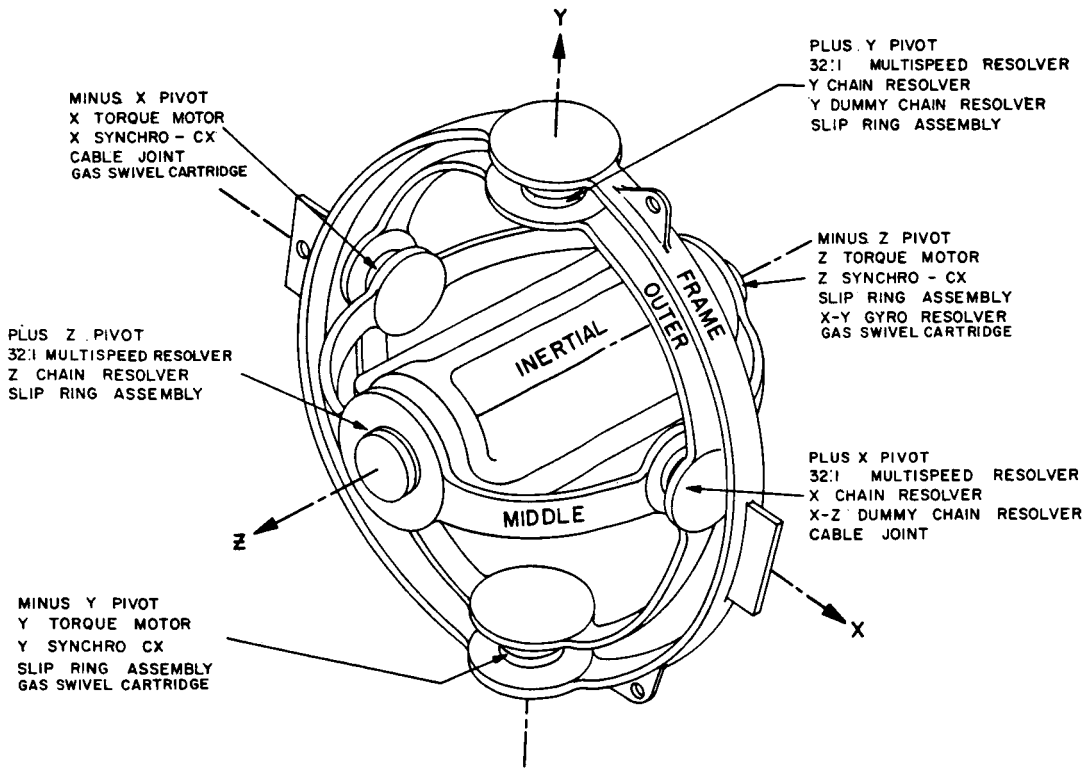

FIGURE 29. THREE GIMBAL CONFIGURATION.

The dual resolver has both a 32-speed and a single-speed winding on the same magnetic structure. The 32-speed winding has 32 electrical rotations for one mechanical shaft rotation. The reference or the resolver excitation (V_1) is 26 volts, 1016 Hz. The output winding drives an RC bridge network as shown in Figure 30.

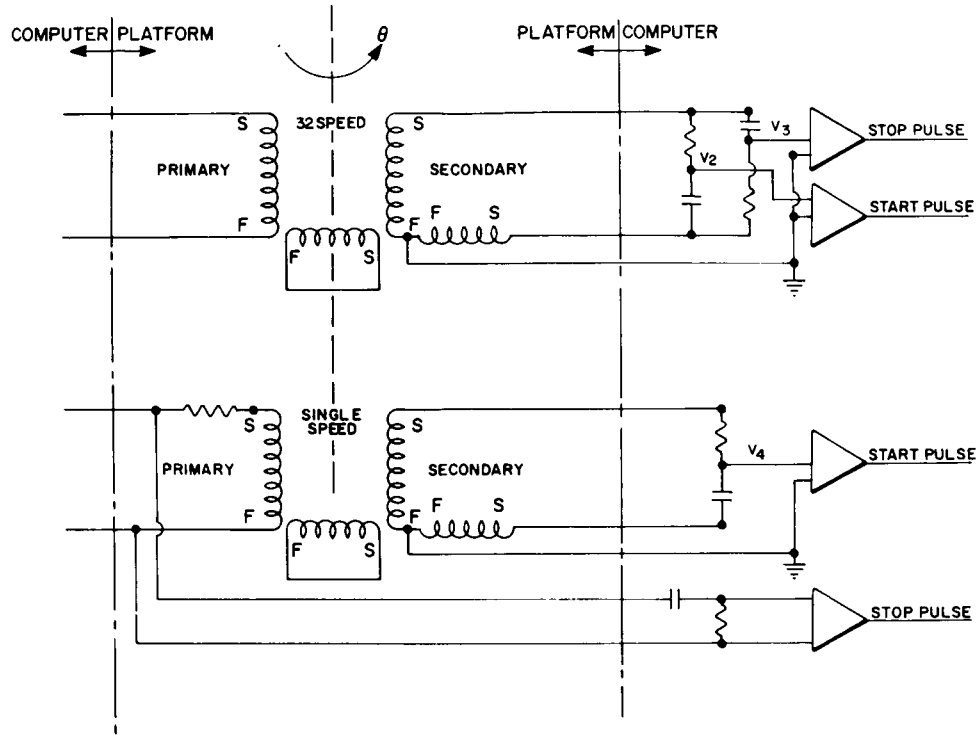

FIGURE 30. TWO-SPEED RESOLVER SCHEMATIC.

The voltage V_2 at the input to the start pulse generator can be expressed as

$$V_2 = \frac{E}{\sqrt{2}} e^{j(32\theta - \pi/4)}$$

and the voltage V_3 at the input to the stop pulse generator can be expressed as

$$V_3 = \frac{E}{\sqrt{2}} e^{-j(32\theta - \pi/4)}$$

where E is the open circuit resolver voltage and θ is the rotation or mechanical angle in radians.

From the ratio of $\frac{V_2}{V_3} = e^{j(64\theta - \pi/2)}$, it is seen that the phase shift of V_2 with respect to V_3 is 64 times the angle θ or a multiplication by a factor of two occurs in the bridge network.

As the instantaneous voltage V_2 passes through zero with a positive slope, a start pulse is generated which opens a gate; a counter counts a 2.048 MHz clock frequency. As V_3 passes through zero with a positive slope, a stop pulse is generated which closes the gate and stops the counter. The number of cycles counted is a measure of the gimbal angle. (Refer to the vector diagram in Figure 31).

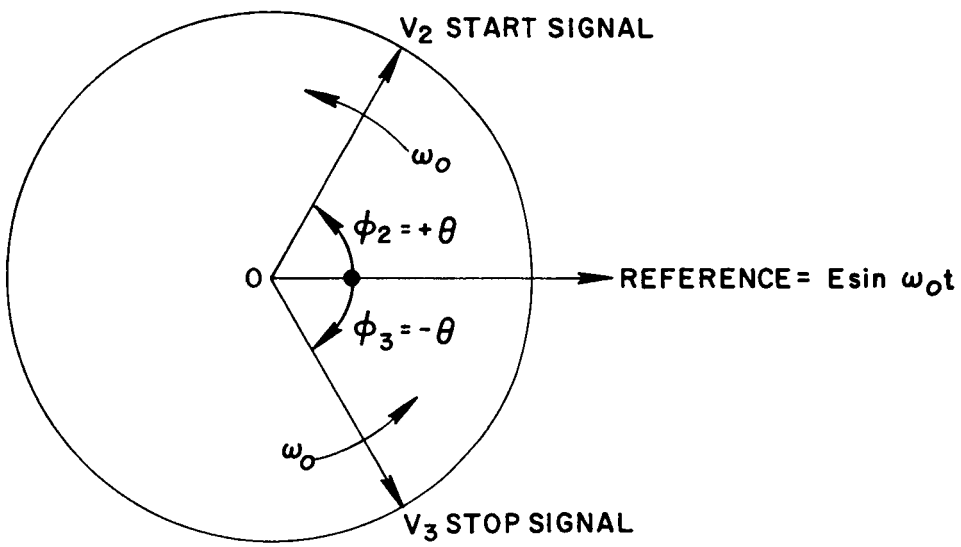

FIGURE 31. PHASE CLOCK VECTOR DIAGRAM.

The single-speed winding uses a single RC passive network which generates a start pulse; the stop pulse is obtained from the reference voltage to the resolver primary as shown in Figure 30. The method of counting is the same for the high-speed windings. This information is utilized only if the multispeed winding is lost. Thus, degraded accuracy occurs rather than complete failure.

The computer system provides two reference sources, one for the multispeed winding and one for the single-speed winding. These references are controlled by the same frequency standard to insure that the gimbal angle measurement will not be lost if one reference source fails.

The multispeed system accuracy is basically insensitive to temperature variation of the resolver as well as impedance unbalance in the output windings. The open circuit voltage of the resolver is the basic reference voltage as shown in the equations.

The resolver and performance characteristics of the angular readouts are:

		32-Speed	Single-Speed
1.	Resolver Characteristics		
a.	Excitation voltage	26 V ±5%	26 V ±5%
b.	Harmonic content of excitation	0.1%	0.1%
c.	Excitation frequency	1016 Hz ±0.01%	1016 Hz ±0.01%
d.	Excitation power	1.8 W	0.08 W
e.	Mechanical accuracy	±10 arc sec	±30 arc min
f.	Secondary voltage maximum (open circuit)	5.0 V	5.0 V

2. System Characteristics

   a. System high speed - 64:1

   b. System low speed - 1:1

   c. Static accuracy - ±30 arc second

   d. Dynamic accuracy (error is proportional to input rate) - 20 arc sec at 0.2 rad/second.

   e. Computer clock frequency - 2.048 MHz ±0.01%

   f. Temperature range for optimum accuracy - ±30° C.

The ST124-M system also contains an analog resolver chain system which can provide vehicle pitch, roll, and yaw attitude steering signals directly to the control system. This is a backup system and is not planned as flight equipment. The capabilities will be utilized in the ground checkout system to program the platform gimbals for vehicle control system calibration.

The resolver chain system includes three servo driven resolvers whose shafts are time programed from the ground computer with a maximum rate of 2 degrees per second; operational rate is 1 degree per second. These units are located in the inertial data box.

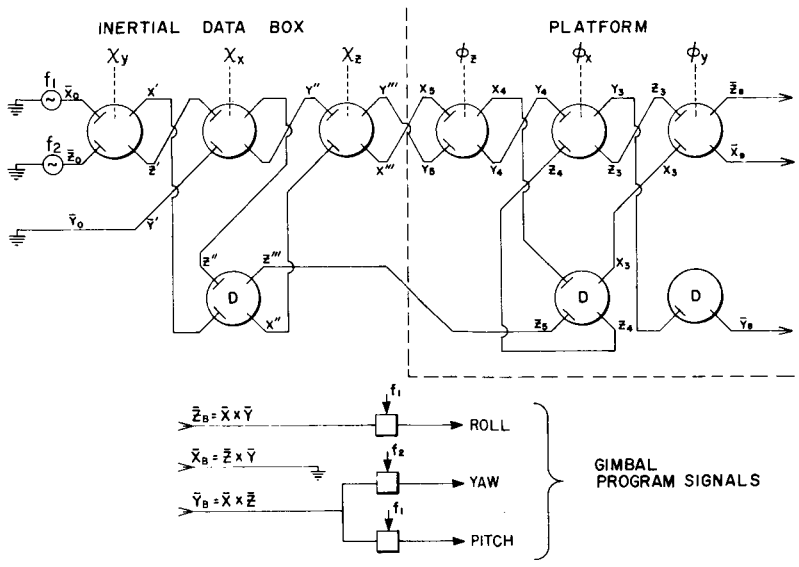

FIGURE 32. RESOLVER CHAIN ST124-M3

The resolver chain schematic is shown in Figure 32. The resolvers χ_y, χ_x, and χ_z are the time programed units. The characteristics of the resolver chain system are:

1. Excitation

   a. f_1 - 26 V, 1.6 kHz

   b. f_2 - 26 V, 1.92 kHz

2. Demodulator Output

   a. To control computer - 3 V dc/degree of arc

   b. To telemetry (fine) - ±2.5 V dc/±3°
      (coarse) - ±2.5 V dc/±15°

   c. Linear range - ±15 degrees

The resolver chain performs coordinate transformation computations. From Figure 32, it can be seen that the resolver chain provides six transformation matrices. With proper detection, two chain references (f_1 and f_2) allow vehicle roll, yaw, and pitch signals to be detected from the transformation matrices. The 1.6 kHz signal on the $\overline{Z}_B$ winding and the 1.6 kHz signal on the $\overline{Y}_B$ at the output of the resolver chain provide the roll and pitch rates, respectively. The 1.92 kHz signal on the $\overline{Y}_B$ winding provides the yaw rate. If redundant steering signals were required, a third reference (f_3) could be inserted at $\overline{Y}'$ and the detection system would provide an additional roll, yaw, and pitch signal at $\overline{X}_B$ and $\overline{Z}_B$.

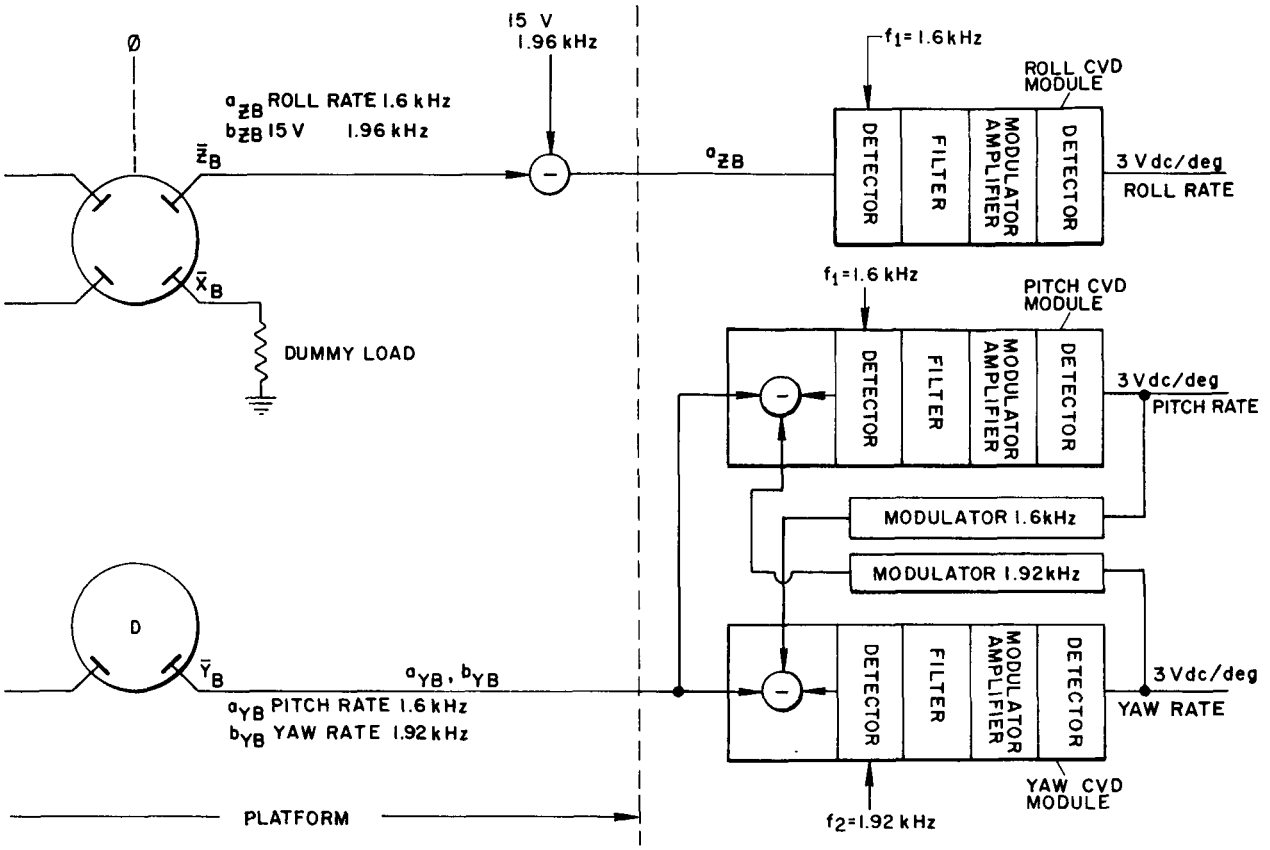

FIGURE 33. BLOCK DIAGRAM OF RESOLVER CHAIN OUTPUT.

The detection scheme for the resolver chain is shown in Figure 33. When the vehicle coordinate system is aligned to the navigational coordinate system, the $\overline{Z}_B$ winding will have a standing voltage of 15 volts, 1.92 kHz, which is in phase with vector $\overline{Z}_O$. This bias voltage is removed by a bucking voltage obtained from $\overline{Z}_O$ (f_2). The signals are filtered and, by means of signal bucking, detection filtering, modulation amplification, and redetection, are separated as shown in Figure 33. The output signals are dc with a scale factor of 3 volts per degree. The 3-sigma accuracy of the resolver chain is 6 arc minutes over a complete cycle.

SECTION VI. PLATFORM ELECTRONICS ASSEMBLY

The platform electronics assembly contains the electronics, other than those located in the platform assembly, required for the platform axis and accelerometer stabilization. Switching electronics for controlling platform system power and checkout functions are also located in the platform electronics assembly. The electronics are printed circuit, modular constructed, and are fitted into the box with an electrical connector for ease of assembly and maintenance.

Components or modules requiring pressurization are protected by epoxy encapsulation. Internal heat sources are heat-sinked to the main casting; heat is removed by conduction into the temperature controlled mounting panels of the Instrument Unit. For system evaluation, critical control signals are conditioned in the platform electronics assembly and supplied to telemetry.

The platform electronics assembly is a cast magnesium structure and is mounted to the vehicle frame with pads that extend out from the box structure. The box has a light-gauge sheetmetal cover and is gasket-sealed and pressurized to 1.7 N/cm^2d (2 psid). The box contains a cast magnesium deck for mounting electronic components and a grooved rack for mounting printed circuit modules. The assembly weighs 19 kg (42 lb).

A gyro servoamplifier card is shown in Figure 34; the torquer power stage is shown in Figure 35. Figure 36 is a view of the platform electronics assembly.

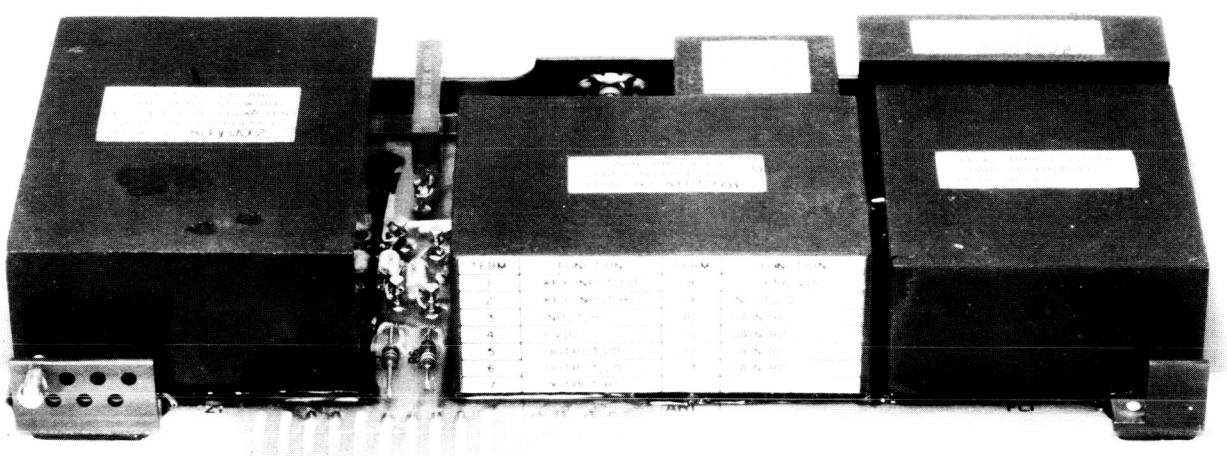

FIGURE 34. SERVOAMPLIFIER VOLTAGE STAGES.

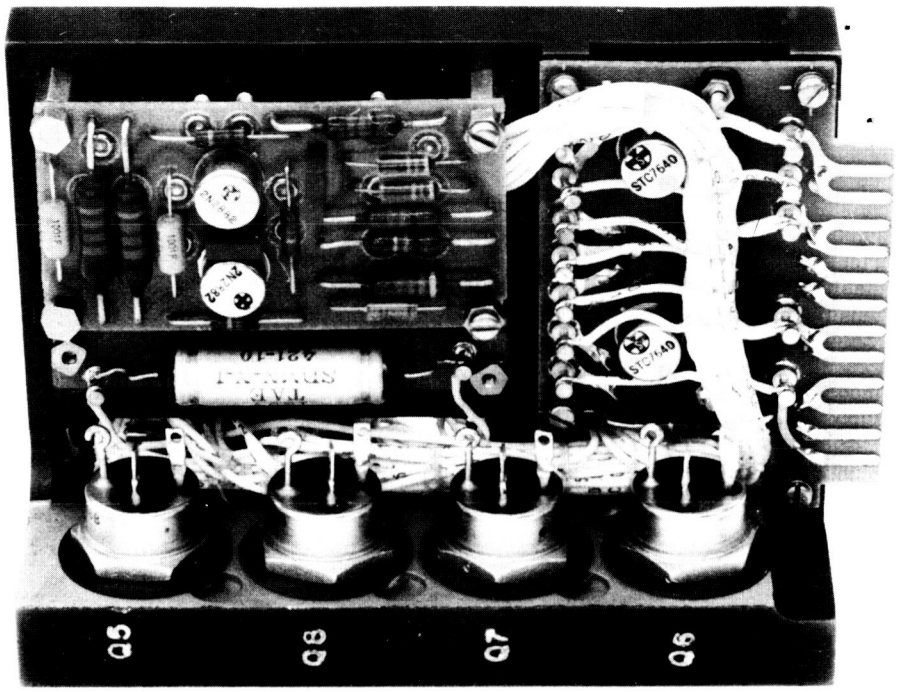

FIGURE 35. SERVOAMPLIFIER POWER STAGE.

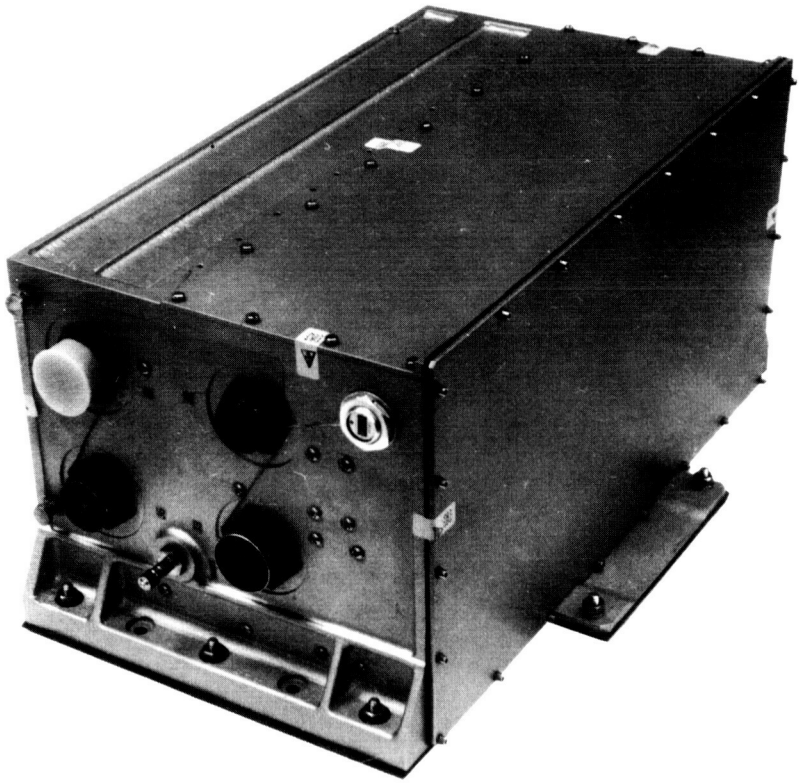

FIGURE 36. PLATFORM ELECTRONIC ASSEMBLY.

SECTION VII. PLATFORM AC POWER SUPPLY ASSEMBLY

The platform ac power supply assembly furnishes the power required to run the gyro wheels, the excitation for the platform gimbal synchros, the frequency sources for the resolver chain references, and the frequency reference for the gyro and accelerometer servosystems carrier. It is a solid-state-regulated three-phase ac power supply, capable of supplying up to 250 VA continuously. With an input voltage from 25 to 30 V dc, it produces a three-phase sine wave output, which is fixed at 26 volts (rms) line-to-line, at a fixed frequency of 400 ±0.01 Hz. Three single-phase 20-volt reference-square-wave outputs of 4.8 kHz, 1.92 kHz, and 1.6 kHz are also provided (Fig. 37).

The oscillator generates a temperature-stable square wave of 19.2 kHz derived by frequency division from a quartz crystal oscillator. This 19.2 kHz square wave is the frequency source from which all the frequency outputs are derived.

The frequency divider network, referenced with the 19.2 kHz square wave, produces two buffered 4.8 kHz square waves. One 4.8 kHz wave becomes the "clock pulse" for the cycle register; the other feeds the regulator-driven amplifier. In addition, the

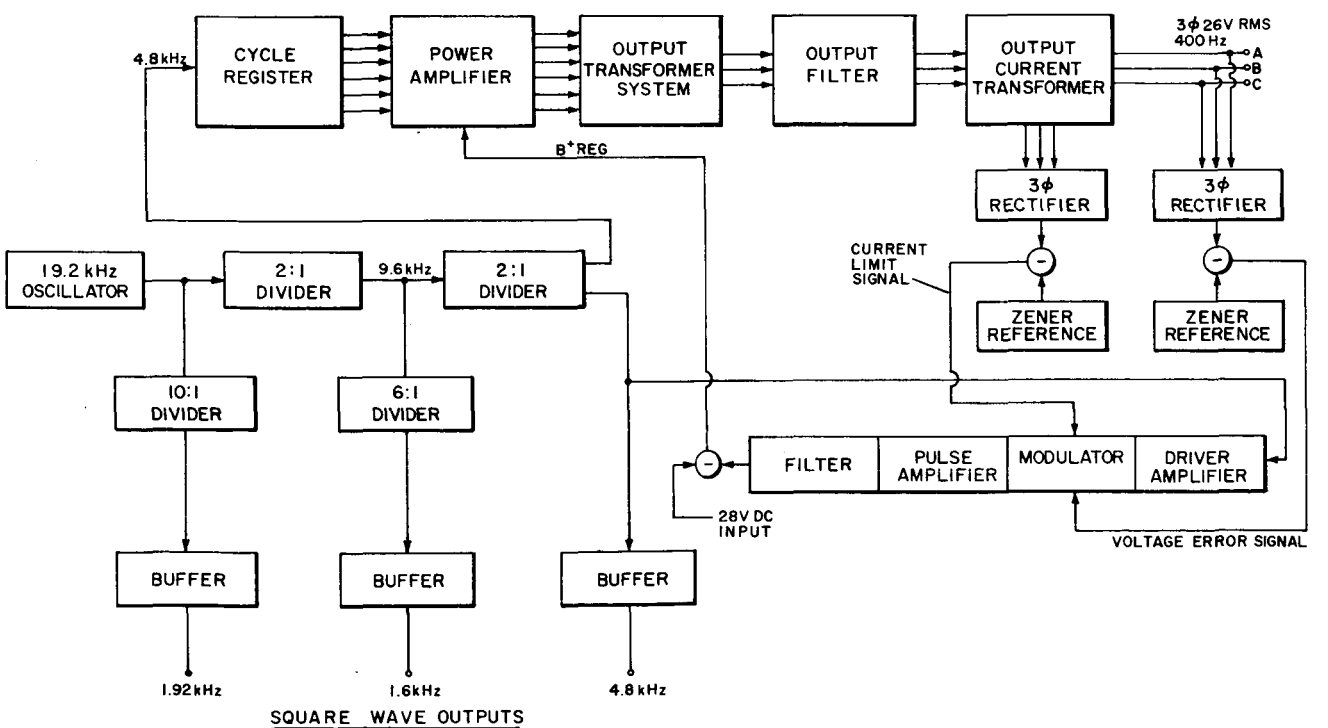

FIGURE 37. BLOCK DIAGRAM OF AC POWER SUPPLY.

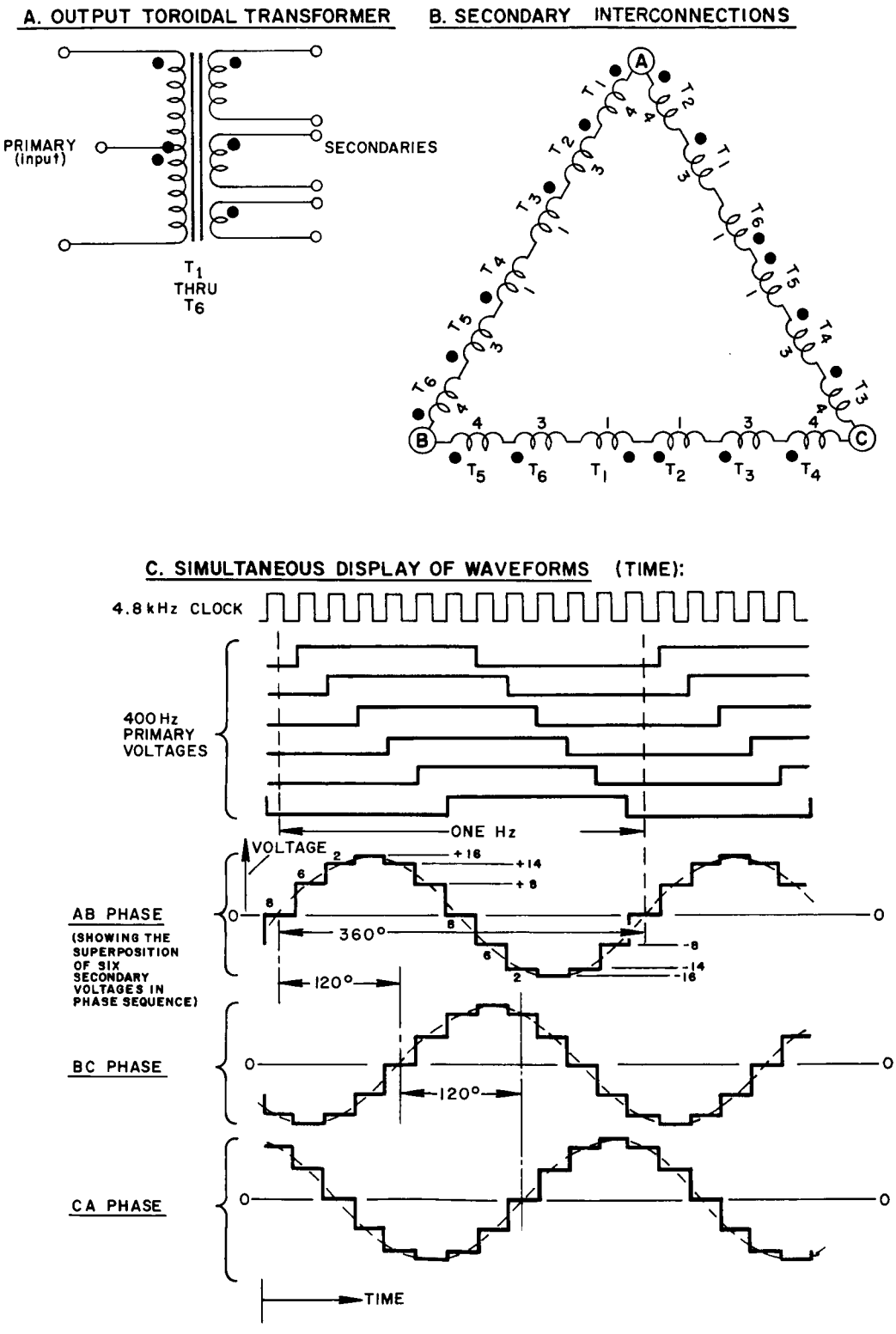

FIGURE 38. GENERATION OF 3-PHASE 400-Hz VOLTAGE.

network provides dividers and buffers for the auxiliary outputs. All frequency-divider circuits use Johnson-type counter logic to provide symmetrical square wave outputs eliminating complicated decoding gates. The network section utilizes integrated circuit construction.

The cyclic register produces six push-pull square-wave 400-Hz outputs spaced in 30-degree increments. The 4.8 kHz signal from the divider network is used as the clock pulse to trigger the six register flipflops. The flipflops are bistable circuits of the same integrated-circuit type used in the frequency divider network.

Each cycle register flipflop drives one channel of the power amplifier. One channel consists of two cascaded push-pull stages which are transformer coupled; all transistors operate in the switching mode, which contributes to the high efficiency of the inverter. Each channel excites a push-pull primary winding of a toroidal output transformer. The secondary windings consist of three per transformer with a 4:3:1 winding ratio (Fig. 38A). Each of the outputs has one winding from each of the six transformers (Fig. 38B) in a combination of three pairs with a 4:3:1 wattage ratio. Figure 38C illustrates the manner in which these ratios are used in the generation of the sine wave output.

The output voltages contain a 15 percent harmonic distortion. A low-pass output filter reduces this distortion by approximately 10:1. The voltage regulator compares a sample of the three-phase output voltage with a stable Zener reference voltage, then amplifies the error, and biases the power amplifier to close the loop.

The 19.2 kHz oscillator, the frequency dividers, the network dc supply, and the cycle register operate in dual redundancy. If the 400-Hz voltage is not detected in channel A, a bistable switching circuit will instantly switch power demand to channel B.

The ac power supply box has a light-gauge sheetmetal cover and is cast of magnesium, gasket-sealed, and pressurized to 1.7 $N/cm^2 d$ (2 psid). Modular-potted construction is used throughout. Motherboard printed circuit boards with integrated circuitry minimize internal wiring. The weight of the assembly is 14.5 kg (32 lb).

SECTION VIII. ACCELEROMETER SIGNAL CONDITIONER ASSEMBLY

The accelerometer signal conditioner assembly accepts the velocity signals from the accelerometer optical encoders and shapes them before they are passed on to the guidance computer. Each accelerometer requires four shapers; a sine shaper and a cosine shaper for the active channel, and a sine shaper and a cosine shaper for the redundant channel. Also included are four buffer amplifiers for each accelerometer, one for each sine and cosine output. The output of these buffers is furnished to the blockhouse for a prelaunch accelerometer calibration check. The accelerometer telemetry velocity signals are also conditioned in this assembly.

The total assembly weighs approximately 4.5 kg (10 lb) and is fabricated from a magnesium casting. Light-gauge sheetmetal covers with gasket seals maintain an internal pressure of 1.7 N/cm^{2}d (2 psid).

Characteristics of the velocity signals are:

1.	Output voltage levels	0-6 volts minimum (3 volt bias) 0-8 volts maximum (4 volt bias)
2.	Signal rise time	50 μs on square wave
3.	Output frequency of acceleration signal	+60 g (50 Hz/g) -30 g (50 Hz/g)

SECTION IX. PLATFORM ERECTION SYSTEM

The erection to the local vertical is accomplished by two gas bearing pendulums fitted to the inertial gimbal. The input axes of the pendulums are parallel to the X and Z accelerometer measuring axes.

The gas bearing pendulum is a single-axis gravity-sensing device. Its sensing element is a gas floated slug which supports a soft iron core as shown in the cutaway view of Figure 39. The iron slug moves inside the coils of a linear differential transformer which provides the electrical output signal. Damping of the slug motion is provided by a chamber and an exhaust orifice while the spring restraint is obtained magnetically.

The characteristics of the pendulums are:

1.	Physical Characteristics		
	a.	Size	2.25" by 1.5" by 1.25"
	b.	Weight	92 g
2.	Gas Bearing		
	a.	Gas pressure	10.3 N/cm^{2}d (15 psid)
	b.	Gas flow	100 cc/min STP
	c.	Gas gap	0.015 to 0.02 mm

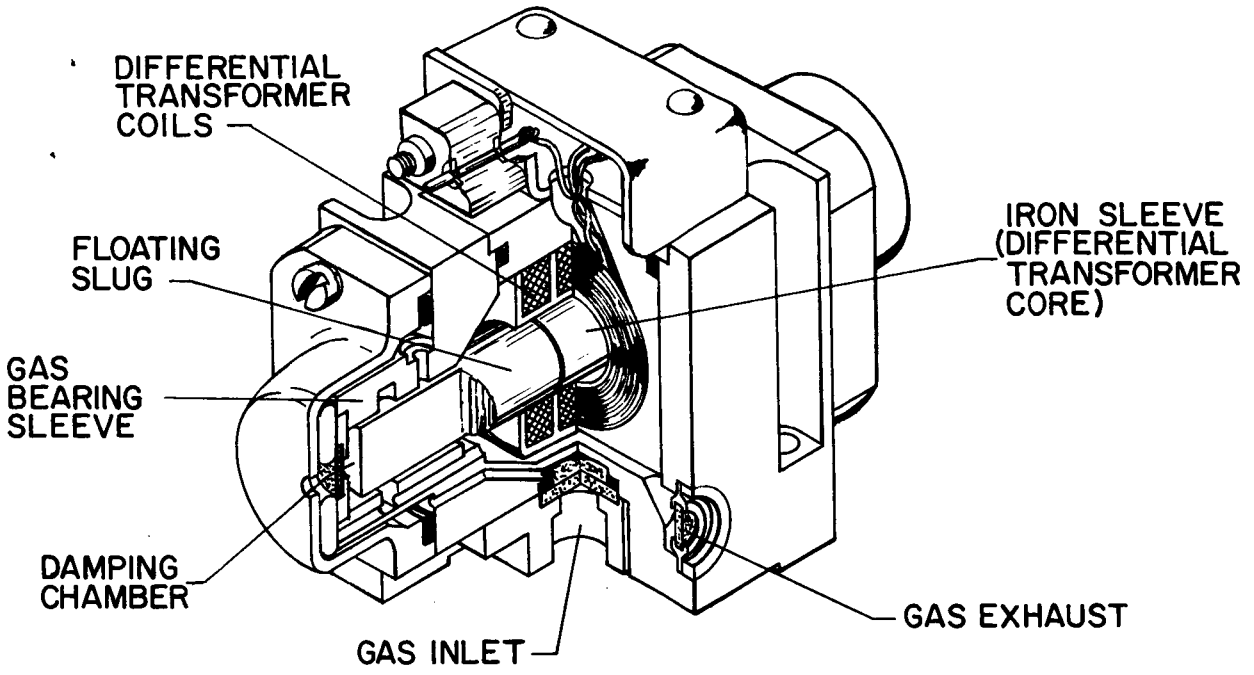

FIGURE 39. GAS BEARING PENDULUM.

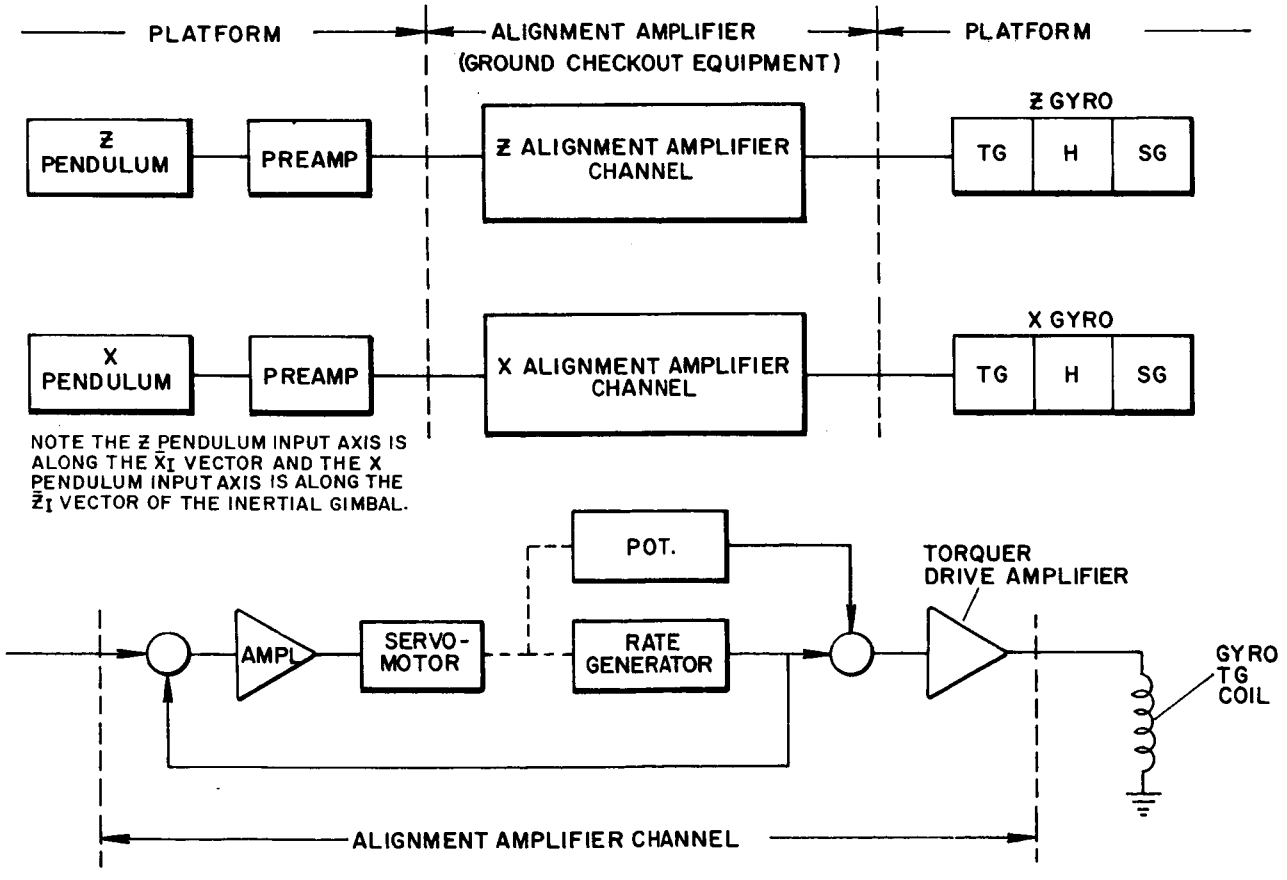

FIGURE 40. BLOCK DIAGRAM OF ERECTION SYSTEM.

3. Signal Generator

a.	Type	Inductive
b.	Excitation	4 V, 400 Hz
c.	Sensitivity	300 mV/°

4. Performance

a.	Leveling accuracy	±2.5 arc seconds
b.	Input range	±0.5° (signal saturation)
c.	Time constant	10 seconds

The block diagram of the erection system is shown in Figure 40. The input axes of the X and Z pendulums are along the inertial gimbal Z and X axes, respectively. The pendulum output is amplified by a preamplifier on the platform and then transmitted to the ground equipment alignment amplifier.

The alignment amplifier provides a proportional plus integral path to the torque driver amplifier, which returns the signal from the ground to the variable coil of the gyro torque generator. The erection system is a second order system with a natural frequency of 0.05 radian per second and a damping ratio of 0.5. The leveling accuracy of the erection system is ±3 arc seconds.

SECTION X. AZIMUTH ALIGNMENT SYSTEM

The azimuth alignment system orients the accelerometers to the desired mission azimuth. To obtain the high accuracy requirement, the azimuth alignment system utilizes electro-optical techniques. The basic elements of the azimuth alignment system are an autocollimating theodolite with detection system, synchro encoder servosubsystem, launch control computer for azimuth programing and reference, and an alignment torquing servosubsystem. Fitted to the inertial gimbal is a porro prism (intermediate infrared) with its dihedral edge parallel to the X axis of the inertial gimbal. A second prism (near infrared) is fitted to the stator of the two-speed synchro which has its dihedral edge free to rotate in the X-Z plane (Fig. 41).

The basic element of the optical system is the SV-M2 theodolite (Fig. 42). The system consists of an autocollimating theodolite with necessary optics and detectors, a penta mirror set, an automatic sway control system, a reference prism with stand, a closed circuit TV monitoring system, and support electronics and controls.

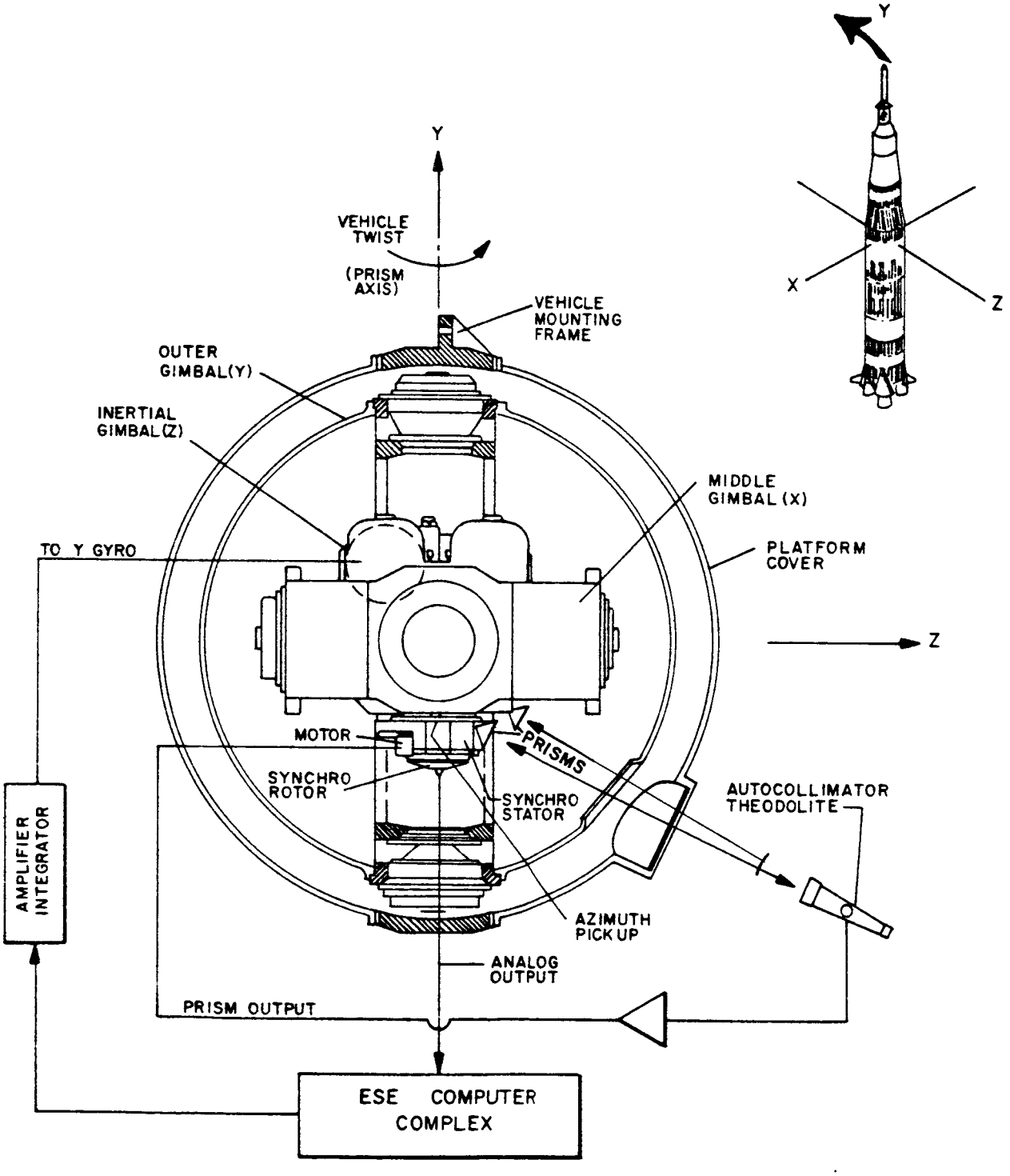

FIGURE 41. AUTOMATIC AZIMUTH ALIGNMENT.

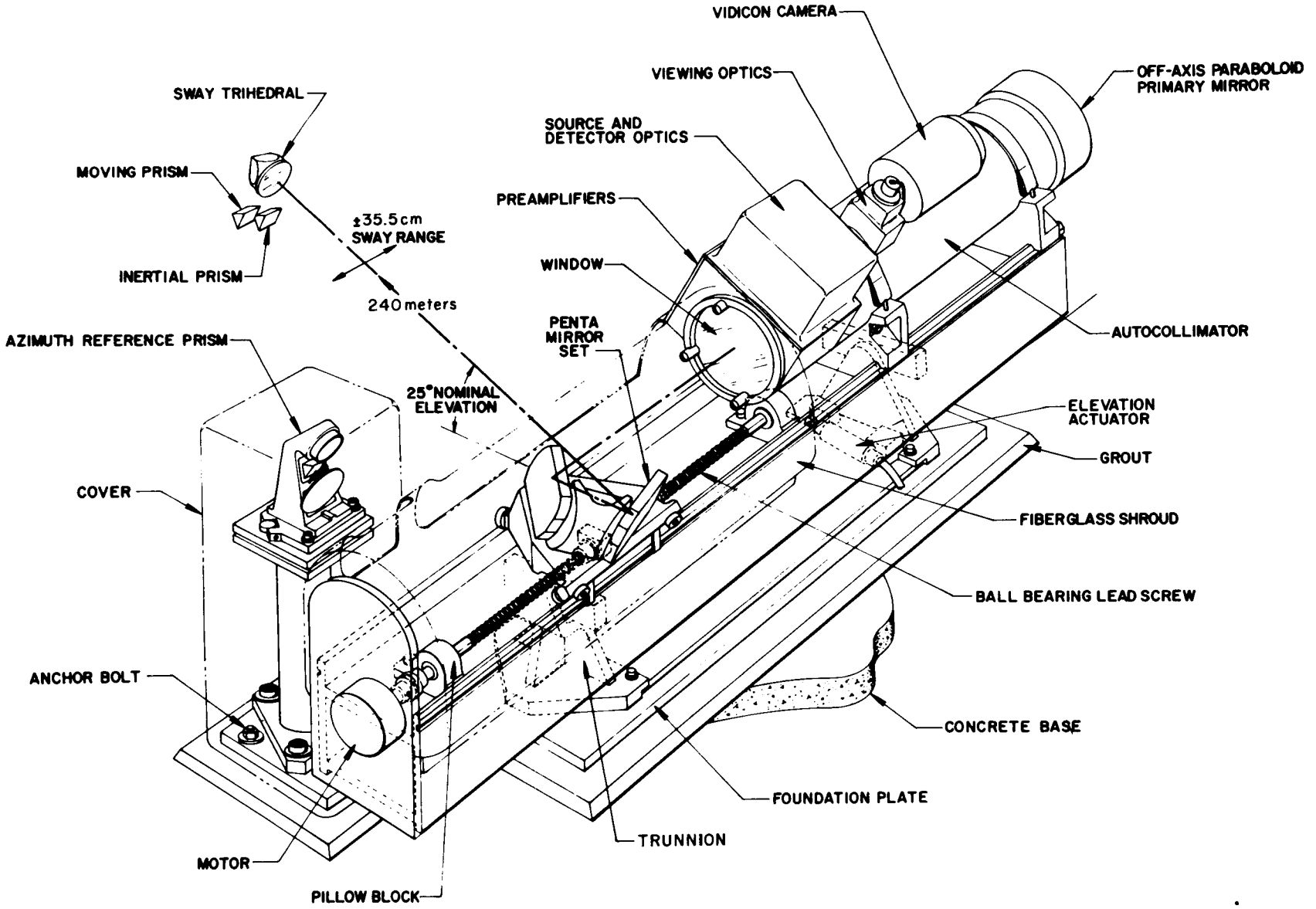

FIGURE 42. SATURN AALT SV-M2 THEODOLITE.

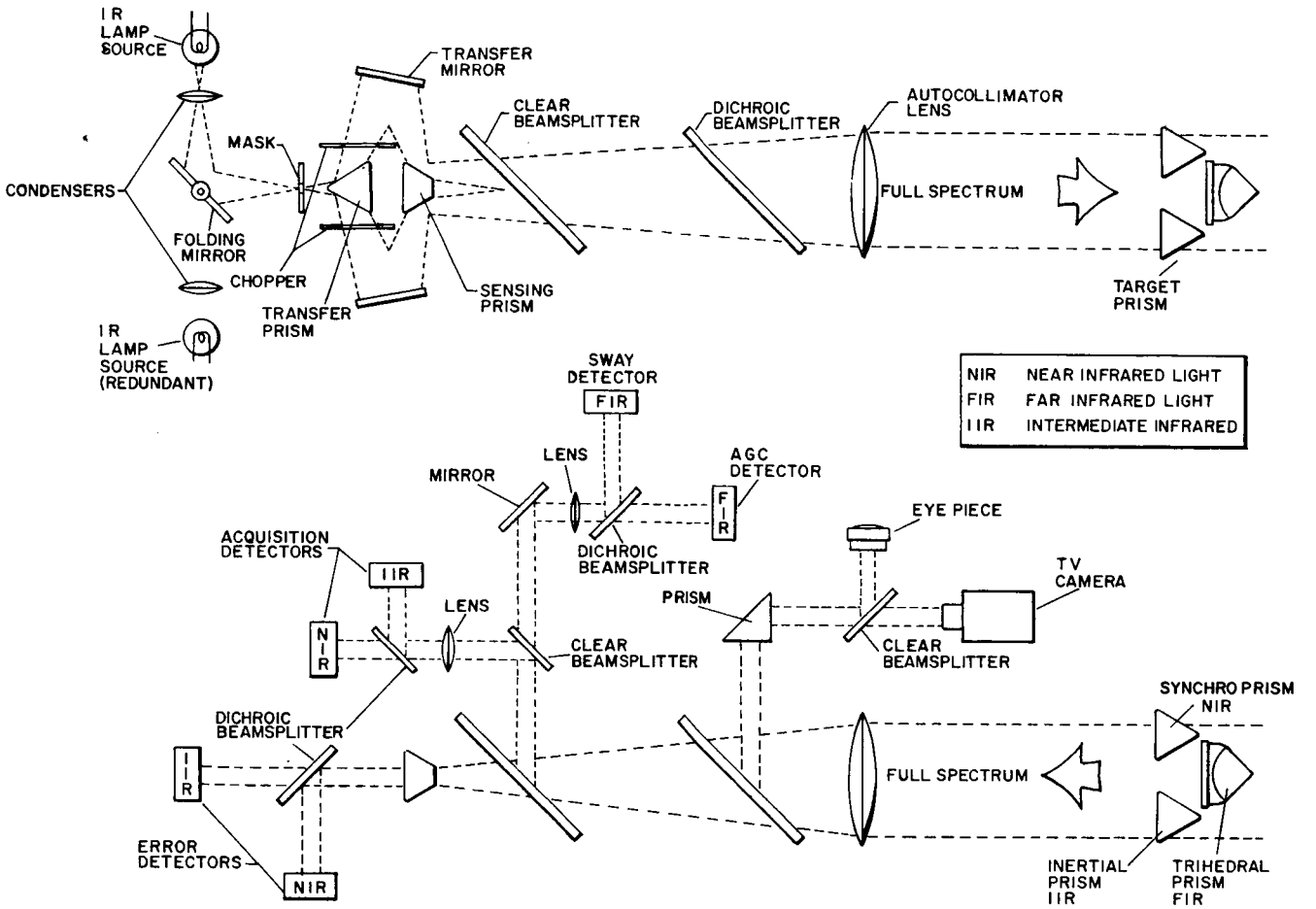

FIGURE 43. OPTICAL SCHEMATIC DIAGRAM OF SV-M2 THEODOLITE.

The theodolite has three control channels: the synchro prism, the inertial prism, and a trihedral prism (Fig. 43). An infrared energy spectrum is generated by a tungsten filament lamp. This spectrum has a bandwidth of two microns which lies between 0.7 and 2.7 microns. Atmospheric absorption of infrared in this bandwidth occurs at 1.35 and 1.8 microns. Therefore, the control channels are divided at 1.35 and 1.8 microns with the 0.7 to 1.35 micron near infrared band assigned to the synchro prism, the 1.25 to 1.8 micron intermediate infrared band assigned to the inertial prism, and the 1.8 to 2.6 micron far infrared band assigned to the trihedral prism (Fig. 44). Each prism has a dichroic multilayer coating that allows only the desired bandwidth of energy to pass.

The angular position of the synchro prism is controlled directly from the theodolite. A theodolite error signal drives a servoamplifier which is located in the mobile launcher. The amplifier output is transmitted to the ST124-M where it excites a servomotor located on the inertial gimbal. The servomotor positions the synchro prism through a gear train of 10^5:1, reducing any angular error to zero. This loop is active throughout countdown until vehicle liftoff. The angle between the inertial gimbal (navigation coordinates) and movable prism is measured by a precision 25:1 dual-speed control

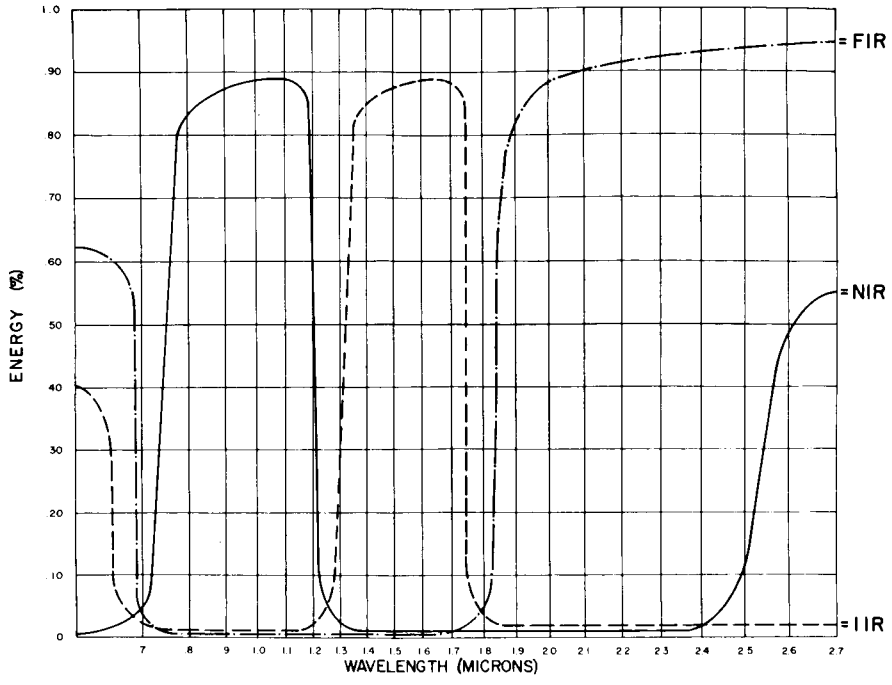

FIGURE 44. SPECTRAL FILTERS FOR THEODOLITE DETECTORS.

transmitter synchro (Fig. 45). The inertial prism is controlled by the theodolite output signal through the roll alignment servoelectronics by torquing the roll gimbal until the prism is in the desired azimuth plane.

The trihedral prism, which is fixed to the vehicle, is used as reference for a servosystem to position the penta mirror that provides the theodolite with the capability of translatory tracking. At the vehicle elevation of the ST124-M platform system, the SV-M2 (Saturn V, Mod 2) will compensate for a ±35.5 cm (±14 in.) translation movement of the vehicle. The trihedral prism servoloop increases the aperture of the autocollimator from 20 cm (8 in.) to 85 cm (32 in.) at a rate of 76 cm/s (32 in./s).

Prism acquisition signals from the three channels are generated with the same infrared coded bandwidths that produce the error signals. These are used to automatically block and/or initiate other events in the vehicle launch procedure and azimuth alignment system. Indicator lights on the theodolite control panel in the launch control center confirm that the three prisms are in the acquisition range of the theodolite. Two closed-circuit TV monitor systems provide the launch control center with a view of the three prisms and a monitor of the theodolite control and display panel in the theodolite hut.

The elevation angle (nominally 25 degrees from horizontal) of the theodolite is set by a dc motor-driven actuator that is manually controlled from the launch control center. At the Saturn V launch complex, the theodolite can operate with a ±35.5 cm (±14 in.) variation in elevation without requiring any adjustment.

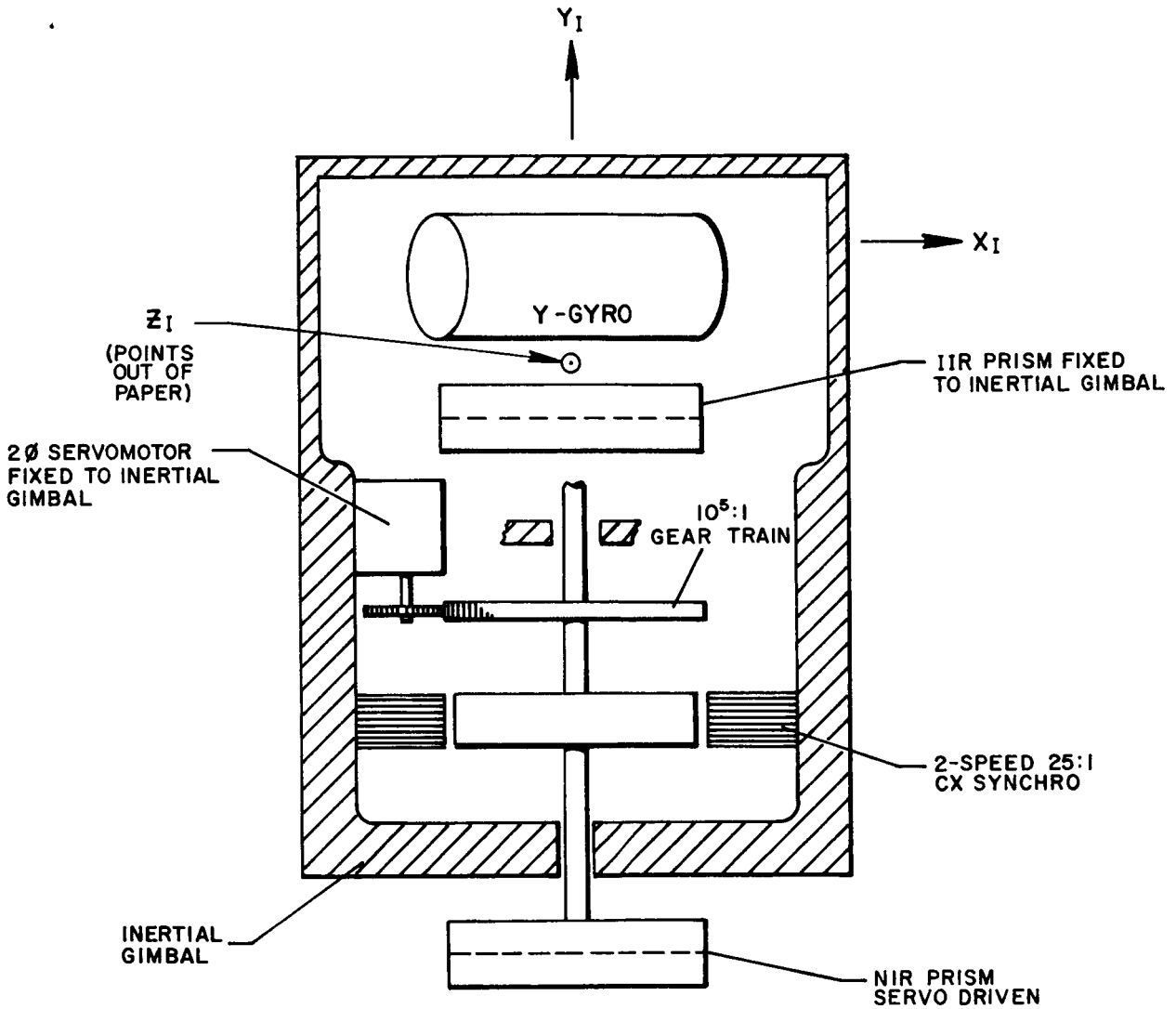

FIGURE 45. SCHEMATIC OF INERTIAL GIMBAL LAYING SYSTEM.

The encoder-synchro package consists of a 25:1 dual synchro, an 18-bit optical shaft angle encoder, and a motor-tachometer-gear assembly. The encoder is provided with an enclosure containing strip heaters to maintain the temperature within ±5° C, maintaining the designed accuracy of ±10 arc seconds. The encoder system has a self-generated encoder sampling time of 20 ms. The output is a cyclic gray code with logic levels of 0 or 28 volts. The 25:1 dual synchro with the platform dual synchro has a back-to-back control transmitter/control transformer (CX/CT) error of ±10 arc seconds.

The reflected infrared energy from the prisms is acquired by the theodolite's optics. From this coded energy, the theodolite detects deviations from the desired position of the prisms. These coded signals are separated into their respective channels by slit prism angle filters and dichroic beam splitters. The dichroic beam splitters have a dichroic multilayer coating similar to that of the prisms. Each of the three channels has acquisition detectors that generate dc signals when the prisms are within the acquisition range of the theodolite. These signals are used to indicate acquisition and to control relay switching in various other vehicle-associated control functions. When an error exists in any channel, a representative portion of the infrared energy passes through the slit prism filter to the dichroic beam splitter and onto a lead sulfide detector. A phase-oriented ac voltage is generated that is directionally proportional to the angular error. This voltage is amplified and demodulated to achieve the desired signal gradient of 100 mV/arc second.

The simplified azimuth block diagram in Figure 46 shows the operation of the azimuth alignment system. After all systems have been energized, the erection system positions the inertial gimbal to the local vertical. The azimuth alignment equipment is

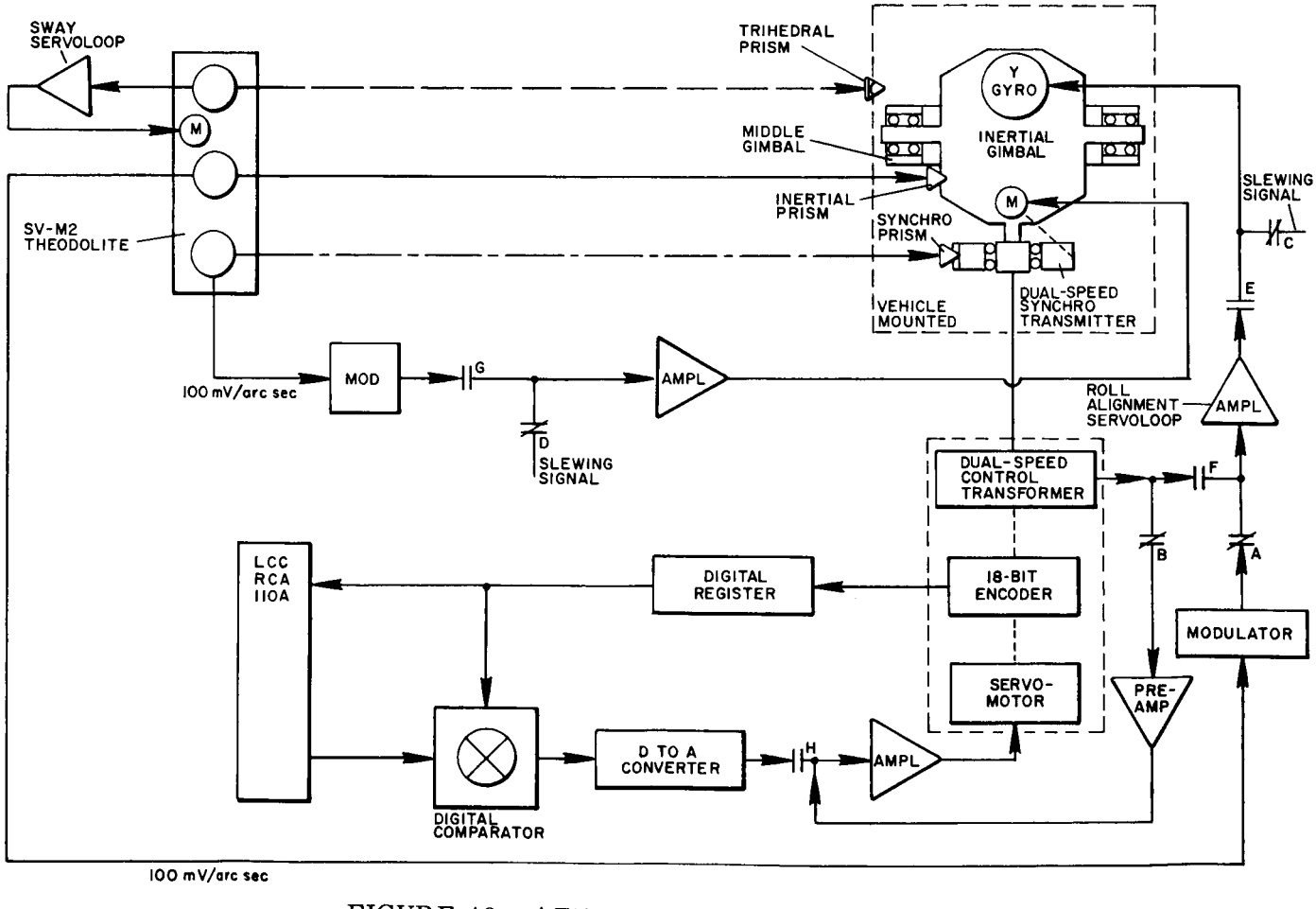

FIGURE 46. AZIMUTH ALIGNMENT SCHEME.

switched into the acquisition mode. This closes contacts A, B, C, and D and opens contacts E, F, G, and H. A bias signal is injected into the synchro prism servoloop, driving this prism into acquisition; the acquisition signal removes the bias and closes the synchro prism servoloop on the theodolite, driving the synchro prism to null.

The output of the dual-speed control transformer drives the encoder-synchro servoloop until the synchro output is zero through contact E. The RCA-110A launch computer reads and stores the position of the 18-bit encoder. Thus the baseline azimuth is stored in the computer. This is the azimuth of the navigation coordinate system and is the reference from which launch azimuth is established. Any deviation from this position will generate an error signal in the CX/CT measurement. This error signal excites the Y gyro torquer which rotates the Y gimbal to cancel the deviation.

The mission azimuth is established with contacts A, B, C, and D open and contacts E, F, G, and H closed. The launch control computer computes the azimuth program angle by comparing the baseline azimuth to the stored mission azimuth and torquing the synchro-encoder repeater until the encoder output agrees with the computer. The error signal from the dual-speed synchro system is fed to the Y gyro alignment loop and drives the inertial gimbal to the mission azimuth, which also nulls the CX/CT unbalance. The synchro prism is held fixed with respect to the optical beam from the theodolite on the baseline azimuth. The inertial gimbal (navigation coordinates) is held on the mission azimuth with the CT acting as an azimuth pickoff. The azimuth angle computation is a function of the predicted launch time. The computer program transforms any deviations from the predicted launch time into a respective azimuth angle change and, through the encoder synchro, repositions the inertial gimbal to the changing azimuth. The mission azimuth is displayed in the launch control center by a digital monitor.

The analysis of the azimuth alignment error shows the RSS system error to be less than ±20 arc seconds.

SECTION XI. SLIP RING CARTRIDGE

The plus Z and plus Y pivots each contain a 100-circuit slip ring cartridge for passing electrical signals across the pivots. The minus Z and minus Y pivots each contain an 80-circuit slip ring cartridge. All critical signals are routed through the plus pivots while all power transmission is over the minus pivots. The base of the slip ring assembly is made up of the wire bundle, cast into a cylinder with a filled epoxy. The slip rings are built up by electrodeposition of 0.04 cm (0.015 in.) of copper into ring grooves machined into the base epoxy. A flashing of nickel over the copper prevents gold migration. A 0.04 cm (0.015 in.) layer of gold electrodeposited over the nickel completes the ring. Thus the rings are dielectrically isolated and supported with a filled epoxy. A one-piece stainless steel cross-spline along the center serves as the main structural member of the ring subassembly (Fig. 47). The leadwire is fastened to the ring by electrodeposition and is routed along the spline to the mounting flange.

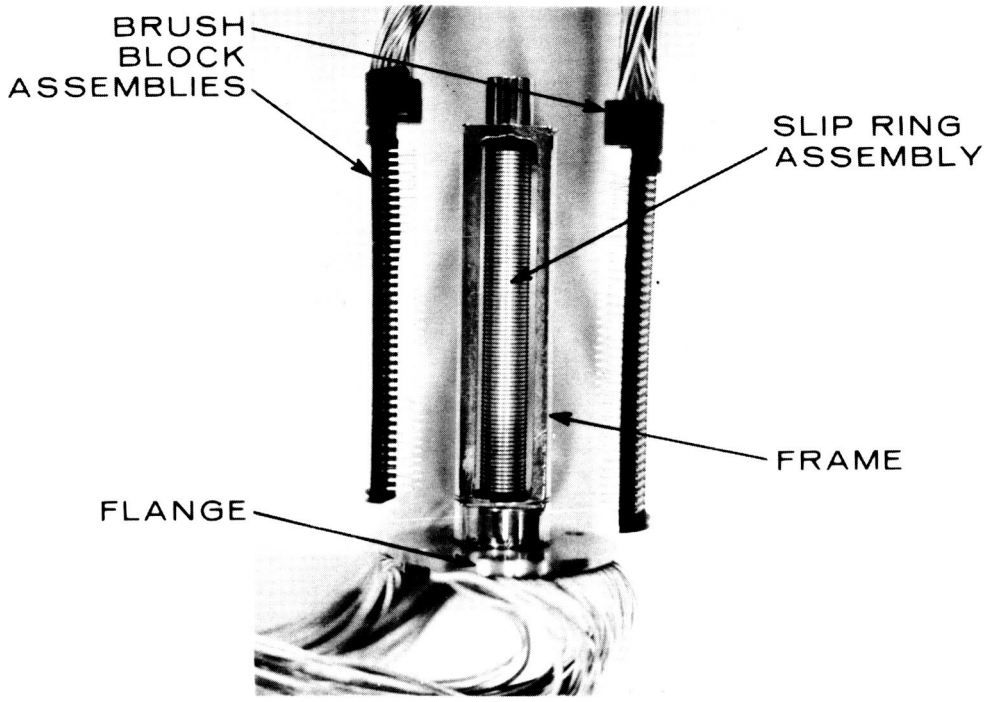

FIGURE 47. SLIP RING CAPSULE.

Machined in the rings is a 90-degree V-groove which serves as a guide for the brushes. Dimensional tolerance on the ring assembly is controlled by a grinding process in which the V-grooves in all rings are ground in a single operation. A set of miniature precision bearings and the mounting frame of the brush blocks complete the ring assembly.

The two brush block subassemblies allow complete redundancy for each brush. The brushes are preformed and prestressed Ney-ORO-28A (75% gold, 22% silver, and 3% nickel) material. The brush blocks are a filled epoxy structure aligned with dowel pins and secured with screws to the frame. The leadwire is an unpigmented teflon-insulated nickel-plated copper, 19/42, size 30 AWG, stranded wire.

Acceptance testing of each unit includes 100 hour run-in time, temperature cycling, noise tests, and an X-ray of the completed assembly.

The following is a listing of the slip ring cartridge characteristics:

1.	Current Rating	1 A at 125 V, 400 Hz continuous per circuit
2.	Noise Limit	10 μV/mA
3.	Contact Resistance	0.125 ohm per circuit

4.	Breakaway Friction	2 g cm/circuit
5.	Environmental	
	a. Temperature	-55° C to +100° C storage 0° C to +60° C operation
	b. Vibration	15 g, 20-2000 Hz 3-hour test time per axis
	c. Shock	30 g, 3 ms 20 g, 11 ms
	d. Acceleration	20 g
6.	Life	
	a. Useful Life	10,000 hours (storage and operating)
	b. Operating Life	1000 hours will meet noise specification 5000 hours with maximum of 100% increase in noise specification

SECTION XII. INERTIAL COMPONENTS

The ST124-M stable platform contains three AB5-K8 gas bearing single-degree-of-freedom gyros and three AMAB3-K8 gas bearing pendulous gyro accelerometers. These components measure the vehicle motion; their performance capabilities define the hardware accuracies of the guidance system. No active compensation is used in the digital computer for instrument error terms, and absolute tolerances are established for the life of the instruments.

The gas bearing gyro is shown in a cutaway view in Figure 48. The cylindrical, externally-pressurized gas bearing suspends the cylinder between the sleeve and endplates, as shown in Figure 49, and provides both axial and radial centering. The endplates are bolted to the sleeve and their assembly forms the case of the gyro.

Dry gaseous nitrogen is passed through two rows of 24 holes with millipore discs in the sleeve acting as flow diffusers and providing the bearing stiffness. The gas in the cylinder chamber generates the hydrostatic bearing and flows symmetrically to both endplates, escaping around the hub at each end of the cylinder. The sleeve, endplates, and cylinder are constructed of beryllium with machined tolerances of 20 μin. in roundness and 20 μin./in. in squareness.

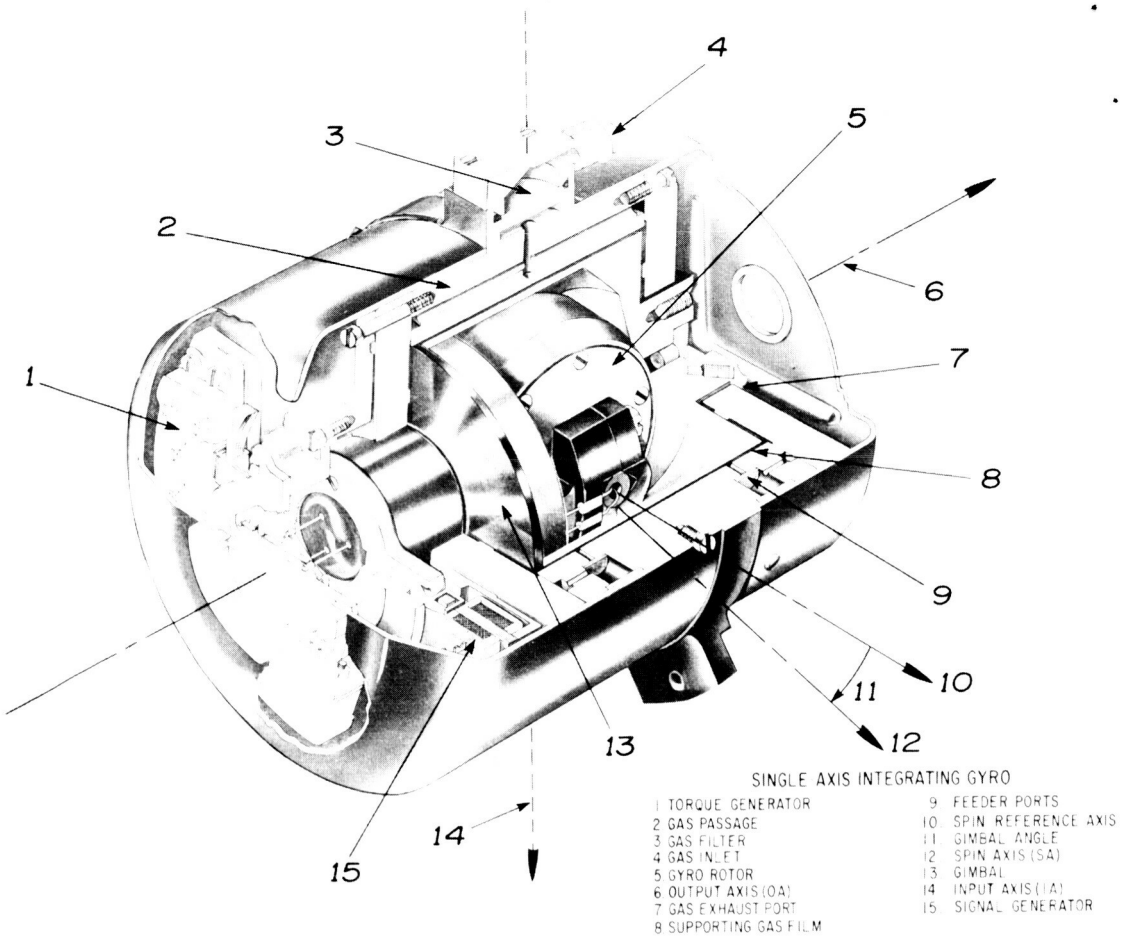

FIGURE 48. SINGLE-AXIS INTEGRATING GYRO.

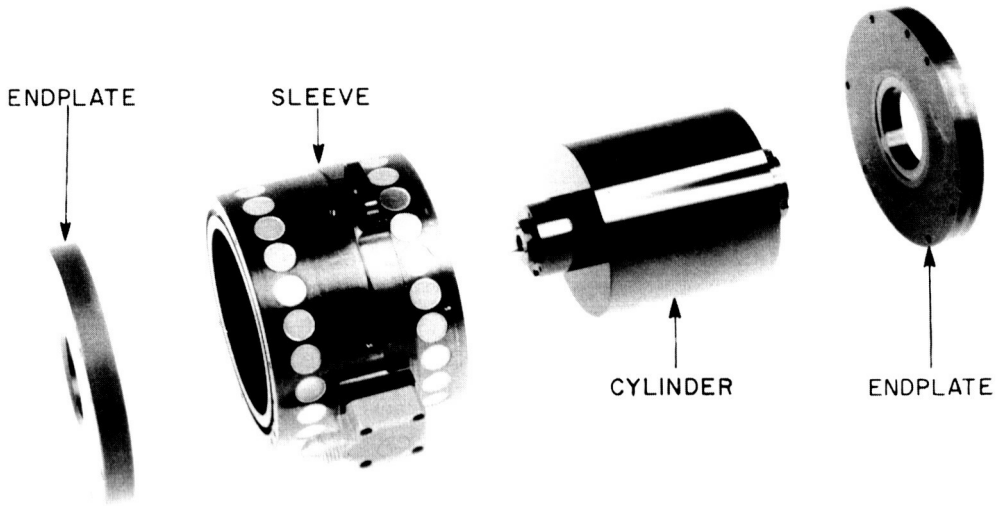

FIGURE 49. AB5-K8 GAS BEARING ASSEMBLY.

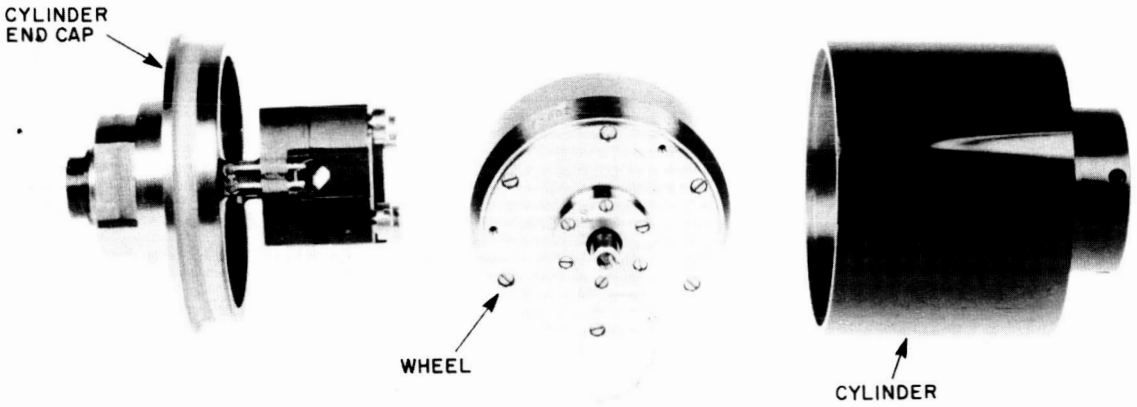

FIGURE 50. AB5-K8 INNER CYLINDER ASSEMBLY.

The gyro wheel, shown in Figure 50, mounts in a yoke of the cylinder endcap. The neck section of the yoke is controlled to minimize the anisoelastic drift of the wheel assembly. The endcap is mounted in the cylinder forming the gyro cylinder assembly. The cylinder is helium filled to reduce windage losses. The wheel is a two-pole, synchronous hysteresis motor. Precision bearings are fabricated to the beryllium shaft with the motor laminations and windings to form the stator of the wheel. The rotor is made up of an Elkonite ring with P-6 hysteresis laminations shrink-fitted into the Elkonite ring and beryllium endbells bolted to each side.

The signal generator and torque generator, shown in Figure 51, are coupled to the cylinder by means of a copper-shorted loop which is mounted on the cylinder. The

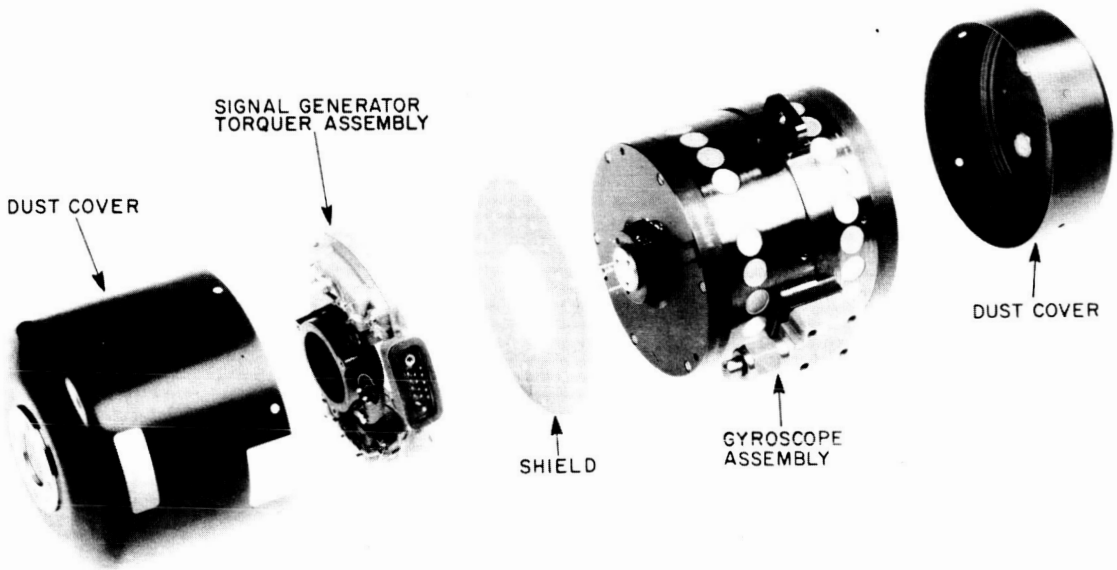

FIGURE 51. AB5-K8 GYRO ASSEMBLY.

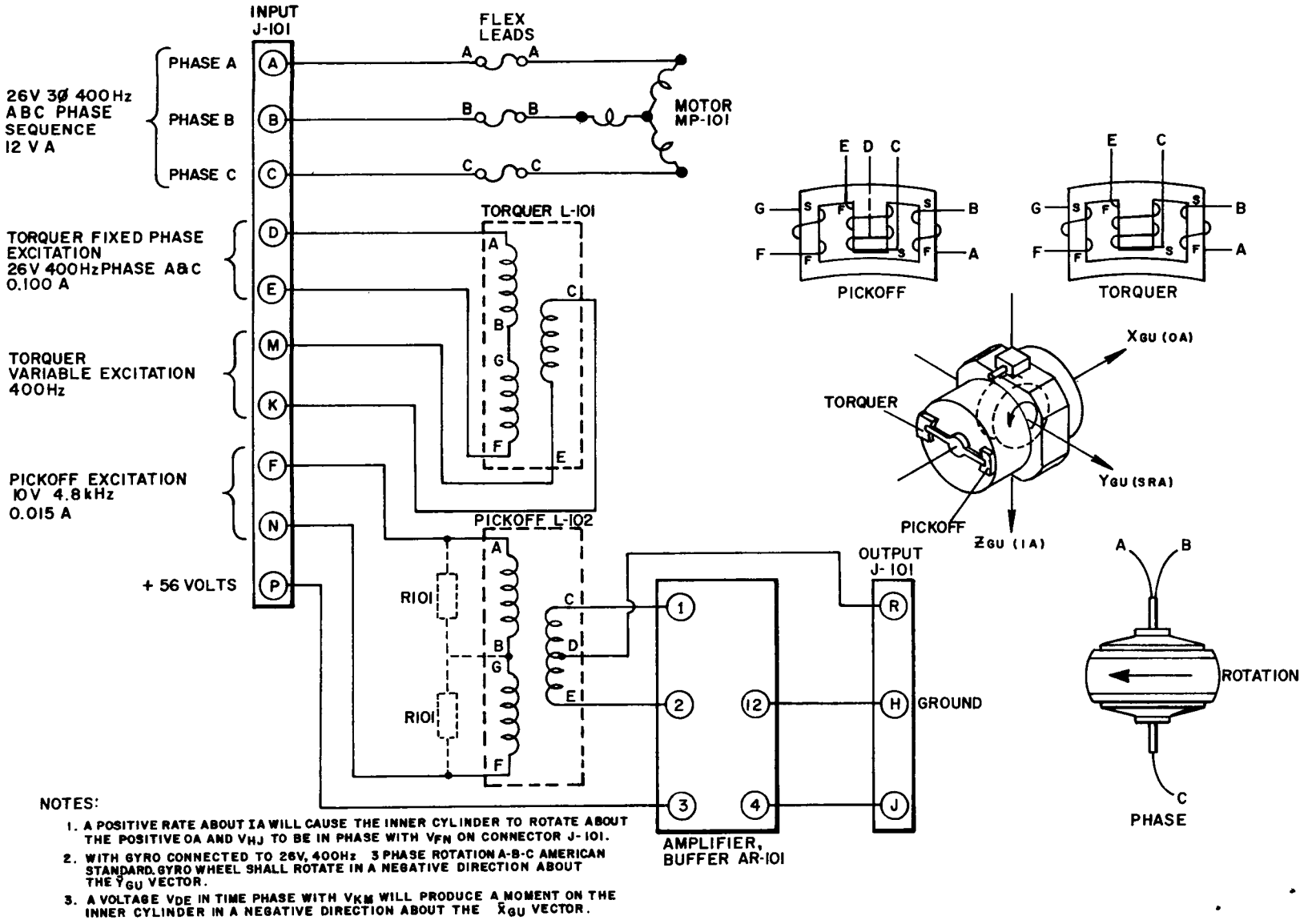

FIGURE 52. GYROSCOPE SCHEMATIC.

signal generator is an ac-type shorted-loop single-winding sensor. It senses the angular displacement of the gyro about its output axis. The torque generator operates like an eddy current motor. It provides only alignment torques for initial erection. The 3-phase 400-Hz wheel power is transmitted by ribbon flex leads to standoffs on the gyro cylinder. A magnetic shield is placed between the gyro case and the signal generator. Dust covers, which are also magnetic shields, complete the assembly.

The electrical schematic for the AB5-K8 stabilizing gyro is shown in Figure 52. Also shown is the coordinate definition for a single gyro. The wheel phase rotation A-B-C, American standard, with the gyro connected to the 26-volt 3-phase 400-Hz supply, causes the gyro motor to rotate in a negative direction about the Y_{GU} (gyro spin reference) vector.

The following list contains the gyro characteristics.

1. Gyro Wheel

a.	Type	Synchronous hysteresis
b.	Angular momentum	2.6×10^6 g cm^2/s
c.	Wheel speed	24,000 rpm
d.	Wheel excitation	26 V, 3 phase, 400 Hz
e.	Wheel bearing preload	3.4 kg, operating
f.	Wheel power at sync	8 W
g.	Wheel life	3000 hours, minimum
h.	Wheel mount	Symmetrical
i.	Wheel sync time	90 seconds

2. Gas Bearing

a.	Gas pressure	10.3 N/cm^{2}d (15 psid)
b.	Gas flow rate	2000 cc/min STP
c.	Gas gap (one side)	0.015 to 0.02 mm
d.	Orifice restrictors	Millipore discs

e.	Sleeve material	Anodized beryllium
f.	Endplate material	Anodized beryllium
g.	Cylinder material	Anodized beryllium

3. Signal Generator

a.	Type	Shorted turn reluctance
b.	Excitation	10 V, 4.8 kHz
c.	Sensitivity	550 mV/° with 10 kΩ load
d.	Float freedom	±3° with +0° and -0.5° tolerance

4. Torquer (for platform erection and earth rate bias only)

a.	Type	Shorted turn reluctance
b.	Normal erection rate	6°/min
c.	Fixed coil excitation	26 V, 400 Hz, 45 mA
d.	Maximum variable coil excitation	30 V, 400 Hz, 50 mA
e.	Impedance	
	(1) Fixed coil resistance	184 ohms
	(2) Fixed coil impedance	555 ∠+31° ohms (400 Hz)
	(3) Variable coil resistance	190 ohms
	(4) Variable coil impedance	330 ∠+53° ohms (400 Hz)

5. Physical Characteristics

a.	Size	3" diameter by 4" length
b.	Weight	900 g
c.	Mounting	3-point flange mounting

6. Temperature Characteristics

a.	Calibration temperature	40° C (gyro housing)
b.	Drift versus temperature gradient	0.009°/h/° C

The AB3-K8 instrument is a pendulous gyro accelerometer; a cutaway view is shown in Figure 53.

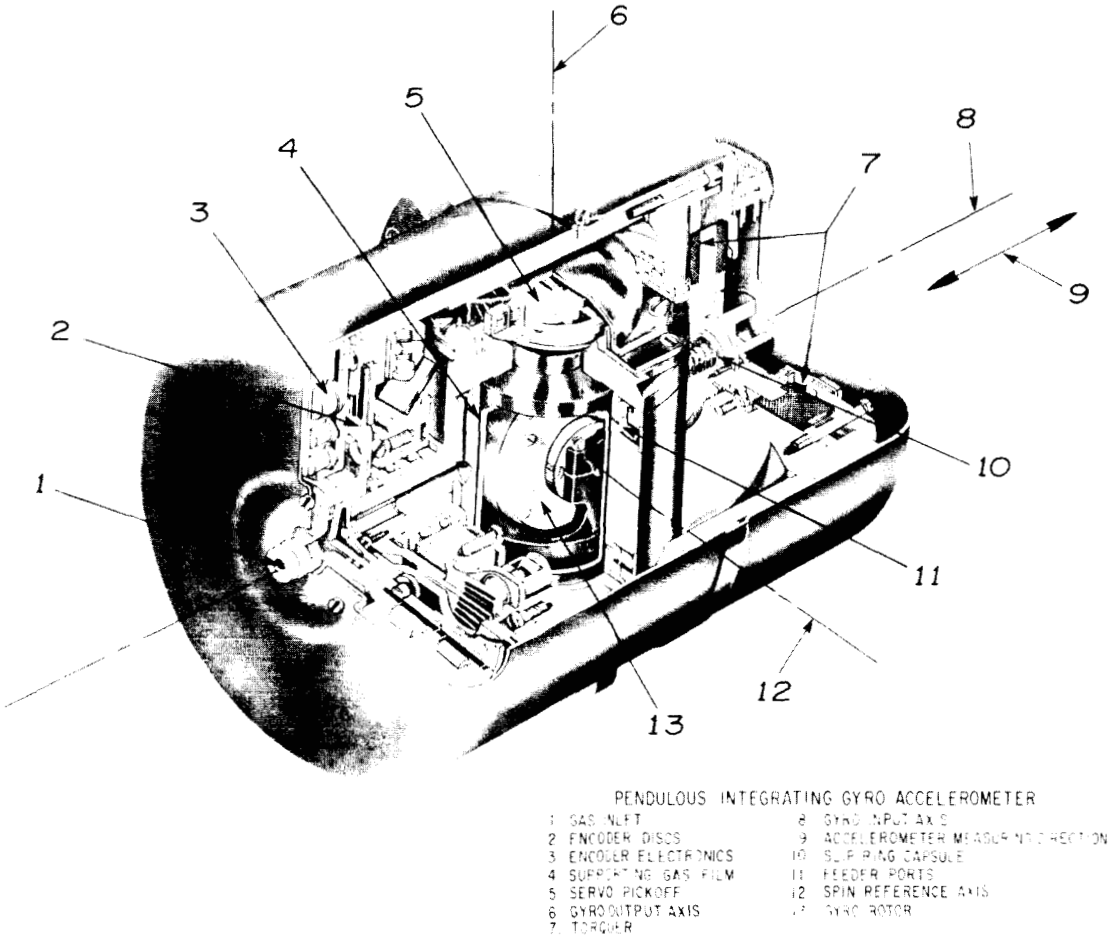

FIGURE 53. PENDULOUS INTEGRATING GYRO ACCELEROMETER.

The accelerometer is a single-degree-of-freedom gyro unbalanced about its output axis. The gyro motor and flywheel of the gyro accelerometer are shifted along the spin reference axis to obtain desired pendulosity about the gyro output axis. The pendulous cylinder is machined with a pair of pivots mounted into a frame with a set of class-seven bearings. Thus the cylinder is free to rotate about the gyro input axis, which is aligned in the acceleration-measuring direction. An unbalance or pendulosity produces a torque

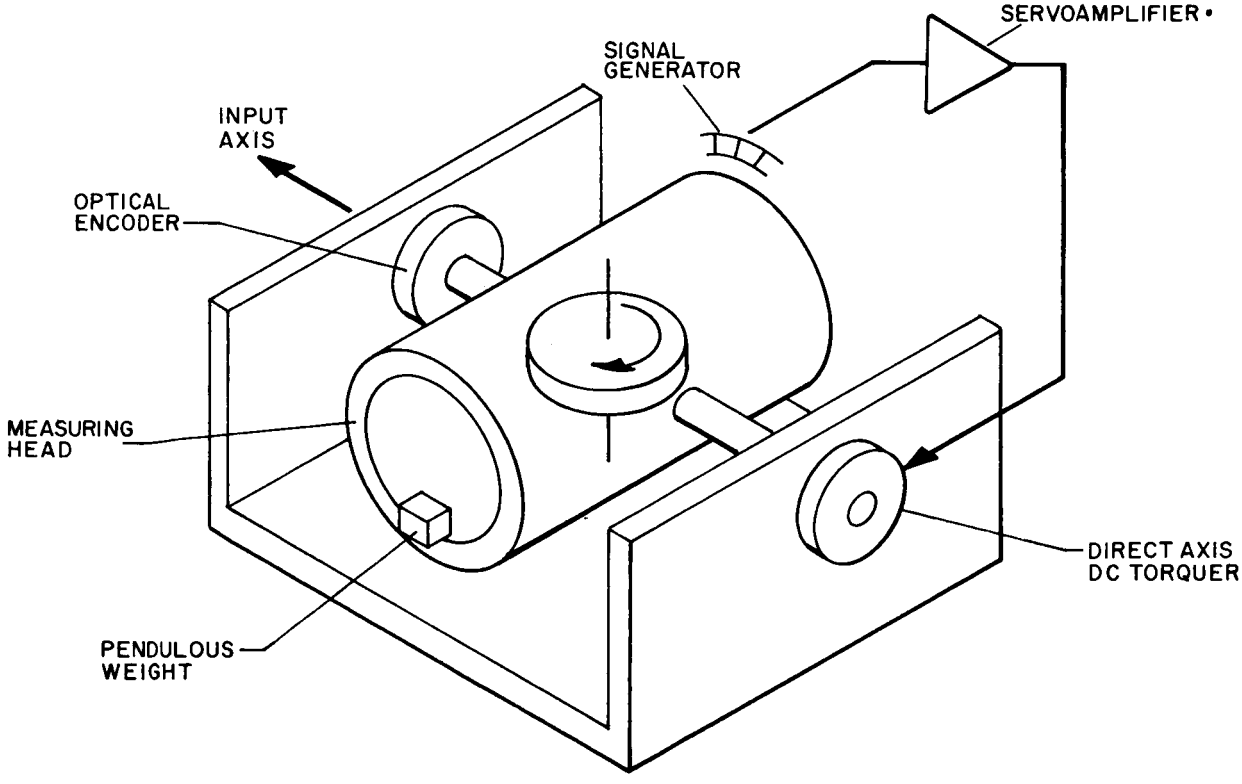

FIGURE 54. SCHEMATIC OF AB3-K8.

proportional to the acceleration to which the pendulous mass is subjected. The precession angle of the gyro is proportional to the acceleration as a function of the measuring head unbalance and friction in the trunnion bearings. A signal generator measures the precession angle and a servo closes the loop to a direct-axis torquer mounted on the gyro input axis (Fig. 54). Thus the gyro measuring head is stabilized and the pendulous weight is held perpendicular to the input axis. The speed of the measuring head or gyro with respect to inertial space is proportional to thrust acceleration along the input axis, and the position of the measuring head is a measure of thrust velocity. An optical incremental encoder is mounted on the input axis and provides a measure of the thrust velocity. The power source for the synchronous spin motor is referenced from a crystal-controlled frequency to guarantee a constant accelerometer scale factor (velocity increment per revolution about the input axis).

The symmetrical gyro wheel is mounted in a cylinder that is suspended on a hydrostatic gas bearing. The gyro is constructed the same as the AB5-K8 gyro except there are two rows of 18 holes for feeding gas into the bearing. All nonmagnetic parts are machined from beryllium except the endplates which are fabricated of Monel to reduce the servoloop nutation frequency.

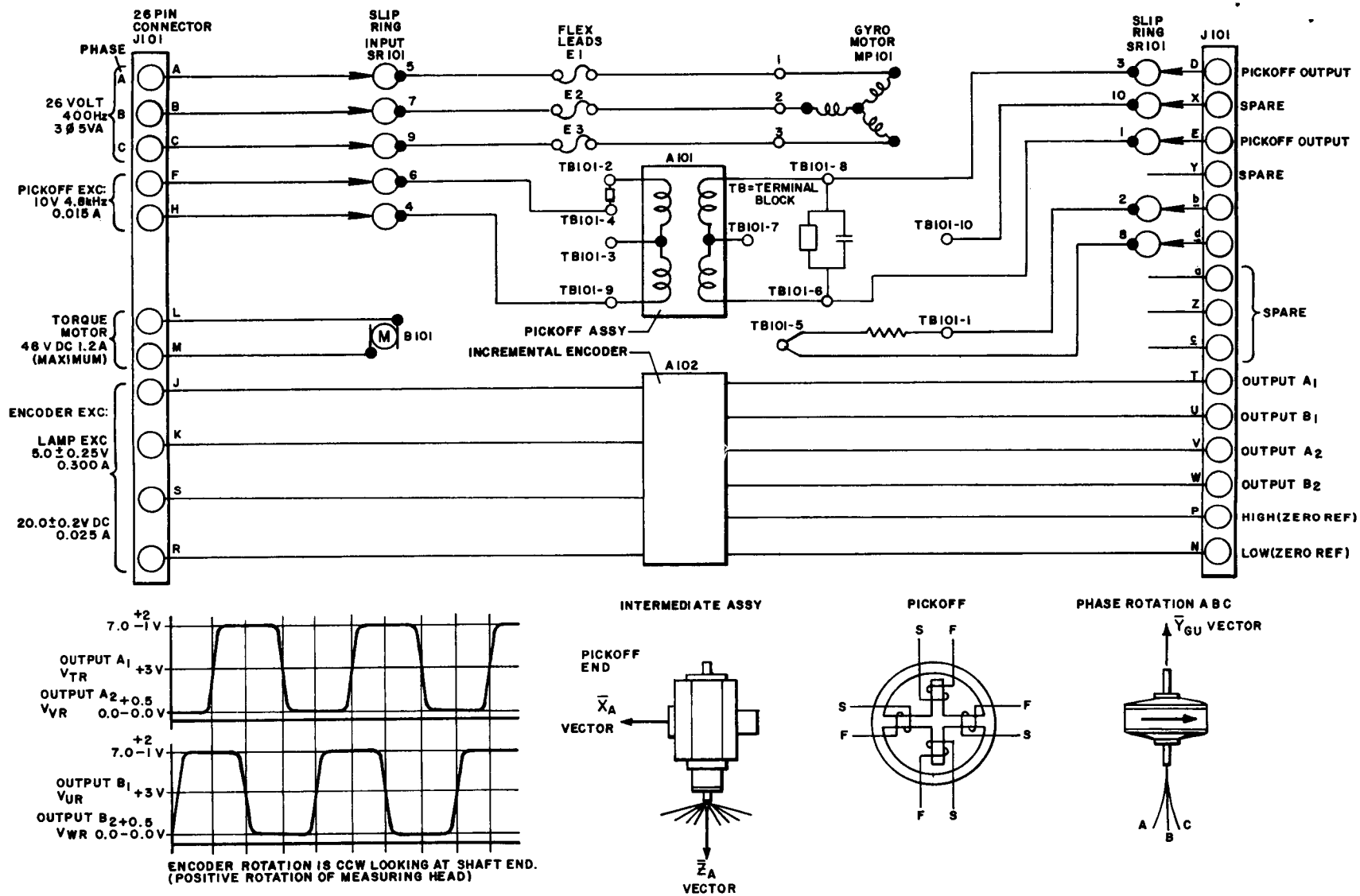

FIGURE 55. ACCELEROMETER SCHEMATIC.

The electrical schematic for the AB3-K8 accelerometer is shown in Figure 55. The wheel phase rotation A-B-C, American standard, with the gyro connected to a 26-volt 3-phase 400-Hz power supply, causes the gyro motor to rotate in a positive direction about the Y_{GU} vector.

The following list contains the accelerometer characteristics:

1. Gyro Wheel

a.	Type	Synchronous hysteresis
b.	Angular momentum	94,000 g cm^2/s
c.	Wheel speed	12,000 rpm
d.	Wheel excitation	26 V, 3 phase, 400 Hz
e.	Wheel sync time	90 seconds
f.	Wheel power at sync	4.5 W
g.	Wheel life	3000 hours, minimum
h.	Wheel mount	Symmetrical
i.	Wheel bearing preload	907.2 g, operating

2. Gas Bearing

a.	Gas pressure	10.3 N/cm^2d (15 psid)
b.	Gas flow rate	2400 cc/min STP
c.	Gas gap	0.015 to 0.02 mm
d.	Orifice restrictors	Millipore discs
e.	Sleeve material	Anodized beryllium
f.	Endplate material	Monel
g.	Cylinder material	Anodized beryllium

3.	Signal Generator	
	a. Type	4-pole shorted turn reluctance
	b. Excitation	10 V, 4.8 kHz
	c. Sensitivity	285 mV/° with 700 Ω load
	d. Float freedom	±3° with +0° and -0.5° tolerances
4.	Torque Motor	
	a. Type	Direct-axis dc torquer
	b. Maximum torque	1.44 kg cm at 1.27 A and 40.7 V
	c. Dc resistance	32.6 ohms
	d. Inductance	12.5 mH
5.	Velocity Pickoff	
	a. Type	Digital encoder (optical grid)
	(1) Count	6000 count/revolution
	(2) Resolution	0.05 m/s/bit
	(3) Output	Incremental with redundant channels
6.	Physical Characteristics	
	a. Size	3.25" diameter by 5" length
	b. Weight	1200 g
	c. Mounting	3-point flange mounting
7.	Performance	
	a. Accelerometer scale factor	300 m/s/revolution of output axis
	b. Pendulosity	20 g cm

8. Temperature Characteristics

a.	Calibration temperature	40° C ambient (on housing gyro)
b.	Ambient temperature range for required accuracies	40° C ±3° C
c.	Accuracy versus temperature gradient	2.5×10^{-5} g/° C of the pendulous cylinder

SECTION XIII. POWER AND GAS REQUIREMENTS

The input power requirements and the expected heat dissipation of the system assemblies are shown in Figure 56. The input power figures show the normal (quiescent) requirements and the peak (maximum disturbing forces and g loading) requirements.

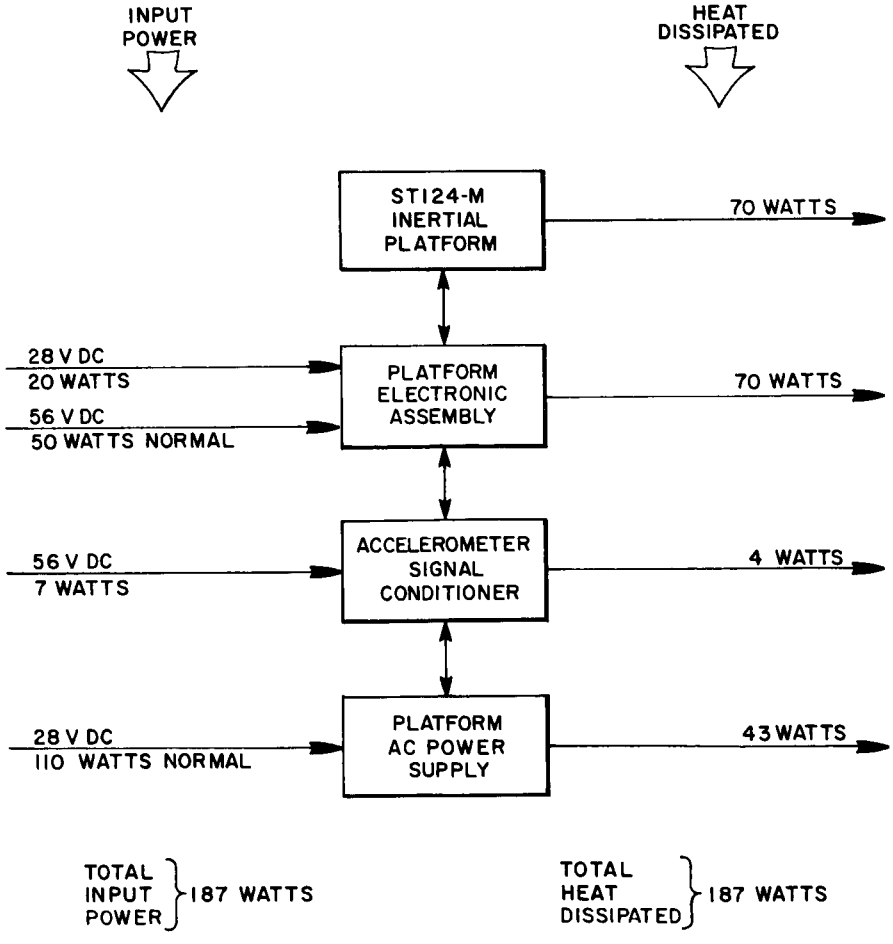

FIGURE 56. SYSTEM POWER REQUIREMENTS AND HEAT DISSIPATION.

The following specifications apply to the power supplies:

1. 28 V DC Supply

a.	Voltage regulation	±2.0 V dc
b.	Ripple content	0.5 V
c.	Normal current	9 A
d.	Peak current	11 A

2. 56 V DC Supply

a.	Voltage regulation	±3 V
b.	Ripple content	0.25 V
c.	Normal current	1.0 A
d.	Peak current	6.0 A

3. Platform Heaters

The platform has 150 watts of resistive heating with the application of 115 volts, 60 or 400 Hz. The heaters are used to assist the platform assembly in reaching its optimum operating temperature. Thermostats, located inside the platform, control the heaters and turn them off when the operating temperature is reached. The platform component heat dissipation maintains this temperature. The heaters will also be available if inflight environment necessitates heating.

Inflight platform temperature is controlled by circulating a constant-temperature fluid through ducts in the platform covers. The exterior of the platform is painted with aluminum to provide an emissivity of approximately 0.4, thus providing a near-constant temperature radiating surface. Blowers will be utilized to circulate the internal gaseous nitrogen and maintain normal temperature gradients across the gimbals.

Gaseous nitrogen is supplied from a 0.056 m^3 (2 ft^3) storage reservoir pressurized to 20.7×10^6 N/m^2 (3000 psi) and regulated to 10.3×10^4 N/m^2d (15 psid) to supply the platform. Temperature conditioning of the gas will be from the water-methanol Instrument Unit coolant system. The platform requires 0.014 m^3/min. (0.5 ft^3/min) of gaseous nitrogen.

SECTION XIV. LABORATORY CHECKOUT EQUIPMENT

Laboratory checkout equipment will be utilized to calibrate and to test the system for accuracy prior to installation in the vehicle Instrument Unit. The final checkout (FCO) equipment will be identical at the manufacturer's plant, launch site, and any intermediate location where verification of system operation is required. The FCO will calibrate all subsystems, servoloops, accelerometers, gimbal pickoffs, and the resolver chain. Platform drift rates will also be measured with the FCO equipment.

The FCO equipment will consist of two main assemblies:

1. Electrical Console

The electrical console will contain the control panels, monitor panels, guidance system simulator panels, program panels, and power supplies. Auxiliary equipment, such as oscilloscopes and voltmeters, will also be contained in this console.

2. Mechanical Stand

The mechanical stand will be used to mount the inertial platform. The stand will contain a gimbal system to simulate vehicle motion and an automatic theodolite to verify the azimuth laying system.

SECTION XV. ELECTRICAL SUPPORT EQUIPMENT

The electrical support equipment (ESE) necessary for activation and prelaunch checkout of the ST124-M inertial platform system is integrated into the Saturn launch complex equipment. The turn-on sequence and checkout procedure is fully automated. Critical measurements and responses will be monitored by the launch computer on a go/no-go basis. Visual displays and readings of the most critical measurements such as the steering signals, azimuth heading, accelerometer outputs, and phi signals (from the data adapter) will be available for monitoring by launch personnel.

The ST124-M ESE is located in three areas. Figure 57 is a block diagram of the ESE located in the mobile launcher, Figure 58 is a block diagram of equipment in the theodolite hut, and Figure 59 is a block diagram of the ESE located in the launch control center. Figure 60 shows how the platform subsystem and its ESE are connected for communication.

The following is a description of the individual panels which constitute the electrical support equipment.

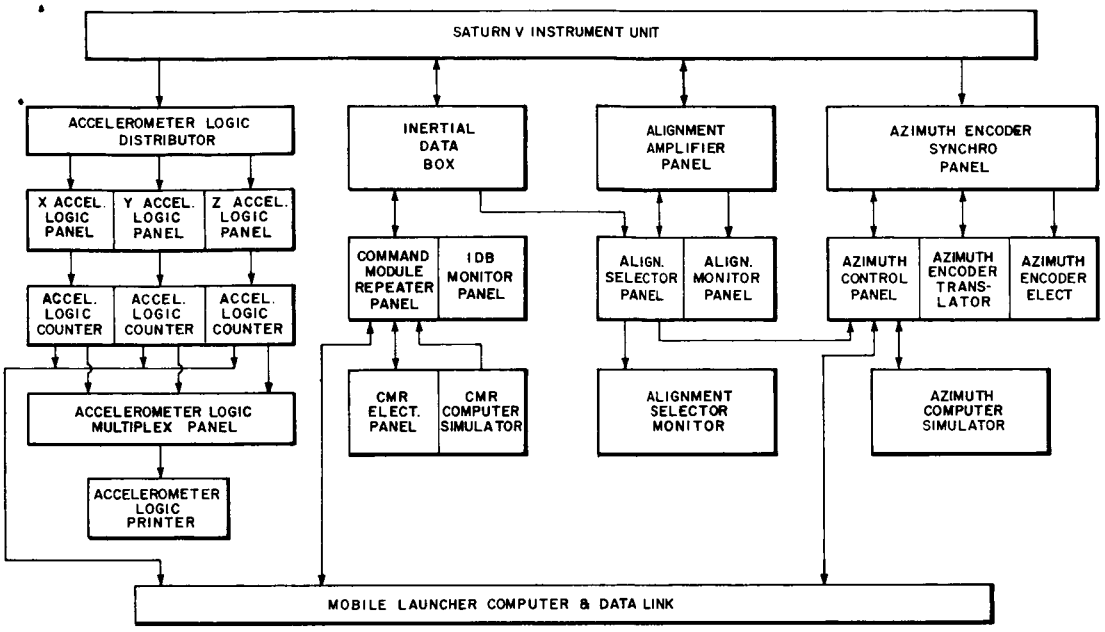

FIGURE 57. BLOCK DIAGRAM OF ST124-M ESE LOCATED IN THE MOBILE LAUNCHER.

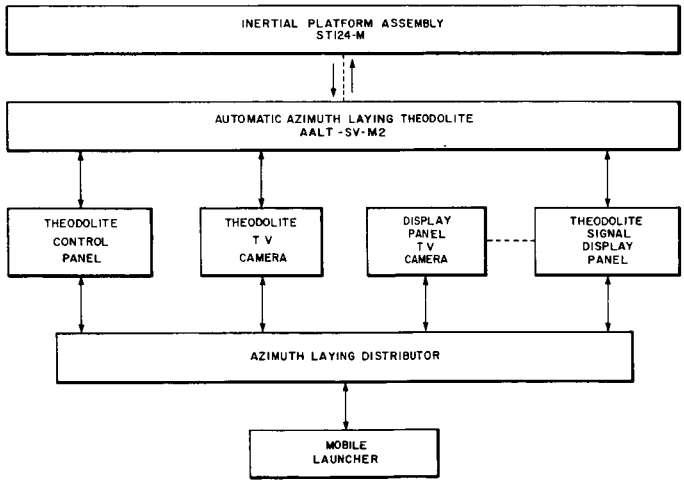

FIGURE 58. BLOCK DIAGRAM OF ST124-M ESE LOCATED IN THE THEODOLITE HUT.

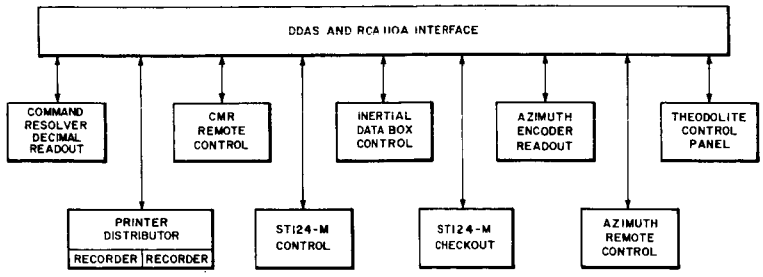

FIGURE 59. BLOCK DIAGRAM OF ST124-M ESE LOCATED IN THE LAUNCH CONTROL CENTER.

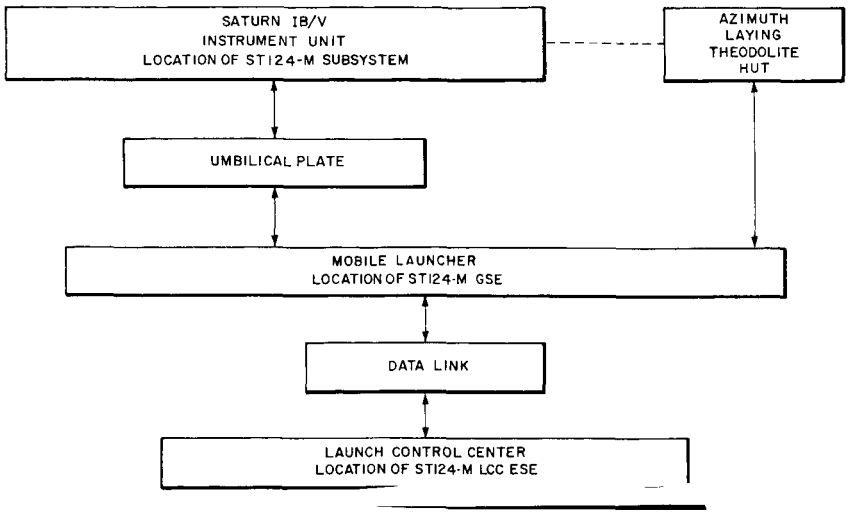

FIGURE 60. BLOCK DIAGRAM OF ST124-M AND LAUNCH ESE.

1. Alignment Amplifier Panel

The alignment amplifier provides circuitry to erect the platform to the local vertical and to align the platform in azimuth to the Y_R pivot sensor or to the inertial prism.

Three similar systems (Fig. 61) are provided for these functions, one for each of the attitude sensors. Each is composed of an integrating amplifier, a motor tachometer, a potentiometer, and a torquer amplifier for providing power to the gyro torquer. The signals for leveling the platform are received from the pendulums and fed to the integrating amplifiers. The potentiometers are driven to a setting to compensate for earth's rate, and the loop is closed through the respective X and Z gyro torquers. The roll loop differs in that it receives its input from a synchro located in the Y_R pivot.

The gyro torquing mode of operation, which is commanded external to the alignment amplifier, provides the means for slewing the platform by applying voltages to the gyro torquers. When torquing, the servo system of Figure 61 is switched out. Any of three different rates in either direction can be manually switched in during torquing.

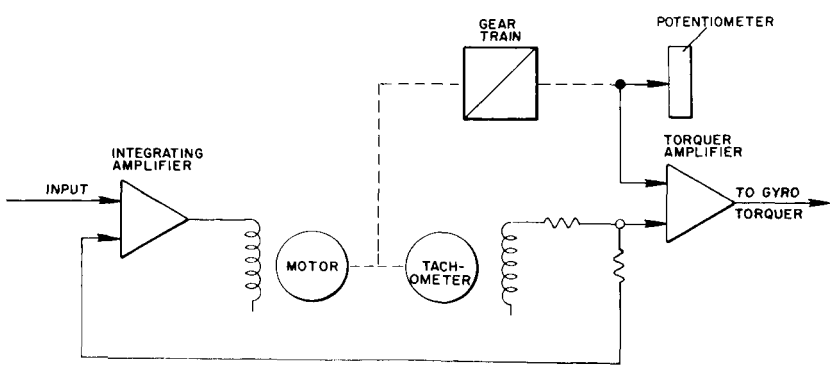

FIGURE 61. ALIGNMENT SERVO CONTROL SYSTEM.

Individual manual controls for each channel are provided within the alignment amplifier for checking out the system. This is accomplished by switching in a reference voltage to the integrator amplifiers and monitoring the torquer amplifier outputs. Verification of the entire amplifier may be commanded externally. Integrator cutouts are incorporated in all loops (X, Y, and Z). Integrator cutout can be commanded (externally) to enable the positioning of any gimbal to any prescribed position for test purposes and still counteract earth's rate. The integrator cutout circuits are activated with the ignition command to "freeze" and thus isolate the three integrators from vibration and erroneous inputs. A test plug is provided for monitoring the functions in the alignment amplifier.

2. Alignment Selector Panel

The alignment selector performs the functions of alignment control and distribution, inertial and synchro prism control, and alignment signal conditioning. All commands for this panel are given by applying 28 V dc to the proper pins on plug J1, which activates relays in this panel. A test plug is provided for monitoring.

The synchro prism may be driven in several operating modes. Manual slewing of the prism in either direction may be commanded at either slow or fast slewing rates. In the automatic slewing mode, prism direction and speed are determined by the output of a phase detector sensing the azimuth synchro repeater position. (This phase detector is in the azimuth control panel.) Upon acquisition of the synchro prism by the theodolite, prism drive modulator-amplifier AM5 is turned on and closes the prism loop (Fig. 62).

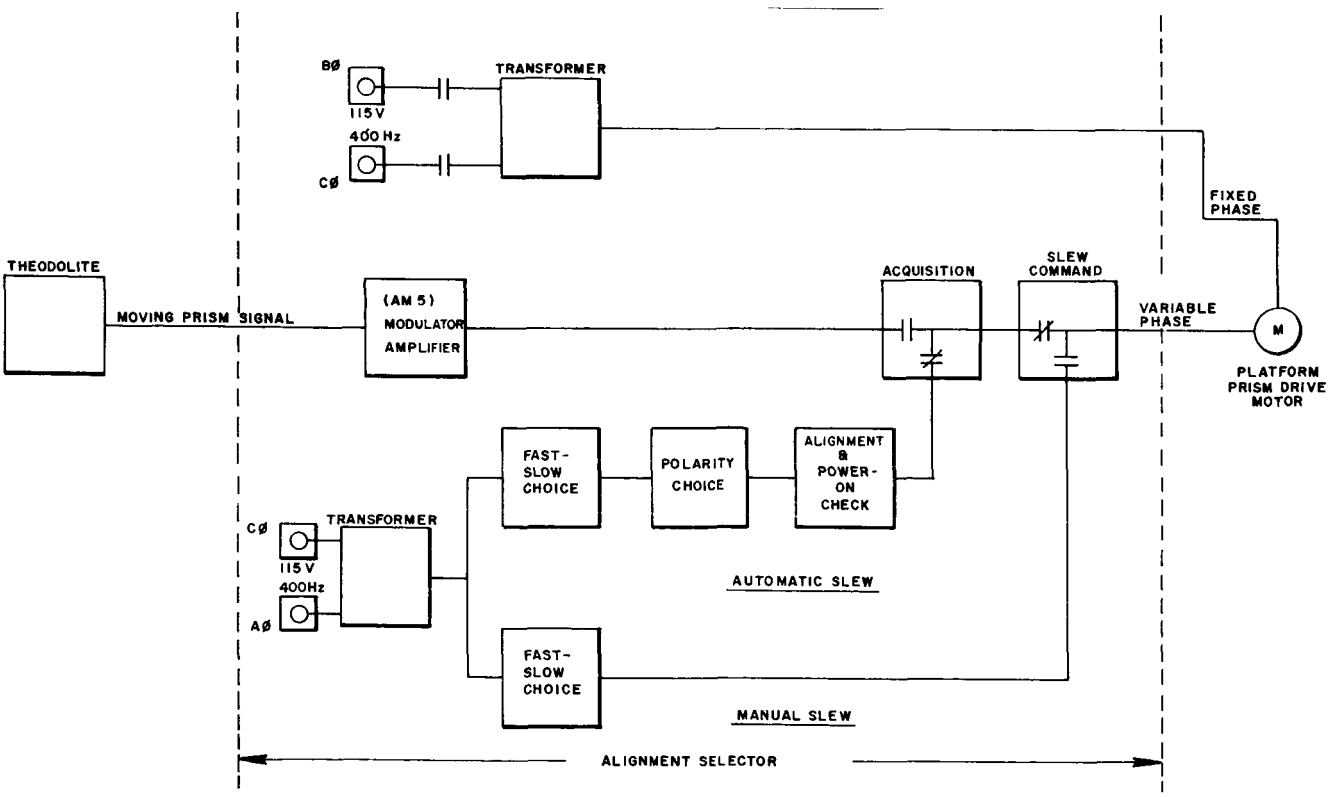

FIGURE 62. SYNCHRO PRISM CONTROL.

The dual prism mode allows both the synchro and inertial prisms to be captured simultaneously by the theodolite. Since the inertial prism is rigidly attached to the inner gimbal, the Y alignment loop is used for inertial gimbal control. A slewing mode is obtained by feeding a voltage to the Y gyro torquer through a transformer. The polarity of this voltage is set by a polarity detector which examines the phi roll signal. In this slewing mode, a command to the Y earth rate bias potentiometer is given to the alignment amplifier. Once the inertial prism is acquired by the theodolite, the Y gyro torquer is controlled by the output of the Y channel of the alignment amplifier, and the inertial prism signal from the theodolite is modulated and amplified and fed to the input of the Y channel of the alignment amplifier. This closes the inertial prism loop (Fig. 63).

Phi signal alignment uses the error voltages from the inertial-data-box command-voltage demodulators as alignment signals for the platform. Since these signals are dc, three modulators, roll (AM6), yaw (AM7), and pitch (AM8), are necessary. The outputs of these modulators may be switched into the input of the alignment amplifier individually by command. In the Y alignment channel, phi roll is used for alignment as a basic mode when the theodolite has not acquired the synchro prism.

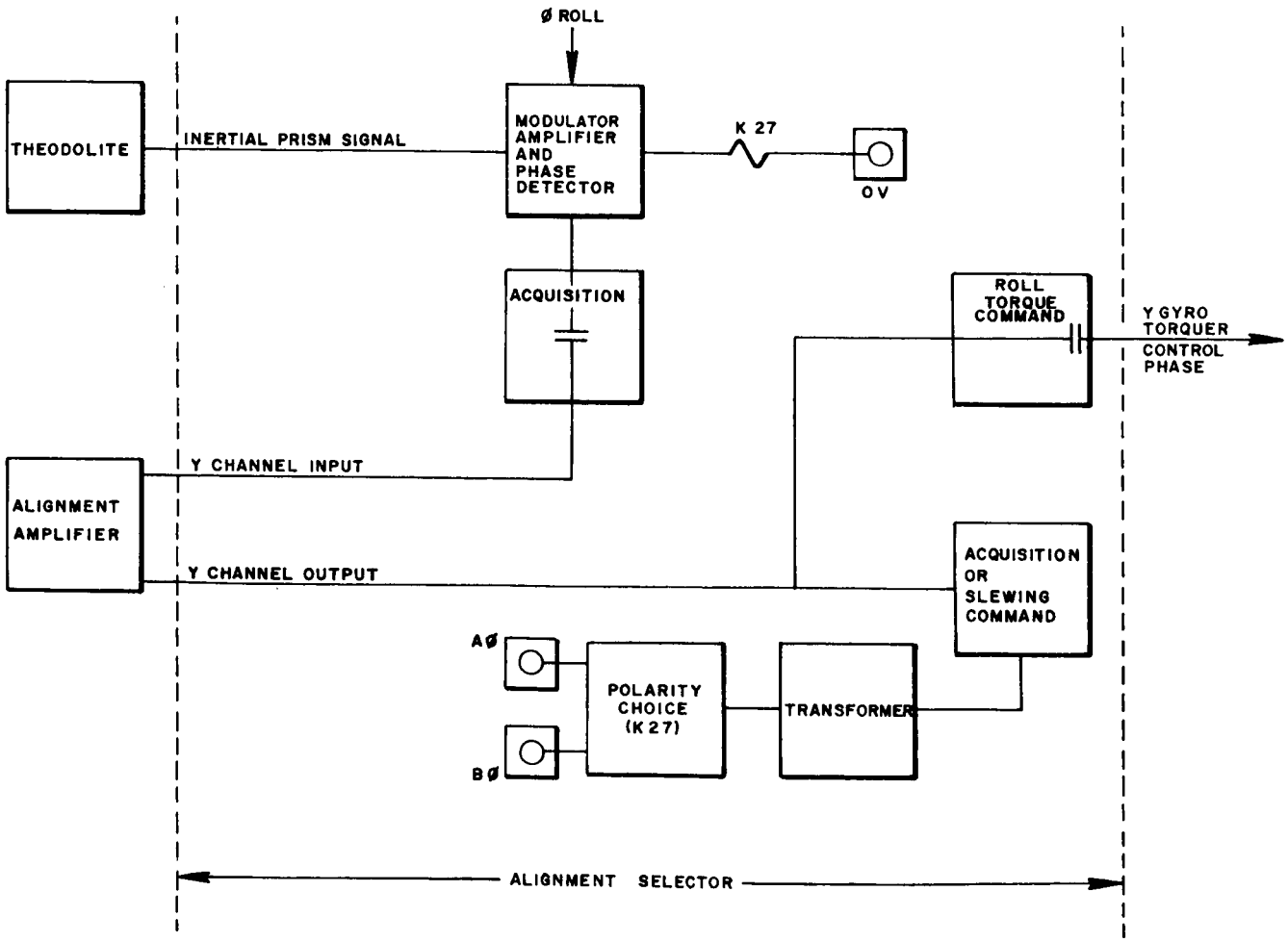

FIGURE 63. INERTIAL PRISM CONTROL.

The output of the Y repeater (either coarse or fine, depending upon the state of the null detector in the azimuth control panel) is fed to a synchro preamplifier, whose output is switched into the input to the Y channel of the alignment amplifier with synchro prism acquisition.

Alignment of the platform to the buffered 400-Hz gimbal resolver repeater outputs may be commanded in each channel individually.

3. Alignment Monitor Panel

The alignment monitor panel monitors the various voltages used in aligning the ST124-M platform and receives its inputs directly from the alignment amplifier. The panel includes meters for measuring the following voltages:

a. X torquer amplifier output

b. Y torquer amplifier output

c. Z torquer amplifier output

d. X integrator amplifier output

e. Y integrator amplifier output

f. Z integrator amplifier output

g. 28-V dc power supply

h. 115-V 3-phase 400-Hz supply (line AB, BC, or AC phase as manually selected)

i. Additional voltmeters are used to measure the excitation voltages to the earth rate bias potentiometers, earth rate bias potentiometer outputs, and tachometer outputs of the X, Y, and Z loops. The position of a rotary switch selects the individual function that the operator requires for measurement.

Each of the meters is equipped with jacks for calibration or for use in external measurement. Jacks are provided for measuring the X, Z, and azimuth alignment amplifier input voltages and phases. Lamps are also included for indicating the following:

a. Proper phasing of the 3-phase 400-Hz supply

b. Erection ON

c. Y earth rate bias zero command ON

A parallel output plug is provided for automatic data acquisition of all monitored voltages.

4. Alignment Selector Monitor Panel

This panel is used to monitor the operation of the alignment selector. ' It contains 8 voltmeters, 8 indicators, and 27 banana jacks. Three of these meters (M_1, M_2, and M_3) read the output of the X, Y, and Z phi signal demodulators in the inertial data box. The next three meters (M_4, M_5, and M_6) monitor the buffer stages output in the gimbal resolver programer. M_7 can be switched in to measure the synchro-fixed phase or variable phase or the Y torquer amplifier output. M_8 can be switched in to read 115-volt 400-Hz AC, BC, or AB phase. The indicators show the presence in the alignment selector of +28 V dc, Y repeater phi detector output, phi roll phase detector output, prism drive relay timer, moving prism drive relay, inertial prism acquisition, and moving prism acquisition. The banana jacks provide monitoring points for the pivot resolvers' outputs, inertial prism theodolite output, and moving prism theodolite output.

5. Azimuth Control Panel

This panel has two modes of operation. The two modes are controlled by either the platform-follow-command switch or the dual-prism-alignment-command switch (both on the theodolite control panel). A block diagram showing the signal flow of this equipment is given in Figure 64. This panel contains the following pieces of equipment:

a. Null detector

b. Phase detector and null detector

c. Preamplifier

d. Drive amplifier

e. Digital to analog converter

In the first mode of operation, the platform-follow-command switch or the dual-prism-alignment-command switch is in the OFF position. Launch control computer functions are fed into the digital to analog converter to the drive amplifier which drives the servomotor/tachometer combination. Since the servomotor is connected mechanically to the stator of the 25:1 synchro repeater, the servomotor drives the control transformer and the platform follows. Essentially, this mode of operation is used to program the platform in azimuth by programing the necessary information into the launch computer.

In the second mode of operation, the platform-follow-command switch or dual-prism-alignment switch is in the ON position. Turning either switch on switches a series of contacts which activate the second mode. In the second mode, the control transformer on the 25:1 synchro repeater follows the 25:1 control transmitter on the platform until the rotor on the repeater is at a null voltage. Thus the 25:1 synchro repeater is slaved to the baseline reference of the platform.

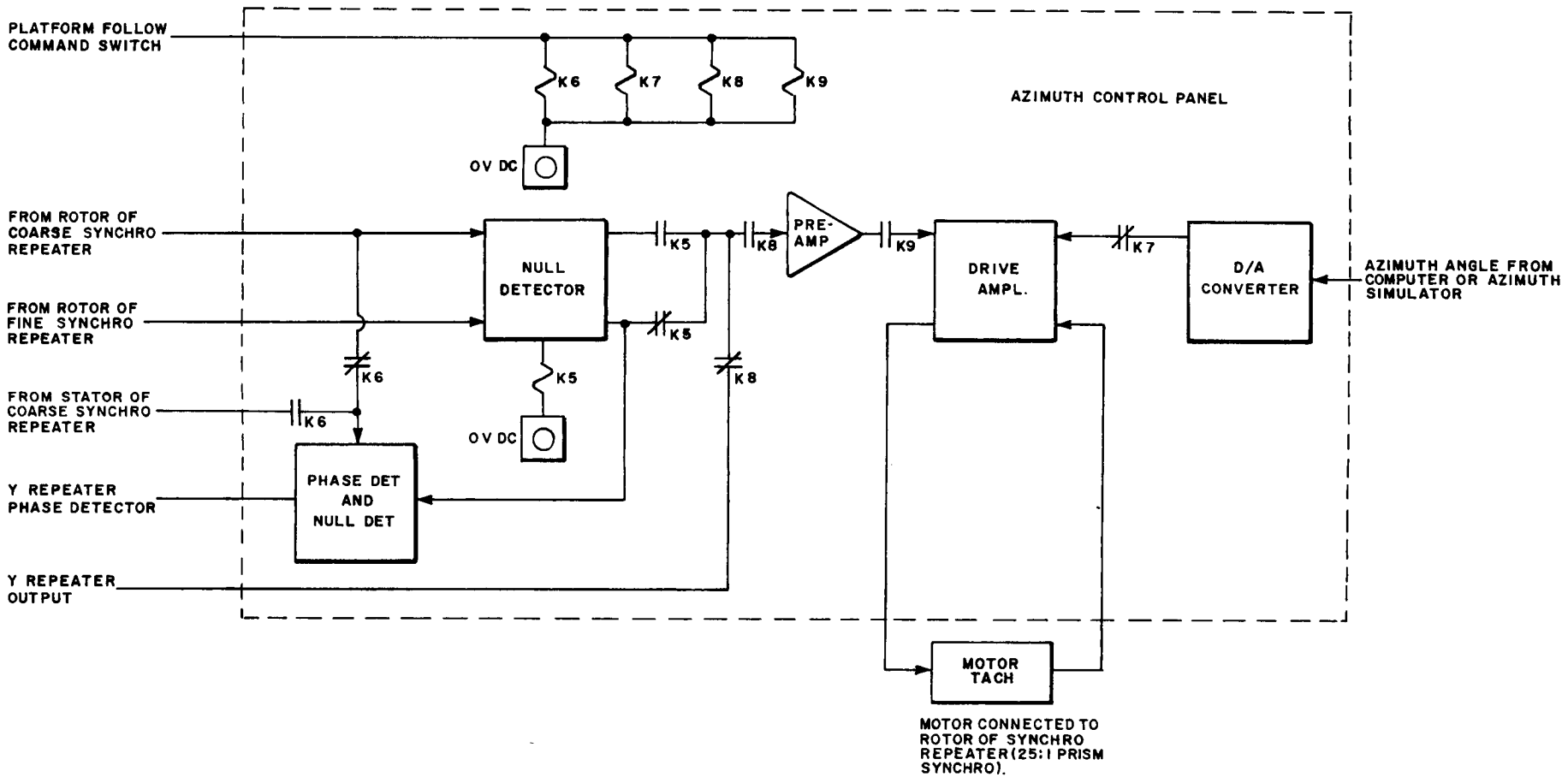

FIGURE 64. BLOCK DIAGRAM OF SIGNAL FLOW FOR THE AZIMUTH CONTROL PANEL.

6. Azimuth Encoder Electronics Panel

The electronics panel is used with the 18-bit encoder in the azimuth encoder synchro panel. It contains the power supplies for the encoder as well as equipment for operation and interrogation of the encoder. The output is conditioned and sent to the azimuth encoder translator.

7. Azimuth Encoder Translator Panel

This panel converts the low-level information outputs from the azimuth encoder electronics panel to 9 and 28 V dc gray code levels to be used by the RCA-110A and the azimuth encoder readout. It also converts the same information into a binary output for test purposes.

8. Azimuth Encoder Synchro Panel

This panel contains a 25:1 two-speed synchro control transformer which is a backup to the 25:1 synchro transmitter on the ST124-M Y_R pivot. Mechanically ganged to the control transformer is a drive-motor/tachometer combination with a 10^5:1 gear box and an 18-bit encoder. The units are kept in a special panel enclosure with its own temperature control system. Maximum synchro drive rate is 18 degrees per minute.

9. Azimuth Encoder Readout Panel

The azimuth and command module repeater (CMR) encoder readout units perform substantially identical functions. Both receive parallel gray-coded angular information from their respective encoders and display the encoder angle as a decimal number in degrees, minutes, and seconds of arc. The same panel functions for both applications with a resolution switch to choose between 16-, 17-, 18-, or 19-bit gray-coded inputs. The azimuth and CMR encoder readout units differ only in that the former requires conversion of an 18-bit input while the latter converts a 16-bit input.

As determined by the resolution control, the number of gray-coded binary bits to be displayed are converted, after buffering and level shifting, to a natural binary number in the gray-to-binary converter. This number is preset into the binary countdown counter and then counted down to zero at a rate of 2.62144 MHz. Concurrent with the countdown process, a binary coded decimal (BCD) counter is counted up from an initial zero state at a rate of 6.48 Hz. When the binary countdown reaches zero, both its clock and that of the BCD counter are stopped. The number in the BCD counter is the BCD representation of the gray-coded input angle times a scale factor equal to the ratio of the two clock frequencies. This ratio is approximately 2.47:1, which is dictated by the conversion factor of 2.47 arc seconds equal one input bit at a conversion accuracy of one part in 2^{19}. This BCD number is stored in a flipflop register, converted to a decimal number, and displayed. The decimal number is also available as parallel output to a printer. The sampling rate may be over the range of 0.2 to 10 seconds.

10. Accelerometer Logic Panel

The accelerometer logic panel accepts accelerometer inputs from an optisyn transmitter, determines the error in precession rate, and measures drift rate. The rate error and drift rate are properly scaled to read in units of meters per second squared and are displayed on a printer.

The accelerometer optisyn has three outputs, two sinusoidal outputs (sine and cosine) yielding 6000 pulses per revolution and a marker channel yielding one pulse per revolution. After the reception of the marker pulse, the leading sinusoid from the optisyn is determined by the rotation sensor. The sinusoid is amplified, shaped, and then counted in the velocity preset counter, which is initially cleared. When the velocity counter reaches 100, it resets itself and starts the 100 kHz period preset counter. The count to 100 provides a delay of sufficient length for the printer to reprint the previous result. Both the velocity counter and the period counter continue to count until either one records a preset value. The first counter to reach its preset value starts the error counter at a 48 kHz rate. The second counter to reach its preset value stops the error counter. The velocity counter counts until it reaches 6000 counts, which is the number of pulses in one complete revolution of the optisyn. The period counter will count at a 100 kHz rate until it reaches the number that represents the nominal time for one accelerometer revolution. Thus, if the velocity counter starts the error counter, the precession rate is too high; but if the period counter starts the error counter the precession rate is too low. The sign of the error thus derived is noted at the printed output by the color of the typing. The ratio of the two clocks (100 and 48 kHz) is such as to cause the error rate to read directly in units of meters per second squared.

The drift rate measurement is initiated manually. Pressing the manual reset clears all counters and starts the period counter counting at a 1 kHz rate. Coincidentally, the velocity counter starts counting the optisyn pulses, which actually represent incremental position changes. When the period counter reaches 313 seconds, it starts the error counter counting at a predetermined rate and starts the velocity counter counting down at a 1 kHz rate. When the velocity counter reaches zero, counting is stopped, and the number in the error counter represents the drift rate in meters per second squared. The value and direction of drift, as determined by the rotation sensor, are printed.

11. Accelerometer Multiplex (Memory) Panel

The accelerometer multiplex is designed to accumulate and assemble the data from three accelerometer logic panels simultaneously so that these data may be printed out on a single printer.

12. Accelerometer Printer Panel

This printer is commercially purchased. It prints on paper tape the data fed to it by the accelerometer multiplex panel.

13. Accelerometer Logic Distributor

The accelerometer logic distributor is a junction box where interconnections between the patch rack, X accelerometer logic, Y accelerometer logic, Z accelerometer logic, and the accelerometer logic multiplexer are made. Accelerometer channel data, are fed through the patch rack to the respective accelerometer logic blocks together with 26-volt 400-Hz power. Accelerometer logic outputs (X, Y, and Z) are fed to the accelerometer multiplexer.

14. Long Range Theodolite

The azimuth alignment theodolite required for the various Saturn vehicles operates at distances of 91.5 to 305 m (300 to 1000 ft) at elevation angles to 25 degrees. It measures separately the azimuth deviation angle of two different vehicle prisms with 5-second accuracy and provides automatic acquisition indications. The theodolite system continues to provide azimuth measurement during vehicle sway of 35.5 cm (±14 in.) amplitude, and sway compensation is made at a rate of 0.76 m/s (30 linear in./s).

The optics of the theodolite provided for this program is a 20.3 cm (8 in.) aperture automatic autocollimator which measures azimuth deviations of two target prisms. A sway compensation system, including a servodriven penta mirror and sway-sensing detectors in the autocollimator, automatically translates the line of sight of the autocollimator to follow the vehicle motion while maintaining precise angular alignment. The autocollimator and the translating penta mirror are on a lathe-bed-type base which may be elevated during setup to acquire the two vehicle prisms. The penta mirror projects the autocollimator beam to the 5 x 5 cm (2 x 2 in.) prisms, and the energy reflected back to the autocollimator generates separate error signals whenever either prism moves from its desired azimuth orientation. The vehicle can be seen on the launch control center TV monitor at all times by the TV camera which views it through the autocollimator. The theodolite can be remotely controlled to center the prisms in the field. The prisms may translate (sway), but once the prisms are acquired, the sway tracking feature automatically translates the penta mirror set to maintain the centering within 1.27 cm (±1/2-in.) over a 71 cm (28 in.) range. Since penta mirror deviation is virtually unaffected by small rotations, its use permits accurate readout of the vehicle prism alignments, even in the presence of sway.

The long range theodolite is equipped with a reference prism located within the range of penta mirror travel and is oriented to the desired alignment direction by survey. Autocollimator zero alignment can easily be checked by positioning the penta mirror in front of the reference prism; therefore, the reference prism is used to check the final alignment of the theodolite and its electronics.

The long range theodolite accomplishes simultaneous but separate alignment of two prisms, the lower or synchro prism and the upper or inertial prism, by spectral separation of the transmitted energy from the two prisms and by spectral discrimination of the returned energy. Spectral separation refers to the spatial separation of the electromagnetic energy in a light beam on the basis of its wavelength. In the long range

theodolite system, a spectral separation is accomplished by the use of dichroic coatings on various optical elements and is utilized to allow the system to serve three independent functions. These functions are alignment of the inertial prism, alignment of the synchro prism, and adjustment of the theodolite with respect to the vehicle (sway compensation).

15. Theodolite Operations Display Panel

The theodolite operations display is a portion of electrical support equipment found in the theodolite hut; it consists of a panel with three meters. One meter indicates penta mirror position (in inches) and the other two meters indicate azimuth error (in arc seconds). On the panel are a sway servoacquisition light, two angular error acquisition lights, and a scale factor control (potentiometer) or gain control. This panel is monitored in the launch control center with a closed loop TV monitor.

16. Theodolite Power and Control Panel

The theodolite power and control panel consists of a master switch to activate the theodolite and controls to operate the penta mirror horizontally and vertically. This equipment will be found in the theodolite hut.

17. Theodolite Distributor Panel

The theodolite distributor, located in the theodolite hut, serves as an interface between the theodolite equipment, the power, and the alignment selector panels in the mobile launcher. The distributor provides voltage monitoring of the theodolite's 28-V dc and 115-volt 400-Hz supplies. A shutter test is manually initiated by pressing a button on the distributor panel.

18. Theodolite Control Panel

The theodolite control panel contains switches and indicators for controlling the azimuth laying scheme of the platform. All switches are three-position (ON-AUTOMATIC-OFF), as is true of the switches on all control panels. Located in the launch control center, this panel has been designed to control the long range theodolite system at the launch site. The controls are:

a. Synchro prism power

b. Inertial prism power

c. Penta mirror drive (left and right)

d. Theodolite elevate and depress

e. Automatic checkout

f. Dual prism align

g. Synchro prism manual control

Indicator lights are:

a. Azimuth alignment null

b. Inertial prism acquisition

c. Synchro prism acquisition

d. Remote power control

e. Sway control acquisition

19. Command Module Repeater Panel

This panel is used to convert RCA-110A position commands into a form that can be used to position the inertial data box chi modules or to read out their position. It contains an 8:1 dual resolver for electrical followup of the 8:1 dual resolver in the inertial data box. The followup dual resolver is mechanically coupled to a 16-bit optical encoder and through a gear train to the drive motor. The panel consists of a single followup servoloop and switching circuits. These are used to select one of the three chi resolvers of the inertial data box to be positioned. Also included in the panel are two digital to analog converter cards, drive amplifier, preamplifier, demodulator, null detector, and a 16-volt transformer for resolver excitation. Figure 65 shows a block diagram of the command module repeater system.

20. Command Module Repeater (CMR) Encoder Readout Panel

This panel contains logic circuitry necessary to give a decimal indication of the CMR angular position. It is essentially identical to the azimuth encoder readout.

21. Command Module Repeater (CMR) Encoder Electronics Panel

This panel provides the buffering for the output of the CMR encoder. It receives a parallel 16-bit, cyclic gray-coded number from the encoder upon interrogation. It amplifies these encoder signals and sends them to the CMR. Input to this panel is in the form of low-level pulses of 5 microseconds duration, occurring at interrogate time. These are amplified and level detected, resulting in a 20-microsecond pulse from the amplifier detector. These pulses are gated into a flipflop buffer register by a 9-microsecond gate pulse. Output amplifiers attached to the buffer register provide high-level outputs.

22. Inertial Data Box

The inertial data box has the following functions:

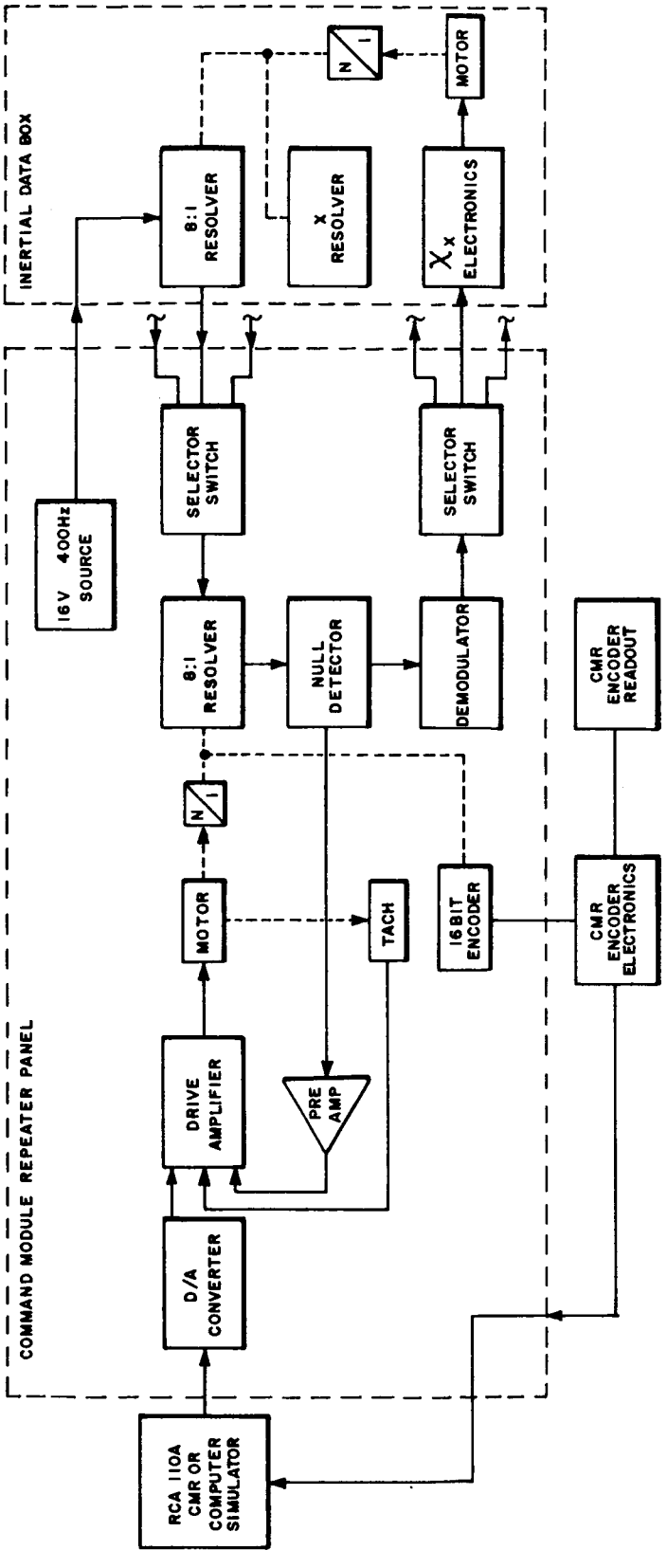

FIGURE 65. BLOCK DIAGRAM OF THE COMMAND MODULE REPEATER.

a. The chi programers generate signals needed to calibrate platform gimbal angle transducers.

b. The command voltage demodulators supply signals proportional to the angular difference between desired gimbal attitudes and programed attitudes.

c. The electronic cards condition the accelerometer outputs to the inputs of the computer.

The following modules are used in the inertial data box:

a. Three chi programers

b. Three command voltage demodulators

c. 1.6 and 1.92 kHz power amplifiers

d. 20-V dc supply

e. Provision for 12 accelerometer buffers and shapers (for flight units only).

The chi programer consists of three channels. Each channel consists of a motor/tachometer, a program resolver, an 8:1 resolver, a potentiometer, a brake, and associated gearing. The chi programer drives a resolver, which is a unit in a resolver chain, and generates the error signals needed for the correct determination of the vehicle attitude. The χ_X channel also has a 1:1 400-Hz redundant gimbal program resolver for controlling redundant gimbal position in the ST124-M4. The input signal to the chi programer is a step input of 48 mV, 5 ms increments. This is summed with the output of the tachometer which is a 400-Hz signal. The tachometer output is converted to a dc signal by means of a buffer, demodulator, and filter. The buffer presents a high impedance to the tachometer to avoid loading. The filter will attenuate any noise and stray signals. The dc input is converted to a 400-Hz signal by a modulator which in turn feeds the chi servoamplifier.

The command voltage demodulator (CVD) provides a dc signal proportional to the error between the platform gimbal and the programer. Three CVD's are in the inertial data box, pitch, roll, and yaw. The pitch and roll CVD uses a 1.6 kHz reference, and the yaw CVD uses a 1.92 kHz reference. The signal for the pitch and yaw CVD comes from the same resolver and therefore is a mixed 1.6 kHz and 1.92 kHz signal. Since the signal is common to both pitch and yaw CVD, a crisscross feedback arrangement is used to cancel out the 1.6 kHz signal in the 1.92 kHz yaw channel and the 1.92 kHz signal in the 1.6 kHz pitch channel.

The pitch CVD has three dc outputs: the computer output, the telemetry output, and the error-nulling-signal output. The computer output signal is proportional to the pitch error 1.6 kHz input signal. The telemetry output consists of two dc signals used for telemetry information. The error nulling signal provides a 1.6 kHz output in opposite phase with the input that is fed to the input summing junction of the yaw CVD. This signal cancels the input 1.6 kHz signal entering the yaw CVD and leaves only the 1.92 kHz yaw error signal. The operation of the yaw channel is the same as the pitch channel except that its carrier is 1.92 kHz.

The 1.6 and 1.92 kHz power amplifiers each supply a 26-volt rms sine wave to excite the program resolver chain and a 20-volt peak-to-peak square wave to the keying circuits of the CVD.

23. Inertial Data Box Control Panel

This panel contains switches and indicators necessary for controlling functions related to the inertial data box. Switches are three-position (ON-OFF-AUTOMATIC). The functions controlled are:

a. Chi mode select (X, Y, and Z)

b. Chi brakes (X, Y, and Z)

c. Phi signal zero (X, Y, and Z)

d. Power

e. CMR follow or drive

24. Inertial Data Box Monitor Panel

This panel monitors the operation of the inertial data box. It contains six voltmeters, two indicators, and a number of banana jacks. The meters have double scales and are connected across binding posts for monitoring and calibrating purposes. Meter M_1 can be switched in to measure the drive amplifier output of either the χ_X, χ_Y, or χ_Z system; meter M_2 can be switched in to measure the program command input of either the χ_X, χ_Y, or χ_Z system; and meter M_3 can be switched in to measure the tachometer output of either the χ_X, χ_Y, or χ_Z system. Meters M_4, M_5, and M_6 monitor the output of the yaw, roll, and pitch demodulators in the inertial data box. Of the two indicators in this panel, one monitor is 28 V dc and the other is 56 V dc. Banana jacks are employed to monitor the χ_X, χ_Y, and χ_Z telemetry potentiometer outputs, the 26-volt 3-phase 400-Hz supply, and the input and output of the 1.6 kHz power amplifiers. A parallel output plug is provided for automatic data acquisition of all monitored signals.

25. ST124-M (Stabilizer) Control Panel

This panel contains a series of lights and switches that are used to turn on the relays in the platform electronics assembly as well as to turn on power to the 56-volt power supply and the ESE panels. The switches all have three positions (ON-OFF-AUTOMATIC). If all the switches are in the AUTOMATIC position, the launch control computer is allowed to control the command lines. In either the OFF or the ON position, the computer is inhibited. Whenever a command line is excited, either manually or by the computer, an indicator will light. Three phase meters are included on this panel along with three manual gyro torquer switches for small angle platform positioning. The functions controlled are:

a. Dc power

b. 4.8 kHz reference

c. Platform blowers

d. Gyro and accelerometer power

e. X, Y, and Z gyro loops

f. Accelerometer and gyro loops

g. Platform heaters

26. ST124-M (Stabilizer) Checkout Panel

This panel contains the command switches and indications for the automatic checkout of the ST124-M platform, i.e., circuit-selection and pulse-application switches The same computer switch principle as used on the stabilizer control panel is applied here. Switches and indicators are also provided for slaving the platform alignment to the attitude (phi) signals. Relays are incorporated within the panel for use with the pulse select indicators for automatic checkout.

27. Servo Monitor (Portable) Panel

The servo monitor is used to monitor voltages and currents supplied to and generated within the platform electronics assembly for the gyro and accelerometers motors and servoloops. The panel includes provisions for measuring the 400-Hz 3-phase voltages and currents, input and output voltages of the servoamplifier power stage, and associated voltage such as amplifier dc supply and 4.8 kHz keying voltage.

Six ammeters continuously monitor the A-, B-, and C-phase gyros and accelerometers. Similarly, the driver outputs for the X, Y, and Z gyro and X, Y, and Z accelerometer servoloops are measured using ammeters with the added provision of a manual switch for each meter for scale change. This permits a reading under normal conditions (no input disturbance) and when input disturbances are present. The servoamplifier input voltages are measured by switching each in separately to a voltmeter. Binding posts are provided to measure all these voltages with a portable voltmeter, which can also measure the 56-V dc supply, 4.8 kHz supply, and 26-volt 400-Hz supply.

A spin protector circuit is provided for protection of the platform gyros and accelerometers. Its function is to detect any malfunction by monitoring the gyro and accelerometer preamplifier outputs. If any output goes over 25 volts, a relay is energized that sends a 48-V dc command through the platform electronics assembly and patch panel to the power distribution panel which shuts off the loops and wheels. An override switch is provided on the front panel.

29. Three-Phase 400-Hz Power Amplifier Panel

This panel will supply 100-VA 115-volt 3-phase power to the ST124-M ESE. The output voltage is referenced to the 26-volt platform ac power supply. Each phase contains a 115-volt to 26-volt stepdown transformer, a Variac, and a transistorized power amplifier. The panel contains three ac ammeters, one ac voltmeter, and a selector switch. One ammeter is used to monitor each phase while the voltmeter monitors all three phases by means of the selector switch. A block diagram of the power amplifier panel is shown in Figure 66.

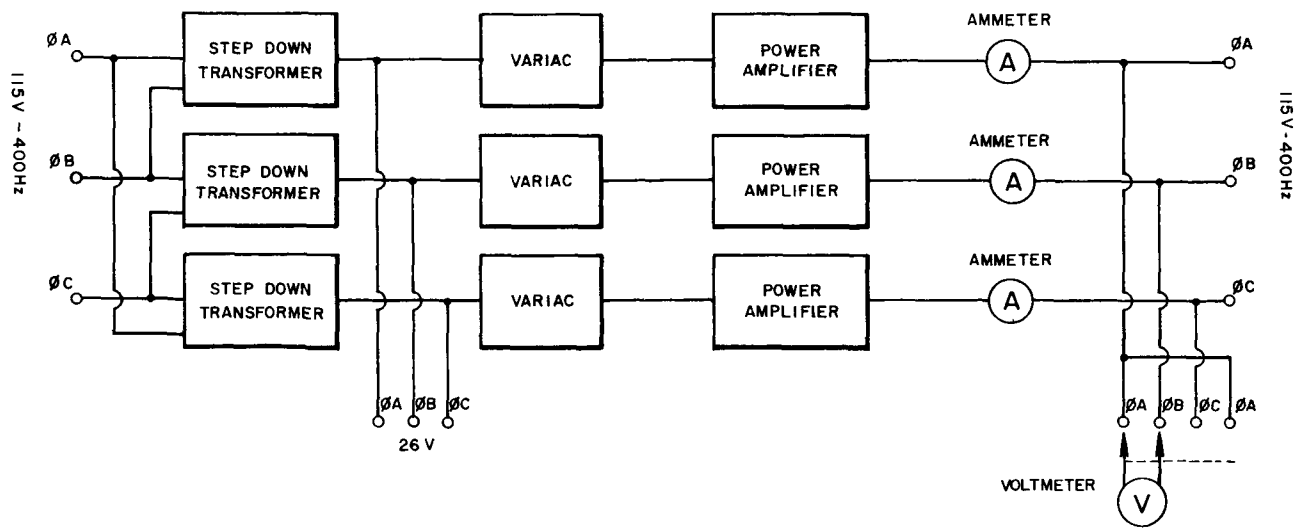

FIGURE 66. BLOCK DIAGRAM OF 3-PHASE 400-Hz POWER AMPLIFIER.

SECTION XVI. CONCLUSIONS

The ST124-M platform system was designed for use with the Saturn IB and Saturn V launch vehicles to support the Apollo mission. It is the latest generation of the ST124 series of platform systems. The ST124 platform system was a system concept developed early in the Saturn program to support the Saturn launch vehicles. When the system design was established, the Apollo program had not been defined; therefore, to allow complete freedom, a four-gimbal system design was utilized.

Eleven ST124 systems were fabricated (nine by contractors and two in-house prototypes). Six systems have been flown and two more are scheduled for flight. One system has been subjected to a series of sled tests and one has undergone temperature and vibration testing under space simulation conditions. The remaining system is the spare flight system to support the Saturn I launch program. The major mission requirements of Saturn I were vehicle development and guidance and control evaluation. The missions of the last three Saturn I vehicles have been allocated to the Pegasus program and a further evaluation of the guidance scheme.

An extensive environmental qualification program has been scheduled for the ST124-M system. A series of rocket sled tests with the system operating will be run at the track facilities at Holloman Air Force Base. This test will subject the system to shock, linear g loading, and extreme random vibration. Vacuum and temperature testing will also be conducted using a space simulation environmental chamber. A failure effect analysis has been completed for the system. A continuous reliability design review for the system has been conducted. Qualification testing to the component level has been initiated. As the results of the reliability program become available, reviews are being conducted and changes are initiated to correct design discrepancies.

Documentation of data generated during test programs and final engineering reports will be distributed to cognizant organizations.

BIBLIOGRAPHY

Fernandez, M., and G. R. Macomber: Inertial Guidance Engineering, Prentice-Hall, Inc., Englewood Cliffs, N. J., 1962.

Haeussermann, W., and R. C. Duncan: Status of Guidance and Control Methods, Instrumentation, and Techniques as Applied in the Apollo Project. Presented at the Lecture Series on Orbit Optimization and Advanced Guidance Instrumentation, Advisory Group for Aeronautical Research and Development, North Atlantic Treaty Organization, Duesseldorf, Germany, October 21-22, 1964.

Jones, C. S.: System Design of Gas-Bearing Gyroscope Servoloops, R-ASTR-G-WP-23-65, July 23, 1964.

Lee, C. E.: Azimuth Alignment System for the ST124-M Stabilized Platform as Used in Saturn IB and Saturn V Vehicles, MSFC, IN-R-ASTR-65-4, January 20, 1965.

Moore, R. L. and H. E. Thomason: Gimbal Geometry and Attitude Sensing of the ST124 Stabilized Platform, NASA TN D-1118, May 1962.

Thomason, H. E.: Multispeed Resolvers for Analog Digital Conversion of Shaft Angles, MTP-ASTR-G-63-7, July 9, 1963.

Thomason, H. E.: Gas Supply System for the ST124 Inertial Platform, NASA TM X-53004, December 2, 1963.

Inertial Guidance, Edited by G. R. Pitman, Jr., John Wiley and Sons, Inc., New York, N. Y., 1962.

Inertial Navigation Analysis and Design, Edited by C. F. O'Donnell, McGraw-Hill Book Company, New York, N. Y., 1964.

O'Connor, B. J.: A Description of the ST124-M Inertial Stabilized Platform and Its Application to the Saturn V Launch Vehicle, The Bendix Corp., Eclipse-Pioneer Division, Teterboro, N. J. Presented at the German Rocket Society Symposium, Darmstadt, Germany, June 26, 1964.

Rowell, J., and H. E. Thomason: A General Description of the ST124-M Inertial Platform System, MSFC, M-ASTR-IN-63-27, September 23, 1963.